1-1-2018

Polypeptoid polymers: Synthesis, characterization, and properties

Brandon A. Chan
Louisiana State University

Sunting Xuan
Louisiana State University

Ang Li
Louisiana State University

Jessica M. Simpson
Louisiana State University

Garrett L. Sternhagen
Louisiana State University

See next page for additional authors

Recommended Citation

Chan, B., Xuan, S., Li, A., Simpson, J., Sternhagen, G., Yu, T., Darvish, O., Jiang, N., & Zhang, D. (2018). Polypeptoid polymers: Synthesis, characterization, and properties. *Biopolymers, 109* (1) https://doi.org/10.1002/bip.23070

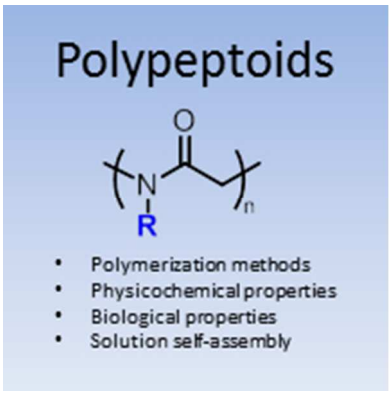

50x50mm (96 x 96 DPI)

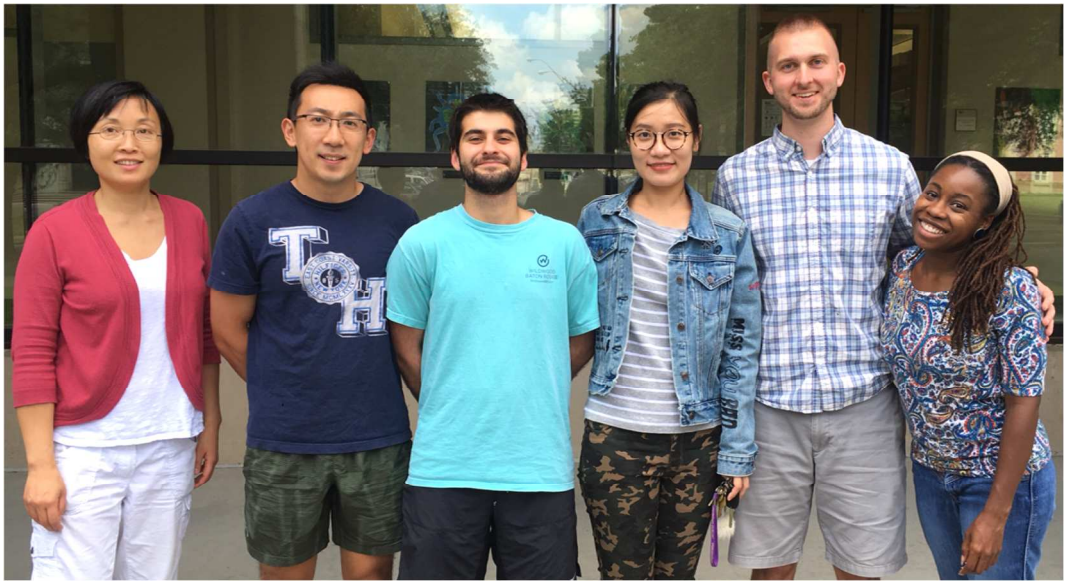

From left to right: Donghui Zhang, Naisheng Jiang, Omead A. Darvish, Tianyi Yu, Garrett L. Sternhagen, Jessica M. Simpson. (Note: Brandon Chan, Ang Li, Sunting Xuan are not included in the photo).

Donghui Zhang is an Associate Professor of Chemistry at the Louisiana State University in Baton Rouge, Louisiana. She obtained B.S. degree in Chemistry from Peking University in 1998 and Ph.D. degree in Chemistry from Dartmouth College in 2003. She did postdoctoral research at University of Minnesota on the synthesis and characterization of biorenewable polymers. Her current research interests include polymerization catalysis towards psudo-peptidic polymers, investigation of structure-property relationship of polypeptoid polymers and sequence-defined macromolecules.

Polypeptoid Polymers: Synthesis, Characterization and Properties

Brandon A. Chan, Sunting Xuan, Ang Li, Jessica M. Simpson, Garrett L. Sternhagen, Tianyi Yu, Omead A. Darvish, Naisheng Jiang and Donghui Zhang*

Department of Chemistry and Macromolecular Studies Group, Louisiana State University, Baton Rouge, LA 70803

Abstract

Polypeptoids, a class of peptidomimetic polymers, have emerged at the forefront of macromolecular and supramolecular science and engineering as the technological relevance of these polymers continues to be demonstrated. The chemical and structural diversity of polypeptoids have enabled access to and adjustment of a variety of physicochemical and biological properties (*e.g.*, solubility, charge characteristics, chain conformation, HLB, thermal processability, degradability, cytotoxicity and immunogenicity). These attributes have made this synthetic polymer platform a potential candidate for various biomedical and biotechnological applications. This review will provide an overview of recent development in synthetic methods to access polypeptoid polymers with well-defined structures and highlight some of the fundamental physicochemical and biological properties of polypeptoids that are pertinent to the future development of functional materials based on polypeptoids.

Introduction

Polypeptoids composed of *N*-substituted polyglycine backbones are structural mimics of polypeptides (Figure 1). Because of *N*-substitution, polypeptoids lack stereogenic centers and hydrogen bonding interactions along the main chains, in sharp contrast to polypeptides. As a result, the global conformations of polypeptoids are strongly dependent on the *N*-substituent structures, giving rise to random coils or well-defined secondary structures [*e.g.*, polyproline I (PPI) helix[1-6] and Σ-sheets][7-12] that are reminiscent of those of polypeptides. The polypeptoid backbone containing tertiary amide linkages is highly polar and hydrophilic. The physicochemical properties of polypeptoids can be tailored by the *N*-substituent structures, enabling control over the hydrophilicity and lipophilicity balance (HLB), charge characteristics,[13,14] backbone conformation,[1-12] solubility,[15-20] thermal and crystallization properties of the polypeptoids.[21-24] Without extensive hydrogen bonding, polypeptoids are thermally processable similar to conventional thermoplastics,[20-24] whereas polypeptides undergo thermal degradation before they can be melt-processed due to the extensive hydrogen bonding interactions. While polypeptoids exhibited enhanced proteolytic stability relative to peptides,[25,26] they can be oxidatively degraded under conditions that mimic tissue inflammation, [27] suggesting their potential *in vivo* uses as biodegradable materials.

Figure 1. Structure of polypeptoids and polypeptides

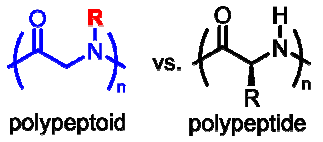

backbone: hydrophilic with strong dipole-dipole interactions
sidechain: tuning the HLB, charge characteristics and chain conformation

Recent advances in the controlled polymerization methods have enabled access to a suite of structurally well-defined polypeptoids with various *N*-substituent structures and molecular architectures, setting the stage for the future development of polypeptoid materials for various targeted applications. Several review articles on the synthesis, properties, and application of polypeptoids for biomedical or non-biomedical uses have been published in recent years.[28-32] As a result, this chapter is not meant to give a comprehensive review of the research activities in the field. It will focus on the recent development in the synthetic methods to access polypeptoid polymers with well-defined structures and highlight some of the fundamental physicochemical and biological properties of polypeptoids that are pertinent to the future development of functional materials based on polypeptoids.

Synthesis of Polypeptoids by Controlled Polymerizations

1. Monomer Synthesis

N-substituted *N*-carboxyanhydride (R-NCA) monomers are typically synthesized from the *N*-substituted glycine precursors **1** from one of the two general routes (Scheme 1). The first involves the initial conversion of the *N*-substituted glycine precursors **1** into the corresponding alkoxycarbonyl protected *N*-substituted glycines **2** followed by cyclization to afford the R-NCAs in the presences of various activating electrophiles (*e.g.*, PCl_3, PBr_3, $AcCl/Ac_2O$, or $SOCl_2$).[16,18, 33 - 37] *N*-substituted glycine precursors can also react directly with phosgene to yield R-NCA monomers.[38,39] The former methods are more popular than the latter due to the avoidance of toxic phosgene as well as the relative ease of purification to afford high purity R-NCA monomers.

Scheme 1. Synthesis of R-NCA and R-NTA monomers

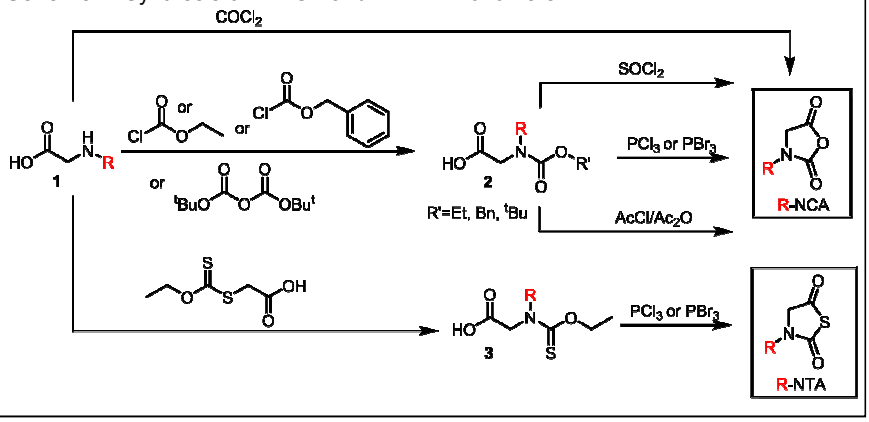

The thioester-analogs of the R-NCA monomers, *a.k.a. N*-thiocarboxyanhydride (R-NTA) can also be synthesized by a similar method through a PCl_3 or PBr_3-mediated cyclization of the thionoalkoxycarbonyl protected *N*-substituted glycine precursors **3** (Scheme 1).[40-42] The R-NTA monomers have proven to be significantly more stable than the corresponding R-NCA analogs so that the monomer synthesis can be conducted in open air versus the air-free atmosphere required for the R-NCA synthesis.[41,42] However, the released COS upon polymerization is toxic, a disadvantage relative to the R-NCAs. These methods have been successfully applied to the synthesis of a variety of R-NCA and R-NTA monomers, as shown in Figure 2.

Figure 2. Chemical structures of *N*-substituted NCA (R-NCA) and NTA monomers (R-NTA) that have been synthesized.

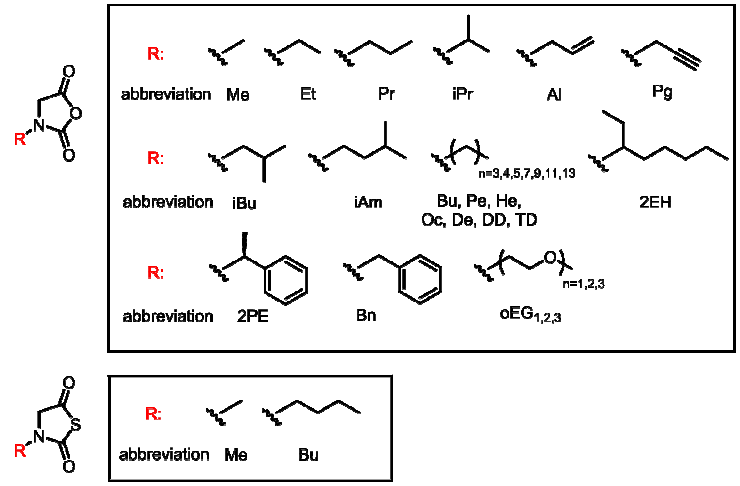

2. Synthesis of Linear Polypeptoids

Ring-opening polymerizations of R-NCA using primary amine initiators. The synthesis of linear polypeptoids can be accomplished by the controlled ring-opening polymerization (ROP) of R-NCA monomers using primary amine initiators (Scheme 2). This method produces polypeptoid polymers bearing the corresponding amide and secondary amino chain ends through a nucleophilic ROP mechanism which has been widely studied for the polymerization of amino acid-derived NCAs using primary amine initiators.[43] The early studies was mostly focused on the polymerization of sarcosine-derived *N*-carboxyanhydride monomers (Me-NCA),[44-55] yielding the water-soluble poly(*N*-methyl glycine) polymer (*a.k.a.* polysarcosine, PNMG). In recent years, the substrate scope for polymerization studies was further expanded to include a variety of R-NCA monomers bearing various *N*-substituents (Figure 2).[5,6,15-22] Luxenhofer *et al* demonstrated that the polymerizations of Me-NCAs using benzyl amine initiators were shown to proceed in a controlled manner without chain transfer or termination events, producing polysarcosines with narrow Poisson distribution (PDI<1.1-1.3) and M_ns that can be controlled by the initial monomer to initiator feed ratios.[56] The molecular distribution remains narrow (PDI=1.01-1.07) even after ten sequential polymerizations of Me-NCA monomers (DP<100), attesting to the robustness of the living polymerization and suggesting the potential uses of the methods towards the synthesis of well-defined block copolypeptoids via sequential monomer addition. For several monomers such as *N*-allyl NCA (Al-NCA)[17] and *N*-2-phenylethyl NCA (2PE-NCA),[5] intramolecular transamidation was kinetically competitive relative to chain propagation, resulting in the corresponding 2,5-diketopiperazine, limiting the accessible chain lengths of the resulting polypeptoids (DP<100). Macroinitiators [*e.g.*, poly(2-(3-butenyl)-2-oxazoline)] bearing a primary ammonium end-group has also been shown to successfully initiate the controlled polymerization of Me-NCA, yielding the corresponding poly(2-oxazoline)-*b*-polysarcosine block copolymers with nearly targeted composition and low molecular weight distribution (PDI=1.15-1.21) (Scheme 2).[57]

Scheme 2. Primary amine-initiated ROPs of R-NCAs to afford the linear polypeptoid. (The solid sphere below signifies the solid support or surfaces bearing primary amine groups).

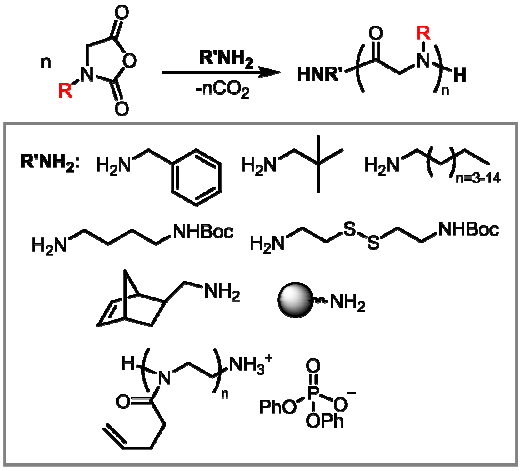

Luxenhofer *et al* also reported a study of combining solid support synthesis with solution phase polymerization to produce polypeptoid polymers.[58] The synthesis of penta-block copolypeptoids comprised of alternating sarcosine and *N*-ethyl glycine blocks was demonstrated. The resulting polymers have broad molecular weight distribution (PDI=2.00-2.20), which was attributed to the much faster polymerization rate relative to monomer diffusion into the solid support resins, resulting in a monomer concentration gradient in the resins. It was shown that the dispersity can be reduced (PDI=1.32) by slowing down the polymerization rate via addition of non-nucleophilic Brønsted acid (HBF_4) and using low capacity resins. The resulting polymer distribution can be described by Poisson distribution with a minor low MW trailing. Penta-block copolypeptoids (DP=50) comprised of sarcosine and *N*-ethyl glycine blocks with relative low PDI (1.34) can also be prepared by sequential immersion of the solid support to different monomer solutions (Figure 3).[58]

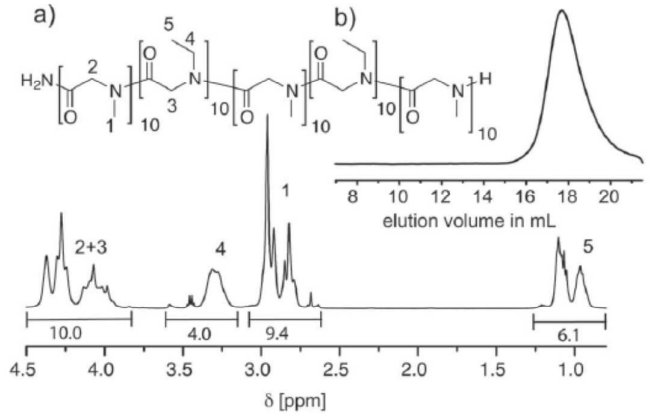

Figure 3. (A) ^{1}H NMR and (B) SEC chromatogram of pentablock copolypeptoids based on sarcosine and *N*-ethyl glycine repeating unit and the structural assignment.[58] Adapted with permission from John Wiley and Sons.

The surface-confined polymerization of Me-NCAs and Bu-NCAs using a surface-tethered primary amine initiator has also been investigated by Luxenhofer and Jordan *et al* to produce hydrophilic, hydrophobic, or amphiphilic polypeptoid homopolymer or block copolymer brushes.[59] Polypeptoid thin films up to 40 nm can be produced by this method. Surface-confined growth of polypeptoid brushes in conjunction with micro-patterning has also enabled access to micro-patterned polypeptoid thin films.[60] Garno and Zhang *et al* have also combined surface-confined polymerization of *N*-allyl NCA with nanoparticle lithography to create nano-patterned poly(*N*-allyl glycine) nanorods which has been characterized by AFM techniques.[61]

ROP of R-NCA using alcohol initiators and 1,1,3,3-tetramethylguanidine. Zhang *et al* recently reported that benzyl alcohol in conjunction with a catalytic amount of 1,1,3,3-tetramethylguanidine (TMG) can mediate the controlled polymerization of Bu-NCAs in low dielectric solvent (THF or toluene) (Scheme 3), whereas the alcohol alone does not initiate the polymerization of Bu-NCA under the same conditions.[62] MS and NMR analysis revealed

that majority of the polypeptoids bear the corresponding ester end group, consistent with benzyl alcohol initiating the polymerization. By contrast, in more polar solvents such as CH_2Cl_2 and DMF, low molecular weight polypeptoids were formed regardless of the initial monomer to benzyl alcohol feed ratios, indicating a lack of controlled polymerization behavior. Further ^{1}H NMR analysis revealed that TMG promotes polymerization of Bu-NCA by forming a hydrogen bonding complex with the alcohol (Scheme 4). This results in enhanced nucleophilicity of the alcohols and facilitates the nucleophilic ring-opening addition of the alcohols to the Bu-NCA monomer as part of the initiation step. The initiation efficiency of the hydrogen bonding complexes is strongly dependent on the steric and electronic properties of the alcohols. For alcohols that are less sterically hindered, such as methanol, ethanol, propanol, and benzyl alcohol, the initiation was efficient relatively to propagation, giving rise to controlled polymerization characteristics where the polymer molecular weights (M_n) agree reasonably well with theoretical prediction in the DP<100 range. As the alcohols become increasingly sterically hindered such as isopropanol or *tert*-butanol, the initiation becomes less efficient relative to propagation, resulting in significantly diminished control of polymer molecular weight. The resulting polypeptoids having significant higher M_ns than theoretical values based on the initial monomer to alcohol feed

Scheme 3. TMG-promoted ROPs of Bu-NCAs using alcohol initiators to afford the linear PNBG polypeptoid.

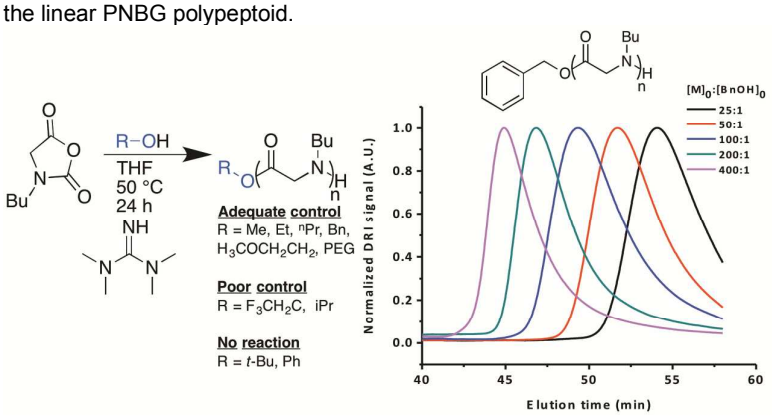

Scheme 4. Proposed mechanism of the TMG-promoted polymerization of Bu-NCA using alcohol initiators

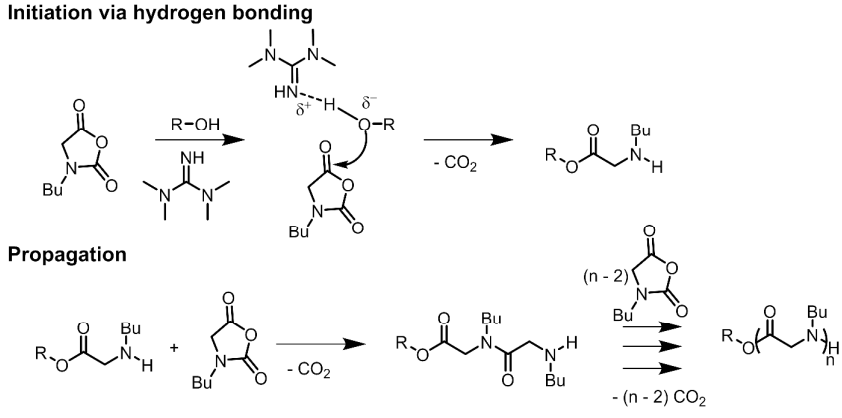

ratios when isopropanol is used as the initiator, whereas no monomer conversion was observed with *tert*-butanol initiator under the same reaction conditions. The electronic characteristics of the alcohols are also important in the initiation efficiency. Increasing deviation from controlled polymerization characteristics was observed with alcohols having enhanced acidity (*i.e.*, ethanol<2-methoxyethanol<2,2,2-trifluoroethanol). In the case of 2,2,2-trifluoroethanol, the M_ns are significantly higher than the theoretical prediction based on a controlled polymerization. Clearly, the nature of the alcohols is important to the polymerization characteristics. To investigate whether this method is useful towards the synthesis of heteroblock copolymers comprised of a polypeptoid segment, a poly(ethylene glycol) (PEG) bearing a hydroxyl terminus was examined as a macroinitiator in conjunction with catalytic TMG to mediate the ROP of Bu-NCA. The resulting heteroblock copolypeptoids have well-defined structures and the polymer molecular weights and compositions agree well with the theoretical prediction for a controlled polymerization and single-site initiation with the PEG macroinitiator.

ROP of R-NTA using rare earth metal borohydride or primary amine initiators. Apart from polymerization of R-NCAs to yield the polypeptoids, Ling *et al* have recently reported the ring-opening polymerization of Bu-NTA and Me-NTA using rare earth metal borohydrides ($[RE(BH_4)_3(THF)_3$, RE = Sc, Y, La, Nd, Dy and Lu]) in THF or CH_3CN (Scheme 5a).[41] The reactions at higher temperature (60 °C) yielded polysarcosines (up to DP=390) with higher dispersity (PDI=1.26-1.40) and in greater yields than those conducted at lower temperature (PDI=1.18 or 1.25 at 25 or 40 °C respectively). The architecture of the resulting polypeptoids is presently unknown. Primary amines [*i.e.*, $BnNH_2$, PEG-NH_2, amine-terminated poly(ε-caprolactone) (PCL-NH_2)] have also been used as initiators for the polymerization of Me-NTA, Et-NTA and copolymerization of Me-NTA and Bu-NTAs in 60 °C THF or acetonitrile (Scheme 5b). The reactions exhibit controlled polymerization characteristics, producing the corresponding linear polypeptoids with well-defined end-group structures, predictable molecular weight (up to DP = ~200) and moderate molecular weight distribution [poly(*N*-methyl glycine): PDI = 1.13-1.31; poly(*N*-ethyl glycine): PDI = 1.12 – 1.17; poly(*N*-methyl

Scheme 5. ROPs of R-NTAs using rare earth metal borohydrides or primary amine initiators to produce polypeptoids or their copolymers

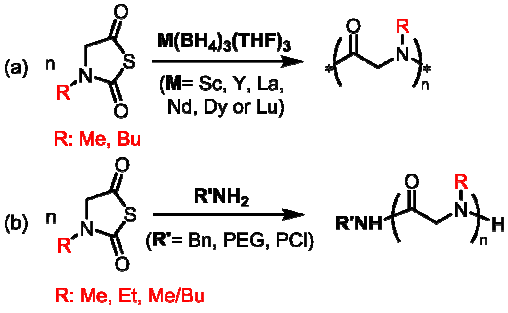

glycine)-*r*-(*N*-butyl glycine)] random copolypeptoids PDI=1.26-1.46].[19,41,63] We have also studied the polymerization of Me-NCA and found that the solvent is important to the polymerization rate. In CH_2Cl_2, the ROP of Me-NTA using benzyl amine initiator proceeds rapidly at room temperature and reach quantitative conversions within 18 h ($[M]_0$=1.0M, $[M]_0$:$[BnNH_2]_0$=25:1-400:1), yielding mono-modal polysarcosines with DP up to 300 and narrow dispersity (PDI=1.03-1.14).[64]Ling *et al* has also investigated a series of aminoalcohol initiators for the ROP of Me-NTA or Et-NTA in acetonitrile or THF (60°C) to access telechelic water-soluble polypeptoids (Scheme 6).[65] It was found that amino alcohols (**1-3**, Scheme 6) in which the alcohol groups are activated through intermolecular or intramolecular hydrogen bonding can initiate the polymerization of R-NTA at both the amino and alcohol ends, yielding a mixture of α-diamino-terminated polypeptoids and α-hydroxyl-ω-amino-terminated polypeptoids. By contrast, for aminoalcohols (**4** and **5**, Scheme 6) where hydrogen bonding is absent, only the amino end of the initiators initiates the polymerization, producing exclusively α-hydroxyl-ω-amino-terminated polypeptoids with controlled molecular weight (up to DP =~100) and moderate molecular weight distribution (PDI = 1.1-1.3) in good yields.

Scheme 6. Aminoalcohol-initiated ROP of R-NTAs (R=Me, Et) to produce telechelic polypeptoids.

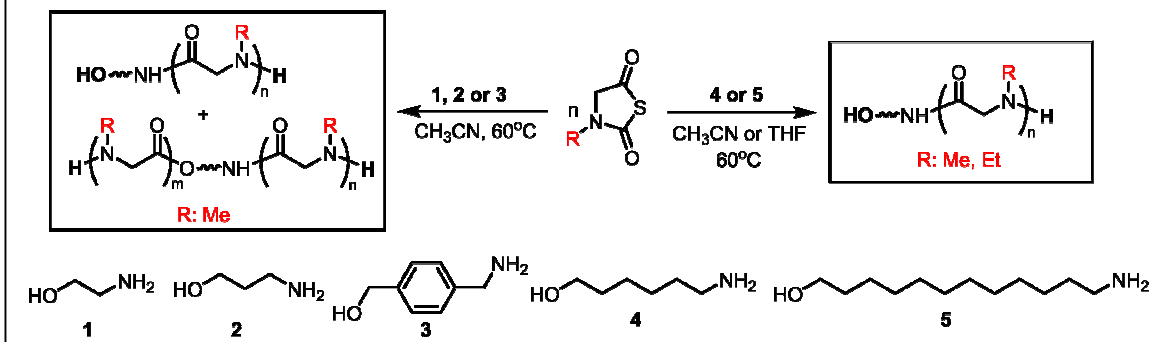

3. Synthesis of Cyclic Polypeptoids

NHC-mediated ZROP of R-NCA. Zwitterionic ring-opening polymerizations (ZROPs) have recently emerged as a promising strategy to synthesize high molecular weight cyclic polymers with diverse backbone structures (*e.g.*, polyether, polyester, and polyamide).[66] Zhang *et al* have reported ZROP of Bu-NCA using *N*-heterocyclic carbenes (NHCs) as nucleophilic initiator to produce the corresponding cyclic polypeptoids [*i.e.*, poly(*N*-butyl glycine)] with narrow dispersity and tunable ring sizes (Scheme 7).[37, 67] The polymer molecular weight and the ring size can be adjusted by controlling the initial monomer to NHC feed ratio. The polymerization proceeded through a zwitterionic propagating intermediate where the two oppositely charged chain ends are held in proximity through electrostatic interaction (Scheme 7). The zwitterionic species is in equilibrium with a dormant

Scheme 7. NHC-mediated ZROPs of R-NCAs to afford cyclic PNBGs and post-polymerization conversion of the cyclic PNBGs into the linear and NHC-free cyclic polymeric analogs.

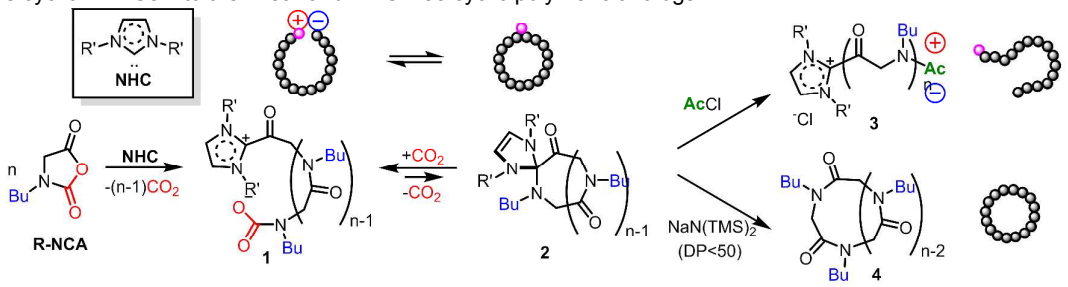

spirocyclic propagating species. The reaction exhibited pseudo-first order polymerization kinetics and polymerization rate is dependent on the steric characteristic of NHCs due to the intramolecular counter ion effect. The reactions proceed in a controlled manner in low dielectric solvents such as THF and toluene. In more polar solvents (*e.g.*, DMF, DMSO, and nitrobenzene), only low molecular weight mixtures of cyclic and linear polypeptoids were obtained, due to the competitive intramolecular transamidation relative to chain propagation. The zwitterionic species can be isolated and treated with $NaNTMS_2$ to give NHC-free cyclic polypeptoids. However this method is limited to polypeptoids with low MW (DP<50); the macrocyclization efficiency was found to vary for high molecular weight zwitterionic polypeptoid precursors. In addition, treatment of the zwitterionic species with electrophiles (*e.g.*, AcCl) afforded the corresponding linear polypeptoid counterparts. This method has been used to polymerize a variety of R-NCA monomers (Me-NCA, Et-NCA, Pg-NCA, Bu-NCA, De-NCA, 2EH-NCA and 2PE-NCA) to produce cyclic polypeptoids with different *N*-substituent structures including those adopting polyproline I (PPI) helical conformations[5,6] and cyclic random and block copolypeptoids.[15,37,68,69] Cyclic random copolypeptoids comprised of *N*-butyl glycine and *N*-propargyl glycine repeating units have also been grafted with short PEG (550 Da) sidechains to yield cyclic bottlebrush copolymers, which appear as toroid structures in AFM images, in support of the cyclic architecture of the polypeptoid backbone (Figure 4).[69]

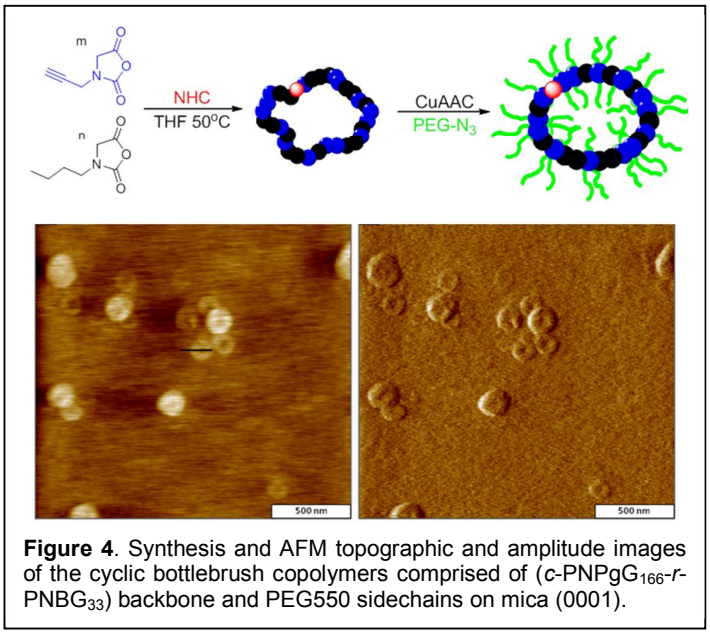

Figure 4. Synthesis and AFM topographic and amplitude images of the cyclic bottlebrush copolymers comprised of (*c*-$PNPgG_{166}$-*r*-$PNBG_{33}$) backbone and PEG550 sidechains on mica (0001).

DBU-mediated ZROP of R-NCA. It was recently reported that 1,8-diazabicyclo[5.4.0]undec-7-ene (DBU), a bicyclic amidine, can also mediate the controlled ZROPs of Bu-NCA similar to NHCs (Scheme 8).[70] The reaction occurs in a controlled manner in low dielectric solvents (*e.g.*, THF and toluene), allowing access of polypeptoids having low to medium molecular weights (DP<300) and narrow PDI (1.02-1.12), similar to what has been reported for NHCs. By contrast, in DMF, only low molecular weight polymers (DP<40) were formed regardless of the initial monomer to DBU ratios. In toluene, the initiation rate was found to be comparable to that of the propagating rate. The propagating species have a zwitterionic structure with positively charged DBU moieties at one chain end and negatively charged carbamate group at the other. The cyclic polypeptoid architecture was verified by a combination of end-group analysis with NMR and MS method and AFM and SANS analysis.[70,71] While the ZROP of Bu-NCA using DBU initiators is comparable to that with NHC initiators in rate, DBU has the advantage of being air and moisture stable, in contrast to NHCs. This makes DBU a more robust initiator relative to NHCs towards the ZROP of R-NCAs.

Scheme 8. DBU-mediated ZROPs of Bu-NCAs to afford cyclic PNBGs

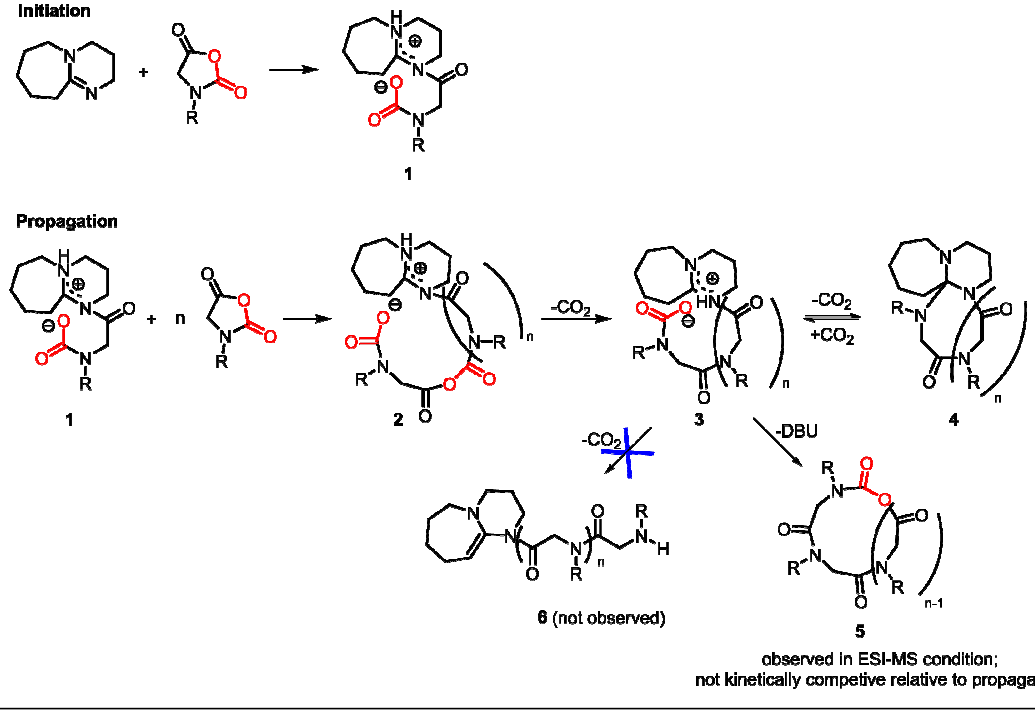

4. Synthesis of Bottlebrush, Branched and Star-shaped Polypeptoid Copolymers

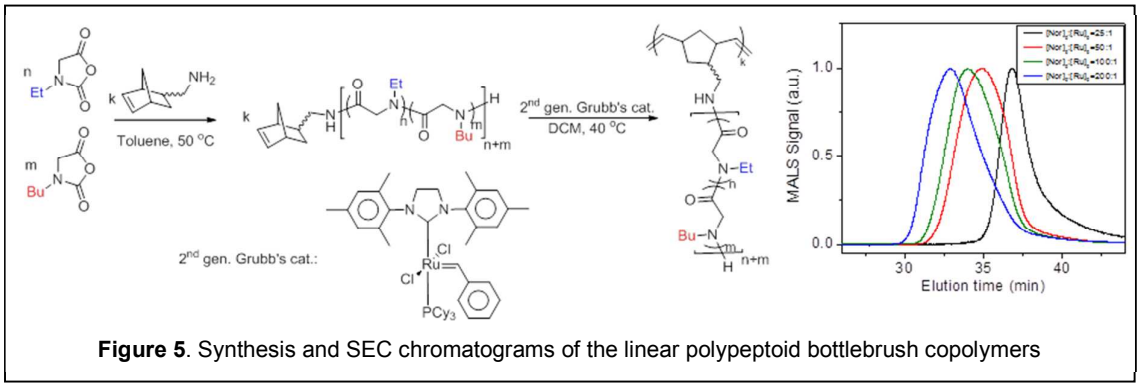

Figure 5. Synthesis and SEC chromatograms of the linear polypeptoid bottlebrush copolymers

Zhang *et al* reported the synthesis of polypeptoid bottlebrushes using a grafting-through approach by combining primary amine-initiated ROP of Et-NCA and Bu-NCA using norbornene methylamine initiator and the ring-opening metathesis polymerization (ROMP) method (Figure 5)[72] The resulting bottlebrush copolypeptoids are thermally responsive with a cloud point transition that is strongly dependent on the thermal history of the solution. Schmidt *et al* recently reported the synthesis of a polysarcosine bottlebrush polymer and core-shell bottlebrush polymers bearing an internal poly(L-lysine) and an external polysarcosine block using polymeric macroinitiators having primary amino groups on the sidechains.[73] The cationic bottlebrush polymers were examined as effective carriers for siRNA delivery with a 70% knock down efficiency of ApoB100 mRNA in AML-12 hepatocytes. Aoi *et al* also reported the synthesis of water-soluble polysarcosine-grafted chitosan and chitin through a grafting-from approach by using high molecular weight chitosan or chitin bearing amino groups as macroinitiators.[74, 75] Due to the poor solubility of the chiotosan and chitin in common

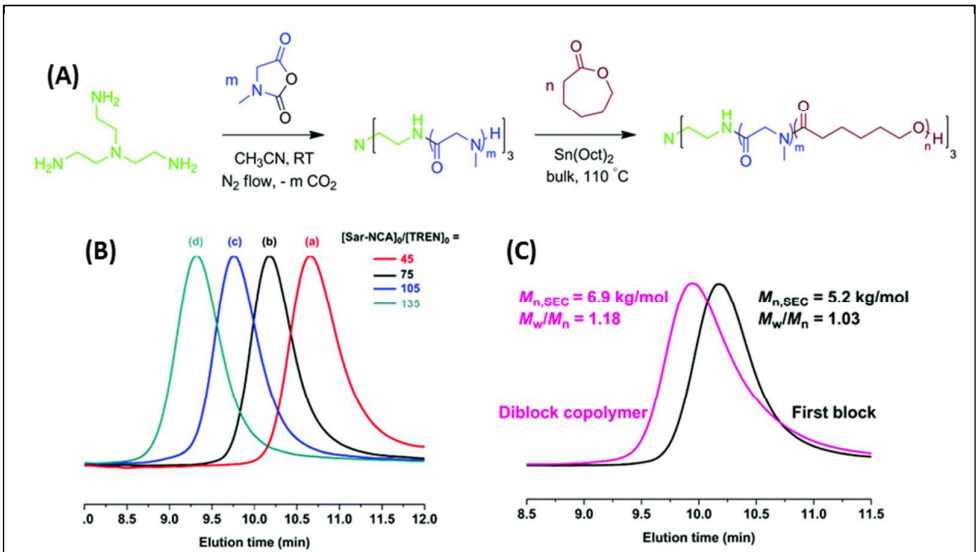

Figure 6. (A) Synthesis of star-shaped polysarcosine and polysarcosine-*b*-poly(ε-caprolactone) block copolymers; (B) SEC-DRI traces of star-shaped polysarcosines with varying molecular weight; (C) SEC-DRI traces of the initial star-shaped polysarcosine and the polysarcosine-*b*-poly(ε-caprolactone) copolymer obtained from the chain extension by the one-pot synthesis.[77] Adapted with permission from John Wiley and Sons.

organic solvent, it was shown that nicotinic or isonicotinic acid has to be added to slow down the polymerization to control the degree of polymerization (DP) and degree of substitution (DS) of the polysarcosine sidechains in the chitosan-*graft*-polysarcosine in DMSO. It was also revealed that the DP and DS of the chitin-graft-polysarcosine affect the molecular recognition of the polymers by the chitinase, lysozyme and WGA (lectin). Okada *et al* reported the synthesis of star-shaped polysarcosine copolymer using a poly(trimethylenimine) (PTMI) dendrimer with 64 primary amino termini as the macroinitiator.[76] The final copolymer was obtained in high yields (91-99%) with low polydispersity (PDI=1.01-1.04) tunable polysarcosine segment length in the DP=2 to 30 range. Guo *et al* has recently reported the one-pot synthesis of three-arm star-shaped polysarcosines and polysarcosine-*block*-poly(ε-caprolactone) copolymers with controlled molecular weight, composition and low polydispersity (PDI<1.1) using *tris*-(2-aminoethyl)amine initiators (Figure 6).[77] The star-shaped polymers have reduced intrinsic viscosity relative to the linear analogs of identical molecular weights, in agreement with the more compact architecture of the former than the latter. Barz *et al* has also investigated the synthesis of three-arm star-shaped polysarcosines and poly(ε-*N*-protected-L-lysine)-*b*-polysarcosine block copolymers using disulfide-containing initiators (Figure 7).[78] Treatment of the star-shaped polymers with glutathione (100 mM) in aqueous solution resulted in the disintegration of the three-armed polymers,

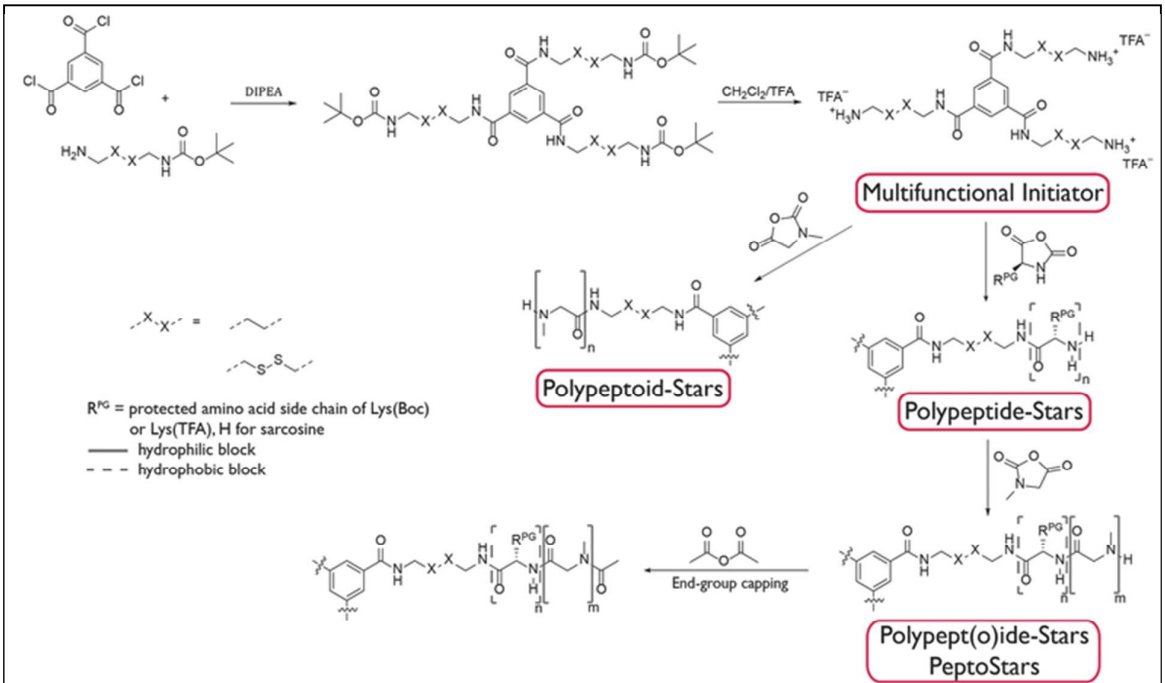

Figure 7. Synthesis of stable and disulfide containing tri-arm star-shaped polysarcosines, poly(ε-*N*-protected-L-lysine) polymers and poly(ε-*N*-protected-L-lysine)-*b*-polysarcosine block copolymers.[78] Adapted with permission from John Wiley and Sons.

yielding the linear arms having Poisson-like molecular weight distributions with low dispersity (PDI = 1.05-1.12).

5. Post-Polymerization Modification of Polypeptoids

The majority of the R-NCA monomers and polypeptoids that have been investigated so far contain either saturated or unsaturated aliphatic *N*-substituent. Post-polymerization represents a valid strategy to increase the *N*-substituent structural diversity. Schlaad *et al* have reported the post-polymerization functionalization of poly(*N*-allyl glycine) (PNAlG)[17] and poly(*N*-propargyl glycine) (PNPgG) via radical thiol-ene chemistry to install different functional moieties (*e.g.*, monosaccharide or glycerol) (Scheme 9).[14] MS analysis indicates quantitative modification of PNAlG via thiol-ene addition chemistry. Poly(*N*-propargyl glycine) homopolymer and copolymer can also been functionalized with azido-containing compounds by CuAAC chemistry. Grafting of low molecular weight ionic or neutral species by CuAAC was efficient with nearly quantitative conversion of the alkyne into the triazole functionality. This has been used to synthesize a library of cationic polypeptoids bearing various *N*-substituents towards gene delivery applications (Scheme 10).[79] Zhang *et al* found that grafting efficiency of polymeric sidechains (*e.g.*, PEG500) was significantly higher for the poly[(*N*-propargyl glycine)-*r*-(*N*-butyl glycine)] [P(NPgG-*r*-NBG)] random copolymer than the PNPgG homopolymer.[69] This was attributed to the strong tendency of PNPgG to

Scheme 9. Post-polymerization functionalization of polypeptoids

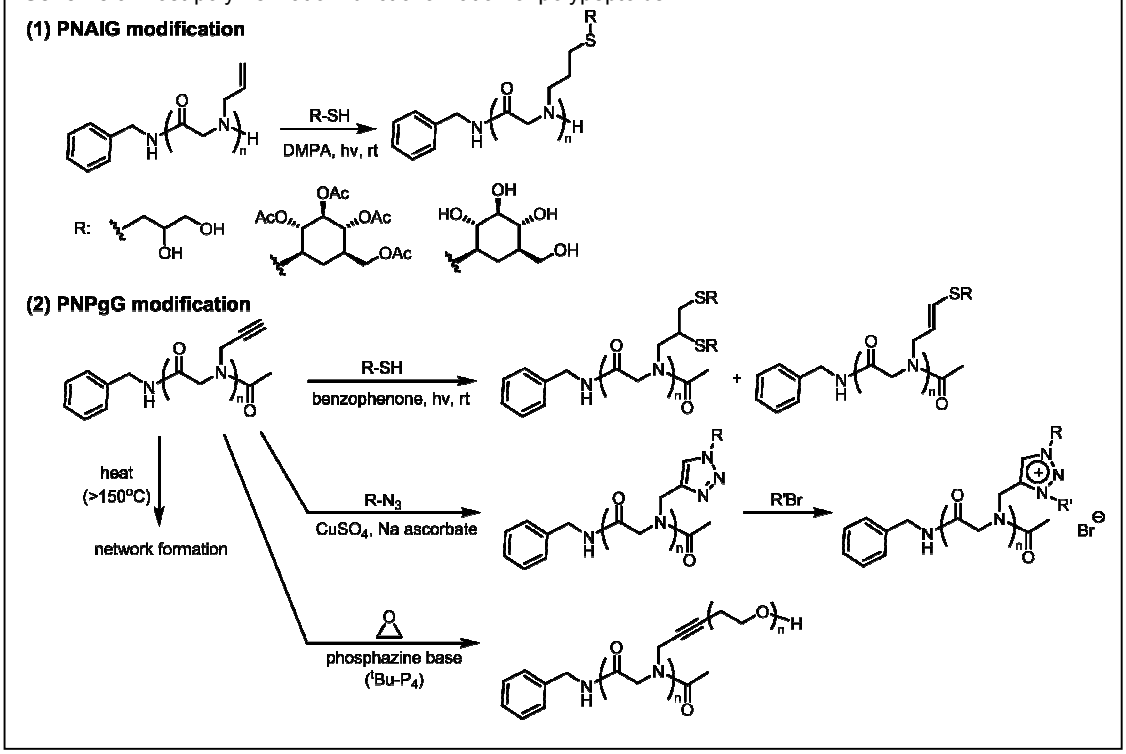

aggregate in solution, limiting the access of the propargyl groups by the azide and Cu catalyst. Schlaad *et al* also reported that the resulting triazole moieties can be further quaternized with alkyl bromide to produce a polypeptoid ionic liquid (Scheme 9).[14] Apart from CuAAC, the propargyl *N*-substituents in PNPgG can also be deprotonated by strong base to initiate anionic ROP of ethylene oxide or serve to crosslink the polymer under heat.[80] The post-polymerization method proves to be an effective strategy to increase the *N*-substituent diversity of polypeptoids.

Scheme 10. Synthesis of a library of cationic polypeptoids bearing different cationic amino groups (**P1**–**P4**), backbone chain lengths (DPs) (**P4–P7**), hydrophobic linker lengths (**P4**, **P8**, **P9**, and **P10**) and incorporation of hydrophobic *N*-substituents (**P11**).[79] Adapted with permission from the American Chemical Society.

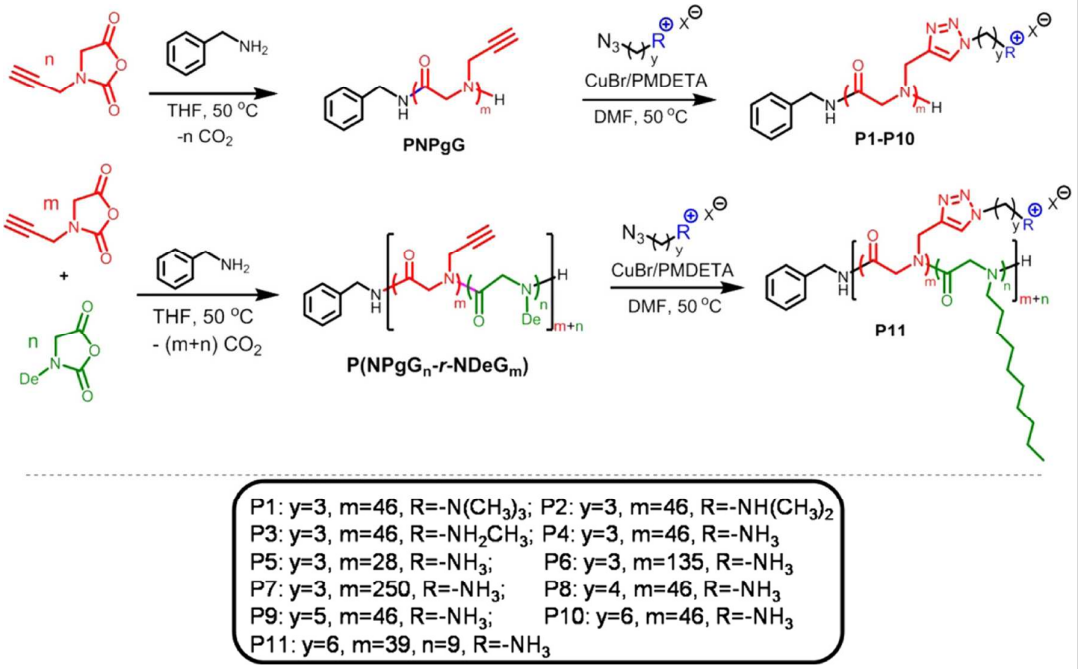

Fundamental Physicochemical Properties

1. Thermal properties of polypeptoids

The thermal properties of the polypeptoid polymers are strongly dependent on the *N*-substituent structures, giving rise to amorphous and semi-crystalline polymers (Figure 8).[20-22,24] Polypeptoids with linear aliphatic *N*-substituents shorter than 2 carbons are amorphous, whereas polymers with longer linear aliphatic *N*-substituents (n=3, 4, 5, 6, 8, 10, 12 and 14) tend to be highly crystalline and pack into lamellar structure in the solid state (Figure 9A).[21,22]Asymmetric branching of the aliphatic *N*-substituents (*e.g.*, 2-ethylhexyl) suppresses the degree of crystallization.[21]

A comparative study of cyclic and linear polypeptoids bearing linear aliphatic *N*-substituents with more than 4 carbons (n=4, 6, 8, 10, 12 and 14) revealed that all polymers exhibited two melting points (T_{m1} and T_{m2}) due to the sidechain and main chain crystalline packing (Figure 9B).[21] The cyclic polymers exhibited higher main chain melting temperature than their linear analogs, whereas the sidechain melting peaks are not affected by the architecture (Figure 9C and 9D). The two modes of chain packing are strongly coupled. Increasing sidechain length causes the sidechain melting temperature to increase and the main chain melting temperature to decrease accordingly for both the linear and cyclic polypeptoids. For polypeptoids bearing short ethyl or 2-ethylhexyl *N*-substituents that do not undergo sidechain crystallization, the main chain crystallization is either completely absent for the former or significantly reduced in the latter.

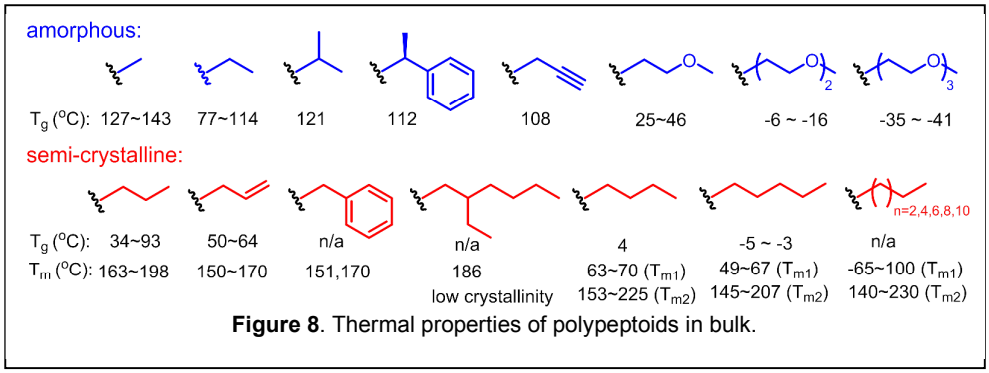

Figure 8. Thermal properties of polypeptoids in bulk.

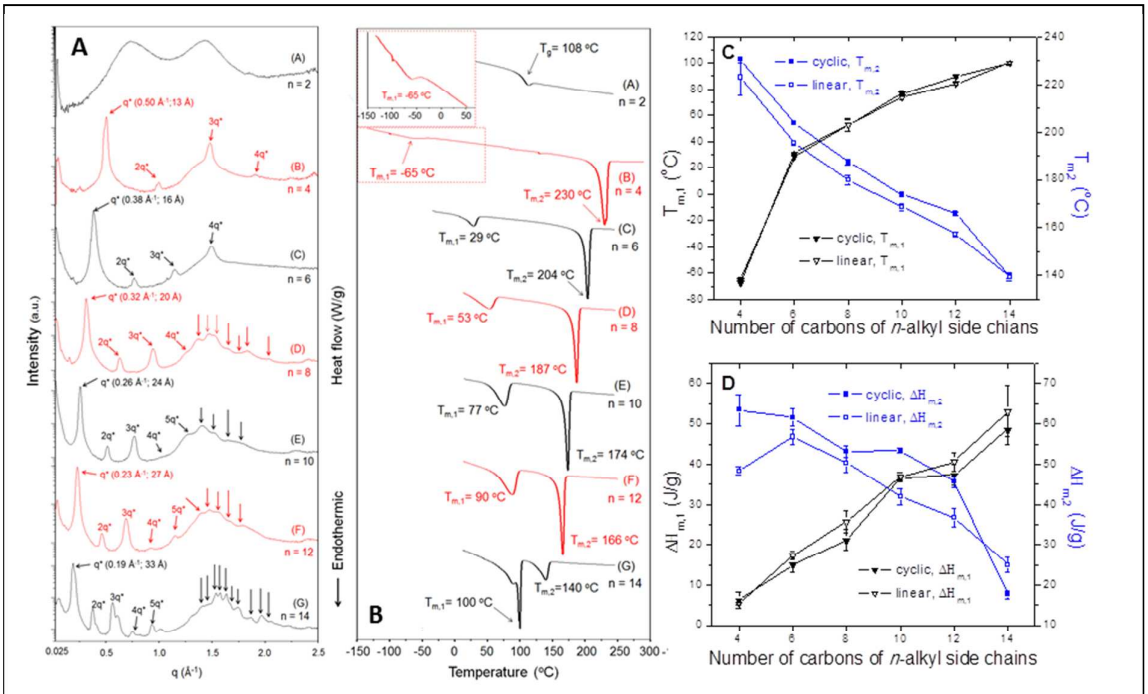

Figure 9. (A) WAXS diffractograms (room temperature) and (B) DSC thermograms (2nd cooling cycle) of cyclic polypeptoids bearing various *n*-alkyl sidechains; (C) plot of T_{m1} and T_{m2} or (D) the associated latent heat (ΔH_{m1} and ΔH_{m2}) versus the number of carbons on the n-alkyl *N*-substituents.

2. Cloud point behaviors of polypeptoid solutions

Polypeptoids have a polar backbone; the overall hydrophilicity and lipophilicity balance (HLB) can be tuned by controlling the *N*-substituent structure. Amphiphilic polymers including polypeptoids often exhibit a reversible temperature-induced cloud point transition where the polymers become dehydrated and undergo hydrophobic collapse with increasing temperature. Polypeptoids bearing methyl, ethyl, or 2-methoxyethyl *N*-substituents have good solubility (20-200 g/L) in water and their aqueous solution do not exhibit cloud point transition.[16,20]

Schlaad *et al* investigated the solution properties of poly(*N*-alkyl glycine) with C3 carbon *N*-substituents.[16] It was found that poly(*N*-propyl glycine) (PNPG), poly(*N*-allyl glycine) (PNAlG) and poly(*N*-isopropyl glycine) (PNiPG) exhibited cloud point (T_{cp}) transitions in water with T_{cp} in the 15-25, 27-54 and 47-58 °C range respectively, depending on the chain length and polymer concentration. Interestingly, the poly(*N*-propargyl glycine)s (PNPgG) also bearing C3 *N*-substituents do not readily dissolve in water. It was also found that prolonged heating of the PNPgG and PNAlG solutions above the respective T_{cp} resulted in the formation of crystalline nanoparticles through the crystallization of the respective polymers in the coacervates.[81]

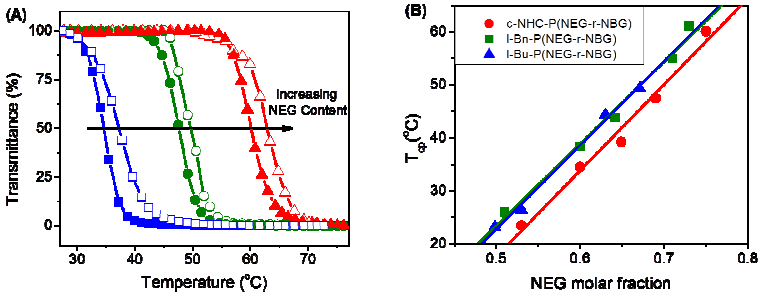

Figure 10. (A): transmittance versus temperature for cyclic P(NEG_{70}-*r*-NBG_{47}) (■,□); cyclic P(NEG_{65}-*r*-NBG_{30}) (●,○) and cyclic P(NEG_{101}-*r*-NBG_{34}) (▲, △) (polymer concentration= 1.0 mg·mL^{-1}; the filled and unfilled symbols designate the heating and cooling cycles respectively. (B) Plots of cloud point temperature (T_{cp}) versus the molar fraction of NEG segment in the cyclic and linear P(NEG-*r*-NBG) random copolymers bearing different end groups and their respective linearly fit curves [cyclic NHC-P(NEG-*r*-NBG) (●, —), linear Bu-P(NEG-*r*-NBG) (▲,—) and linear Bn-P(NEG-*r*-NBG) (■, —)].

The cloud point can also be controlled by copolymerization strategy (Figure 10). Both cyclic and linear poly[(*N*-ethyl glycine)-*r*-(*N*-butyl glycine)] [*c*/*l*-P(NEG-*r*-NBG)] random copolypeptoids have been synthesized by ROPs of the respective R-NCA monomers using either NHC or benzyl or butyl amine initiators and were shown to exhibit cloud point transitions in aqueous solutions.[15] The T_{cp} in the range of 20-60 °C can be readily adjusted by controlling the polymer composition and architecture. Cyclic polypeptoids exhibited lower T_{cp}s than their linear counterparts by 5 °C, which is a result of cyclic polypeptoids forming soluble dimers in water.[82] Linear poly[(*N*-methyl glycine)-*r*-(*N*-butyl glycine)] random

copolymers obtained by primary amine-initiated copolymerization of the corresponding R-NTA monomers also exhibited tunable cloud points.[19]

Bottlebrush copolymers comprised of the linear P(NEG-*r*-NBG) random copolypeptoid sidechains were obtained by ROMP of the norbornene-terminated P(NEG-*r*-NBG) macromonomer (Figure 5).[72] The polypeptoid bottlebrush copolymers also exhibited cloud point transition in aqueous solution similarly to the linear macromonomers. In contrast to the linear macromonomers, the cloud point transition of the polypeptoid bottlebrush copolymers is strongly dependent on the thermal history of the solution (Figure 11).[72] Freshly prepared aqueous solutions of the bottlebrush polymers do not exhibit any notable cloud point transition, whereas the solutions that have been thermally annealed at high temperature exhibit sharp and reversible cloud point transition. Intriguingly, upon inorganic salt addition, the aqueous solutions of the bottlebrush copolypeptoids exhibit normal cloud point transition which is independent of the solution thermal history. It was suggested that the thermal annealing and salt presence facilitated the conformational reorganization of the polypeptoid bottlebrush copolymers to favor hydrophobic collapse and intermolecular aggregation, resulting in a cloud point transition.

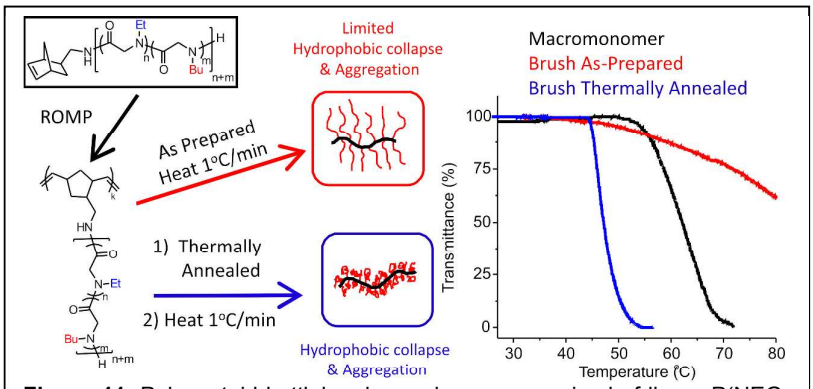

Figure 11. Polypeptoid bottlebrush copolymers comprised of linear P(NEG-*r*-NBG) sidechains exhibited cloud point transitions that are dependent on the thermal history.[72] Adapted with permission from the Royal Society of Chemistry.

Biomedically relevant properties (degradability, cytotoxicity and immunogenicity)

1. Degradability of polypeptoids.

Hydrolytic degradation. Polypeptoids have an *N*-substituted polyglycine backbone with tertiary amide linkages and thus can potentially be hydrolytically broken down. Early studies by Blout *et al* have shown that polysarcosine-*b*-poly(L-proline) copolymer can be hydrolytically degraded into the respective amino acids under highly acidic conditions (6 N HCl, 120 °C, 24 h).[83] We have found that polysarcosine also completely degraded into the corresponding *N*-Me glycine under basic conditions (1.0 M KOH, room temperature, 48 h).[84] It is clear that the polypeptoids can be hydrolytically degraded although the required

conditions are harsh. It is perhaps safe to assume that hydrolytic degradation of polypeptoids in a cellular environment is very slow and minimal.

Enzymatic degradation. Structural variations such as *N*-substitution, incorporation of non-natural amino acid, and homologation are common strategies to develop peptidomimetic therapeutics with enhanced protease resistance. While there has not been any systematic study on the enzymatic degradation of high molecular weight polypeptoids, two early studies by Zuckermann and coworkers on sequence-specific peptoid oligomers revealed that the peptoids cannot be degraded by proteases including carboxypeptidase A, papain, pepsin, trypsin, elastase, and chymotrypsin, in contrast to the peptide analogs that are readily degraded.[25,26] Katchalski *et al* conducted the degradation studies of random copolymers consisting L-proline with D-proline, hydroxyproline, glycine, or sarcosine using proline iminopeptidase.[85] This enzyme is an exopeptidase known to cleave the *N*-terminal L-proline and is widely found in the bacteria and various organs of mammals. For copolymers comprised of L-proline and D-proline or hydroxyproline, the experimentally determined amount of L-proline agrees with the calculation based on exclusive cleavage of bond at the *N*-terminal L-proline and the random distribution of non-L-proline amino acid residue within the polypeptide chain. By contrast, for the copolymer comprised of L-proline and sarcosine, the amount of L-proline was 4.4 times that of the theoretical prediction. This suggests that either the non-L-proline residues are either not randomly distributed along the copolymer chain or the presence of additional sites on this copolymer that can be cleaved by proline iminopeptidase. Blout *et al* has reported that the poly(L-proline) and polysarcosin copolymer have a gradient composition of the two amino acid building blocks with higher content of the sarcosine at the *N*-terminus.[83] Based on these observation, Luxenhofer *et al* made a reasonable hypothesis that proline imminopeptidase may also cleave at the *N*-sarcosine terminus, thus giving rise to increased L-proline content from enzymatic digestion of the copolymer comprised of L-proline and sarcosine.[30]

Oxidative degradation. In cellular environment, oxidative stress can result in significant increase of local concentration of various reactive oxygenated species (ROS), which are widely implicated in various diseased states.[86] Thus, it is important to assess the stability of polypeptoids under oxidative conditions pertinent to an *in vivo* environment. Luxenhofer *et al* recently reported a comparative study on the oxidative degradation of poly(*N*-ethyl glycine), PEG, and poly(2-oxazoline) (POx) using H_2O_2/Cu^{2+} as a source to generate ROS.[27] H_2O_2 together with Cu is known to generate the reactive hydroperoxide ($HOO^{\cdot}$) and hydroxyl ($HO^{\cdot}$) radicals. The degradation studies were conducted in a phosphate buffered saline solution with

a constant initial polymer concentration (1.0 g/L) and $CuSO_4$ concentration (50 μM) and varying H_2O_2 concentration [0.5, 5 or 50 mM (*i.e*, 0.2wt%)]. It was found that all polymers degraded over time with the PEG being significantly more stable than the PNEG and POx at 50 mM H_2O_2 concentration with Cu^{2+} present (Figure 12).[27] Higher H_2O_2 concentration gives rise to faster degradation rate. High molecular weight polymer was shown to degrade faster in terms of percentage molecular weight reduction over time relative to the low molecular weight polymer, which suggest chain scission as a main mode of degradation and that the amine chain ends are presumably more reactive towards oxidation than the amide linkages.

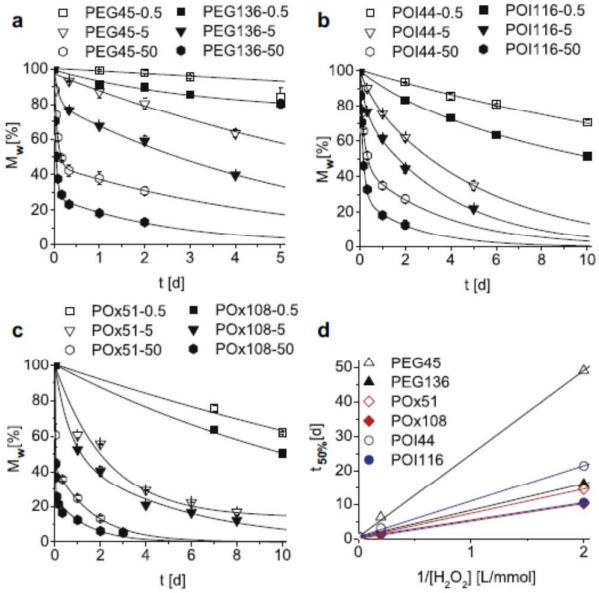

Figure 12. Development of molar masses (a-c) (M_w relative to original M_w) of a) polyethylene glycol (PEG), b) poly(2-ethyl-2-oxazoline) (POx) and c) poly(*N*-ethyl glycine) (POI) upon incubation with 0.5, 5 and 50 mM of H_2O_2 and 50 mM of Cu(II)SO_4 at 37 °C as obtained from SEC elugrams. d) Comparison of determined $t_{50\%}$ (with respect to molar mass M_w) of PEG, POx and POI plotted against 1/[H_2O_2]. Data (a-c) presented as means ± standard error means (SEM) (n=3). Data were fitted with double exponential functions to guide for the eyes.[27] Adapted with permission from Elsevier Limited.

2. Cytotoxicity

Following the recent development of controlled polymerization that enables access to polypeptoids with diverse *N*-substituent structures, a number of water soluble polypeptoids other than polysarcosine and its copolymers has been discovered.[15-20] Several studies have reported the assessment of the cytotoxicity of these polymers. Zhang *et al* synthesized a series of cyclic and linear random copolypeptoids [*c*/*l*-P(NEG-*r*-NBG)] comprised of *N*-ethyl glycine and *N*-methyl glycine repeating units.[15] Cytotoxicity assessment of cyclic P(NEG_{74}-*r*-NBG_{15}) polypeptoid using CellTiter-Blue® assay revealed minimal cytotoxicity of the polymer towards human embryonic lung fibroblasts (HEL229) with 90% or above cell viability in the 0.039-5.0 mg·mL^{-1} polymer concentration range after incubation in PBS buffer at 37 °C for 24 h. This is on par with a low molecular weight poly(ethylene glycol) (PEG, M_n=8.0 kDa), a FDA approved biocompatible polymer. Recently, a series of linear

polypeptoids bearing oligomeric ethylene glycol *N*-substituents (Figure 2) have also been synthesized by benzylamine-initiated ROPs of the corresponding NCAs. Cytotoxicity of the poly(*N*-2-methoxyethyl glycine) (PNMeOEtG) with different molecular weights (3.26−11.1 kg/mol, PDI = 1.04-1.10) has been assessed using human epidermoid cancer (HEp2) cells and an MTT assay. All polymers exhibited minimal cytotoxicity toward HEp2 cells, with greater than 90% cell viability in the 0.0625−1.0 mg/mL polymer concentration range.[20]

Ling *et al* also synthesized a random copolymer comprised of sarcosine and *N*-butyl glycine repeating units from primary amine initiated copolymerization of the corresponding NTA monomers (Me-NTA and Bu-NTA) and evaluated their cytotoxicity using MTT cell viability assay at different polymer concentrations.[19] A series of low molecular weight (M_n=6.5-7.2 kDa, PDI=1.31-1.39) copolypeptoids with different compositions [*i.e.*, P(Sar_{48}-*r*-NBG_{26}) P(Sar_{47}-*r*-NBG_{30}), P(Sar_{42}-*r*-NBG_{36}) and polysarcosine (M_n =5.7kDa, PDI=1.47)] in varying concentrations (0.05-3.0 mg/mL) was incubated with the human heptoblastoma cells (HepG2) at 37 °C for 48 h in DMEM cell culture medium. The relative cell viability was found to be dependent on the polymer composition and concentration. It was found that relative cell viability decreases with increasing polymer concentration for all polymers (Figure 13).[19] P(Sar_{48}-*r*-NBG_{26}) exhibited minimal cytotoxicity (>75% cell viability) at the whole concentration range comparable to that of polysarcosine. P(Sar_{47}-*r*-NBG_{30}) and P(Sar_{42}-*r*-NBG_{36}) showed drastic reduction of percentage cell viability at a 3.0 mg/mL concentration, which has been attributed to the partial precipitation of the polymers at this concentration due to their onset cloud point being close to the incubation temperature.

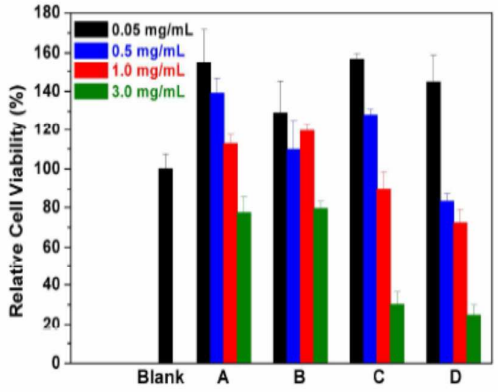

Figure 13. MTT cell viability assay of linear poly(*N*-methyl glycine-*b*-*N*-butyl glycine) random copolymer with different composition (P(Sar48-*r*-NBG26) P(Sar47-*r*-NBG30), P(Sar42-*r*-NBG36)) and polysarcosine at different concentrations.[19] Adapted with permission from the Royal Society of Chemistry.

Luxenhofer *et al* reported the cytotoxicity assessment of polysarcosine homopolymer [M_n =3.7 kDa (NMR), PDI=1.31] and several amphiphilic diblock or triblock copolypeptoids comprised of polysarcosin and poly(*N*-propyl glycine) or poly(*N*-pentyl glycine) segments [M_n=4.2-7.8 kDa (NMR), PDI=1.09-1.32]. [87]The polymers in different concentration (0.01-10 mg/mL below CMCs) was incubated with HepG2 cells in DMEM medium for 24 h. WST-1 assay revealed minimal cytotoxicity with 90% or above cell viability for all polymers. In

comparison, Barz *et al* evaluated the cytotoxicity of tri-arm star-shaped polysarcosines having different arm lengths in several cell lines [*i.e.*, HeLa, human embryonic kidney cells (HEK 293) and murine dendritic cells (DC 2.4)],[78] the cytotoxicity is notably higher than those reported by Luxenhofer *et al* for the linear polysarcosines.[87] While IC_{50} value was not reached in the investigated concentration range (0.1-1 mg/mL) for all samples, reduction of cell viability was found to occur in a cell-line dependent manner.[78] For example, the tri-arm star-shaped polysarcosine (arm DP=25) at 1.0 mg/mL concentration reduced the HEK 293 cell viability to 56% in comparison to 65-80% cell viability for HeLa and DC 2.4 cells. The tri-arm polysarcosine with longer arms (arm DP=100) appears to be less cytotoxic than its counterpart with shorter arms (DP = 25), giving rise to cell viability in the 80-100% range for HEK 293, DC 2.4 and the 65-80% range for HeLa cells at 1.0 mg/ml polymer concentration. The dependence of cell viability on the cell type was tentatively attributed to the difference in cell metabolism and robustness.

Zhang *et al* recently also reported the cytotoxicity assessment of core-crosslinked polypeptoid micelles with poly(*N*-ethyl glycine) (PNEG) corona and poly[(*N*-propargyl glycine)-*r*-(*N*-decyl glycine)] [P(NPgG-*r*-NDG)] core that was crosslinked with either a redox-responsive disulfide containing crosslinker (CCLM) or a non-redox responsive permanent crosslinker (ICCLM, Scheme 12, *vide infra*). [88] Both polypeptoid micelles exhibited no or minimal cytotoxicity with 95% or above cell viability towards HepG2 cells (Figure 14A) after incubation for 48 h in MEMS medium in the 0.01-1.0 mg/mL concentration range, as determined by MTT assay. Doxorubicin (DOX) loaded micelles exhibited time and dosage dependent cytotoxicity towards HepG2 cells (Figure 14B and 14C). DOX-loaded ICCLM also exhibited cytotoxicity at a reduced level relative to the DOX-loaded CCLMs with a 100 μg/mL IC_{50} for the former and 40 μg/mL for the latter. This suggests the release of DOX from ICCLMs presumably through polymer degradation in the

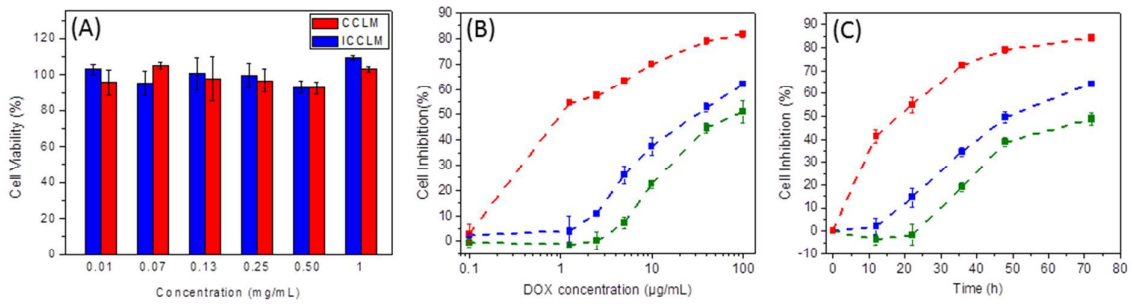

Figure 14. (A) MTT assays to assess the cytotoxicity of CCLMs and ICCLMs based on $E_{204}Pg_{13}D_{15}$ block copolypeptoids. (B) The plots of percentage cell inhibition versus DOX concentration and (B) time-resolved cytotoxicity at 40 μg·mL^{-1} equivalent DOX concentration for the DOX-loaded CCLMs (■), DOX-loaded ICCLMs (■) and free DOX·HCl (■). HepG2 cells were used in the study.

cellular environment. The higher cytotoxicity of DOX-loaded CCLMs relative to the DOX-loaded ICCLMs is attributed to the cleavage of the disulfide crosslinking sites under reductive environment in HepG2 cells, thereby enabling more efficient release of DOX and resulting in more HepG2 cell death from the CCLMs than the ICCLMs.

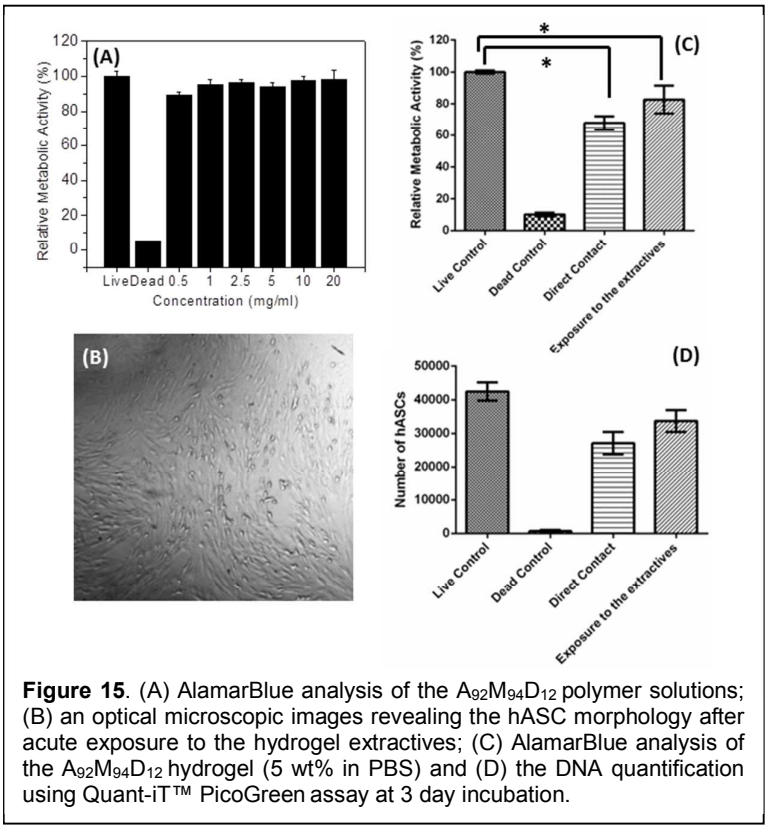

Figure 15. (A) AlamarBlue analysis of the $A_{92}M_{94}D_{12}$ polymer solutions; (B) an optical microscopic images revealing the hASC morphology after acute exposure to the hydrogel extractives; (C) AlamarBlue analysis of the $A_{92}M_{94}D_{12}$ hydrogel (5 wt% in PBS) and (D) the DNA quantification using Quant-iT™ PicoGreen assay at 3 day incubation.

Another study reports the cytotoxicity assessment of amphiphilic ABC triblock copolypeptoid ($A_{92}M_{94}D_{12}$) comprised of a thermo-responsive PNAlG block with cloud point transition, hydrophilic PNMG middle block and hydrophobic PNDG end block in dilute polymer solution or as hydrogel. [89] Alamarblue assay revealed no cytotoxicity towards human adipose derived stem cells (hASCs) in the dilute polymer solutions in the 0.5-20 mg/mL range (Figure 15A). The polymer solution forms hydrogel at 5 wt% at 37 °C. AlamarBlue assay was further used to investigate the effect of ABC hydrogel on hASCs metabolic activity. It was found that the relative metabolic activity of hASCs decreased significantly (P-value < 0.05) compared to the control sample after 24 h culturing in the ABC hydrogel extractives or 3 d culturing within the hydrogel matrix in direct contacting (Figure 15C). Quantification of the corresponding total DNA content by Quanti-T™ PicoGreen® assay indicated no significant inhibition of hASC proliferation compared to the live control when hASCs were exposed to the ABC hydrogel extractives for 24 h or directly cultured within the

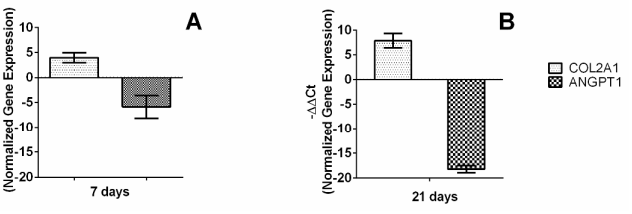

Figure 16. QPCR analysis of gene expression within the $A_{92}M_{94}D_{12}$ triblock copolypeptoid hydrogel matrix.

hydrogel matrix for 3 d (Figure 15D). Moreover, hASC maintained a healthy spindle shape both when exposed to hydrogel extracts and cultured within hydrogel matrix (Figure 15B). The results indicated that the slight decrease of cells proliferation rate does not correlate with a decrease in metabolic activity and may be indicative of stem cells leaving the proliferative cell cycle to differentiate. The differentiation pathway of hASCs happened within the hydrogel matrix was further investigated by the quantitative real-time polymerase chain reaction (QPCR) analysis (Figure 16). The expression of two marker genes, *Col2a1* and *ANGPT1*, for chondrogenesis and endotheliogenesis respectively, was quantified by QPCR after 7 and 21 d incubation point. It was shown that the expression of *Col2a1* gene was upregulated and that of *ANGPT1* gene was down-regulated, suggesting hASCs may have committed to chondrogenesis pathway. These results suggest the potential use of polypeptoid hydrogel as benign scaffold biomaterials for stem cell based tissue repair.

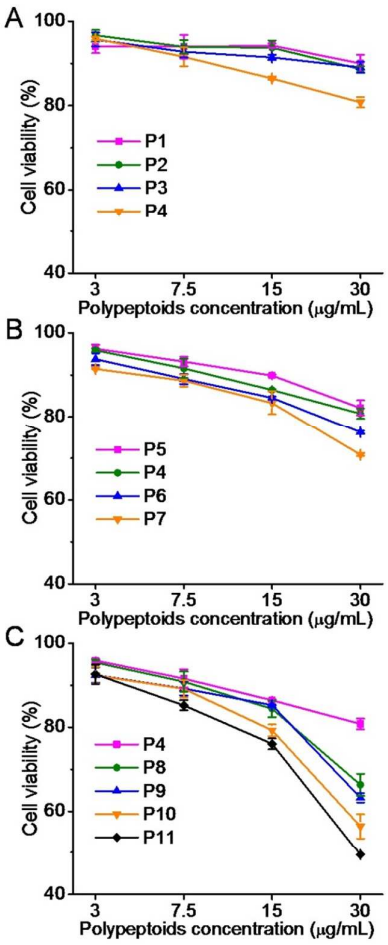

Figure 17. Cytotoxicity of cationic polypeptoids at various concentrations in HeLa cells as determined by the MTT assay (n = 3). (A) Polypeptoids with different cationic amino structures; (B) polypeptoids with different backbone chain length; (C) polypeptoids with different hydrophobic linker lengths and incorporating hydrophobic decyl group on the *N*-substituents.[79] Adapted with permission from the American Chemical Society.

Polypeptoids in the above cytotoxicity studies are all charge-neutral. Once polypeptoids are rendered positively charged, their cytotoxicities are notably enhanced due to the increase of their membrane activities. For example, a library of cationic polypeptoids with varying backbone length, cationic *N*-substituent structure and incorporation of hydrophobic *N*-substituents have been synthesized and investigated towards the gene delivery applications (Scheme 10, *vide supra*). Cytotoxicity of the cationic polypeptoids towards HeLa cells were assessed using MTT assay in the 3-30 μg/mL polymer concentration range (Figure 17).[79] The cytotoxicity of the polypeptoids was found to increase with an elevation of polymer concentration. **P4** bearing primary amine groups showed higher cytotoxicity than its analogs containing secondary, tertiary, and quaternary amines (**P1**, **P2**, and **P3**,

Scheme 10). Polypeptoids with longer backbone length exhibited higher cytotoxicity in the order of **P5** (28 mer) < **P4** (46 mer) <**P6** (135 mer) < **P7** (250 mer). Enhancing the *N*-substituent hydrophobicity also contributed to elevated cytotoxicity, as reflected in the order of **P4** < **P8** < **P9** < **P10** having increasingly elongated hydrophobic linker length between triazole and amino groups on the sidechains. Consistently, **P11** with pendent decyl groups also displayed higher cytotoxicity than its homopolymer analog **P10** at high concentrations. Hydrophobic modification on the *N*-substituents has been known to effectively promote interaction of charge-neural polypeptoids with lipid membranes.[90] These results indicate that excessively high membrane activities can cause irreversible damage to cells. Transfection studies have shown that cationic polypeptoids bearing a primary amino group (**P4**) exhibited significantly higher transfection efficiency than that of its analogs containing secondary, tertiary or quaternary amino groups. Elongation of polypeptoid backbone length from DP = 28 to 251 has resulted in enhanced DNA condensation and cellular uptake level at the cost of increased cytotoxicity. Elongation of the hydrophobic linker length on the cationic *N*-substituents or incorporation of hydrophobic *N*-substituents also significantly enhanced the transfection efficiency presumably due to increased membrane activities. Based on the above transfection and cytotoxicity results, it is concluded that a proper balance between membrane activities and cytotoxicity is required to achieve maximal transfection efficiency, and the excessive membrane activities would decrease rather than increase the transfection efficiency by compromising the cell viability and transcription/translation functions. As such, a cationic polypeptoid random copolymer (DP = 46) bearing 80 mol% cationic *N*-substituents with primary amino groups and 20 mol% *N*-decyl substituents (**P11**, Scheme 10) was identified to exhibit the most optimal gene transfection efficiency.[79] The polymer out-performed the commercial transfection agent poly(ethylenimine) (PEI) by four orders of magnitude in serum-containing

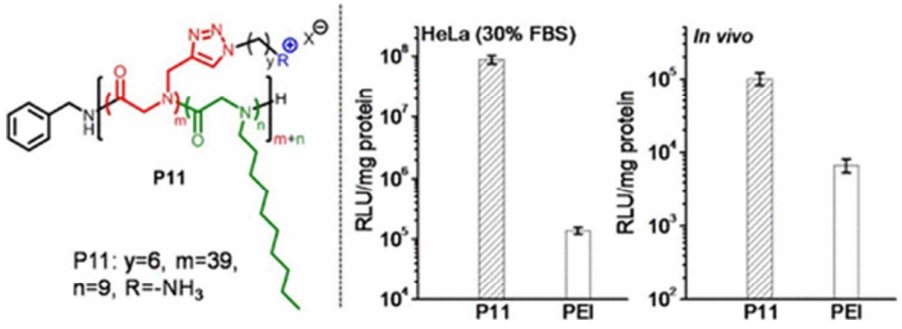

Figure 18. (Left) chemical structure of **P11**; (middle) transfection efficiencies of polyplexes based on **P11** or PEI in HeLa cells with 30% FBS serum (n = 3); (right) *in vivo* transfection efficiencies of polyplexes based on **P11** following intratumoral injection in B16F10 xenograft tumor-bearing mice at 40μg DNA/mouse (n = 4).[79] Adapted with permission from the American Chemical Society.

conditions (Figure 18). Following intratumoral injection to melanoma-bearing mice, **P11** also produced higher effective gene transfection than PEI *in vivo* (Figure 18).[79]

3. Immunogenicity

Low immunogenicity has been indicated for polysarcosine in several different animal models[91,92] Maurer investigated antigenicity of several synthetic homo-polypeptides and copolypeptides and found that all homo-polypeptides including polysarcosine (M_n=3.5kDa) and poly(L-proline) (M_n=50kDa) to be non-antigenic in rabbits using passive cutaneous anaphylaxis (PCA) test.[91] Only one copolypeptide (M_n=38 kDa) comprised of L-glutamic acid and L-lysine in a 6:4 molar ratio was found to be antigenic. Moran *et al* reported the synthesis of the conjugates of polysarcosine with grass pollen allergen extracts.[93] It was found that the conjugate can efficiently suppress the induction of IgE responses in mice. The suppression is allergen-specific and requires covalent linking of the polysarcosine to the allergen.[94] The reduced IgE response was transient[95] and was attributed partly to a short-lived antigen-specific T cell suppression.[96] It was further demonstrated that intranasal application of the conjugate can reduce the serum IgE antibody response that was brought about through exposure to the grass pollen extract,[97] providing a method to treat allergy. Kimura *et al* found that immune response of nanoparticles with identical hydrophilic polysarcosine corona depends on the grafting density of the hydrophilic polysarcosine.[92,98] Spherical micelles (d=36 nm) based on AB type amphiphilic block copolymer [*i.e.*, polysarcosine$_{64}$-*b*-poly(L-lactic acid)$_{30}$] were rapidly captured by the liver upon second administration[99] and cleared from the bloodstream, whereas the micelles (d=22 nm) based on A_3B type polymers [*i.e.*, (poly(sarcosine)$_{23}$)$_3$-*block*-poly(l-lactic acid)$_{30}$] with high grafting density of polysarcosine blocks showed *in vivo* disposition by accumulating in the tumor region similar to that of at the first administration.[92] This has been attributed to the significantly reduced interaction of the micelles with densely grafted polysarcosine corona with the B lymphocyte receptors and hence the suppression of antibody production. It was also found that the polymeric micelles are T cell-independent antigen that can trigger antigen production without the help of T cells[100] and the polysarcosine was found to be the epitope from the competitive inhibition assay (ELISA).[99]

In spite of these reports on polysarcosine, the immunogenicity of other polypeptoids with different *N*-substituent structures or compositions are unknown. As a result, one should be cautioned about making generalization about the immunogenicity of polypeptoid polymers. This area represents a fertile ground for research, as it will provide fundamental

understanding of the interactions between polypeptoids and immune systems, which is critical for the further development of polypeptoid biomaterials for *in vivo* applications.

Solution aggregation of polypeptoid copolymers

Self-assembly of block copolymers into various nanostructures (*e.g.*, micelles, vesicles, network, *etc.*) in solution can be utilized towards a variety of applications. A number of amphiphilic or double-hydrophilic hetero-block or graft copolymers comprised of water-soluble polysarcosine segments (PNMG) have been synthesized and their solution aggregation studied. Examples include PNMG-*b*-polypeptides [*i.e.*, poly(ε-*N*-benzyloxycarbonyl-L-lysine), [101] poly(γ-benzyl-L-glutamate),[101] poly(γ-*tert*-butyl-L-glutamate), [102] and poly(*S*-ethylsulfonyl-L-cystine)], [103] PNMG-*b*-poly(ε-caprolactone), [104] PNMG-*b*-poly[2-(3-butenyl)-2-oxazoline],[57] PNMG-*b*-(Leu-Aib)$_n$ [(Leu-Aib)$_n$: helical peptides], [105 - 112] PNMG-*b*-poly(L-lactide) (AB, A_2B, A_3B types), [113] dextran-*b*-PNMG, [114] PEG-*b*-PNMG[42] and $C_{n=12-18}$-PNMG lipopolymers.[115-117] Their solution aggregation behavior has been reviewed by Luxenhofer *et al* [30] and will not be repeated here. We will highlight several recent examples of block copolypeptoid-based solution aggregates, particularly those that exhibit stimuli-responsive characteristics in dilute or semi-dilute solutions.

Luxenhofer *et al* reported the solution aggregation of linear diblock and triblock copolypeptoids comprised of the hydrophilic polysarcosine segment (DP=~50) and the poly(*N*-alkyl glycine) segment with C2-C5 linear aliphatic *N*-substituents in water.[87] Micellation was observed for the diblock copolymers when the linear alkyl chain has 3, 4, or 5 carbons with the critical micellation concentration (CMC) in the 0.6 μM to 0.1 mM range. The tendency to form micelles was found to increase with increasing hydrophobicity or chain length of the solvophobic poly(*N*-alkyl glycine) segment. The aggregate size and distribution are strongly dependent on the temperature and solvent. In general, the aggregate sizes are smaller in buffer (pH=7.4) than in water. Further studies on the self-assembly of block copolymers consisted of polysarcosine and poly(*N*-butyl/pentyl glycine) or poly(*N*-benzyl/2-phenylethy glycine) in water revealed a wide range of nanostructure morphologies including worm-like micelles, vesicles, oligolamellar nanostructures and their formation is strongly dependent on the polymer composition and sample preparation methods.[118]

Redox-responsive polypeptoid aggregates. Barz *et al* reported the synthesis of amphiphilic polysarcosine-*b*-poly(γ-*tert*-butyl L-glutamic acid) diblock copolymers where the solvophilic and hydrophobic segments are connected by a redox responsive disulfide-bearing linker.[102] A bifunctional initiator was used to polymerize the corresponding γ-*tert*-butyl L-glutamic acid NCA and Me-NCA (Scheme 11). The polymer forms micelles in water which gradually disintegrate in contact with glutathione (GSH: 10-100 mM) over time. The micelles are stable in the medium at low GSH concentration (10 μM).

Scheme 11. Synthesis of redox-responsive PNMG-*b*-PGlu(OtBu)

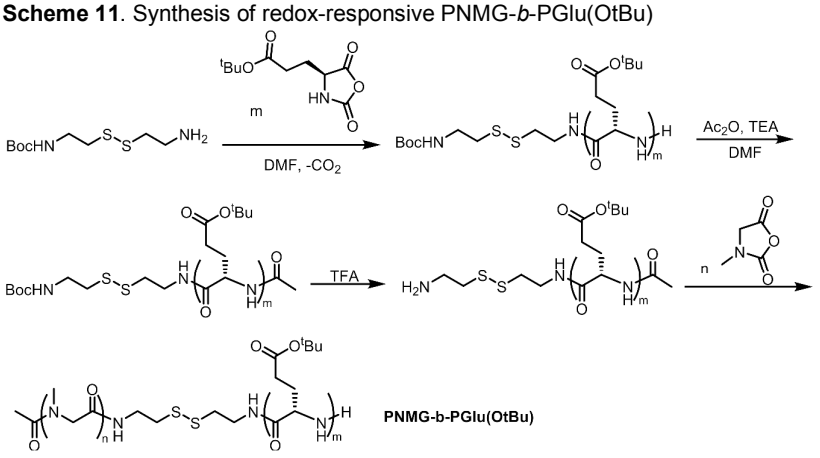

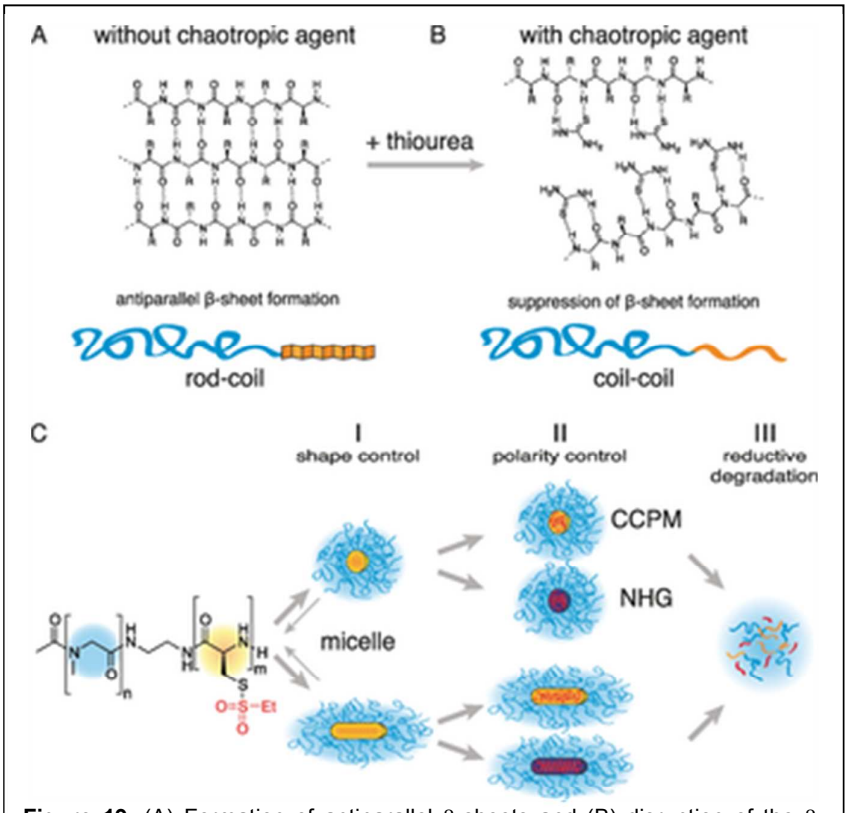

Figure 19. (A) Formation of antiparallel β-sheets and (B) disruption of the β-sheets by thiourea; (C) proposed synthetic system featuring the following phases: I) self-assembly of amphiphilic PSar-*b*-PCys(SO_2Et) block copolymers into different micellar morphologies directed by secondary structure alignment; II) subsequent core cross-linking by disulfides of choice, yielding core-cross-linked polymeric micelles (CCPMs) or nanohydrogels (NHGs); III) disintegration of the system upon a reductive stimulus.[103] Adapted with permission from the Wilev-VCH.

One recent study of the polysarcosine-*b*-poly(*S*-ethylsulfonyl-L-cystine) diblock copolymer [$(PSar)_n$-*b*-$(PCys(SO_2Et))_m$] revealed an intriguing secondary-structure directed self-assembly into different core-shell

nanostructures (*i.e.*, spherical or worm-like micelles) in aqueous buffer solution (Figure 19).[103] Poly(*S*-ethylsulfonyl-L-cystine) segment has intrinsic tendency to form anti-parallel β-she ets, which can be disrupted by the addition of chaotropic agents (*e.g.*, thiourea) to form random coils. The $(PSar)_{407}$-*b*-$[PCys(SO_2Et)]_{28}$ sample having a 15 wt% of the hydrophobic segment ($PCys(SO_2Et)$) was found to form worm-like micelles in aqueous solution in the absence of thiourea, a result attributed to the anti-parallel β-sheet formation in the hydrophobic core. In the presence of thiourea, the block copolymer formed spherical micelles as expected for the coil-coil block copolymer based on their composition. For the $(PSar)_{265}$-*b*-$(PCys(SO_2Et))_{17}$ sample that also has a 15wt% hydrophobic segment but a shorter $PCys(SO_2Et)$ segment, a mixture of spherical and worm-like micelles were observed in the absent of thiourea, whereas spherical micelles were found in the present of thiourea. For the $(PSar)_{97}$-*b*-$(PCys(SO_2Et))_{15}$ that has 30 wt% hydrophobic segment, only worm-like micelles were found with or without thiourea present. It was further demonstrated that addition of neutral or cationic dithiols to the micelles led to the formation of core-crosslinked micelles or nanohydrogels where the pre-crosslinked micellar morphologies are retained (Figure 20A and 20B).[103] The polarity of the micellar core can also be fine-tuned without affecting the micellar size by using various lipoic acid-derived cross-linkers in conjunction with equimolar tris(2-carboxyethyl)phosphine (TCPE) (Figure 20C and 20D).[103] The core-crosslinked micelles or nanohydrogels can be disintegrated in the

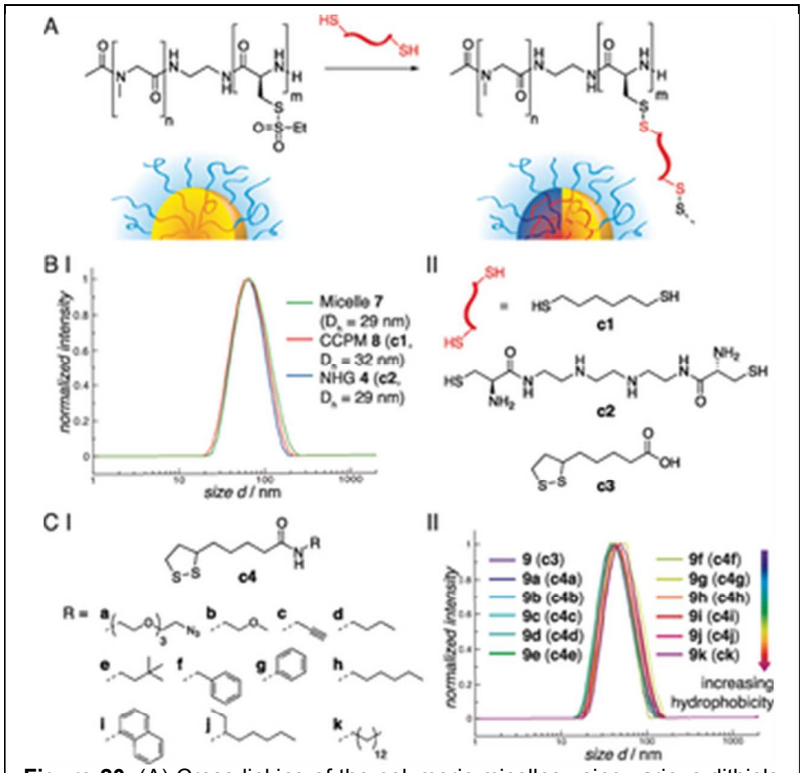

Figure 20. (A) Cross-linking of the polymeric micelles using various dithiols to afford core-crosslinked polymeric micelles (CCPMs, yellow core) and nanohydrogels (NHGs, blue core); (B-I) the particle size remains constant in the presence of various cross-linkers (II) while the core functionality is changed; (C-I) adjusting the core polarity of CCPMs with lipoic acid derived cross-linkers with various side chains without affecting the particle size.[103] Adapted with permission from the Wiley-VCH.

presence of reductive stimuli (*e.g.*, glutathione), highlighting the potential for drug or gene delivery applications.

Zhang *et al* reported the synthesis of a series of linear amphiphilic block copolypeptoids (*i.e.*, poly(*N*-ethyl glycine)-*b*-poly[(*N*-propargyl glycine)-*r*-(*N*-decyl glycine), $E_nPg_mD_k$]) by sequential ROPs of the corresponding R-NCA monomers using benzyl amine initiators (Scheme 12).[88] The polymers form micelles in aqueous solution with critical micellation concentrations (CMC) in the 91-133 µg/mL range at room temperature (22-23°C). Selected samples (*e.g.*, $E_{204}Pg_{13}D_{15}$, the subscript signifies the DP of each segment) form well-defined spherical micelles (NCLMs) in aqueous solution and were then core-crosslinked with two different crosslinkers (CLs) by CuAAC chemistry (Scheme 12). One crosslinker bears a

Scheme 12. Synthesis of redox-responsive and core-cleavable or non-core-cleavable micelles based on amphiphilic block copolypeptoids PNEG-*b*-P(NPgG-*r*-NDG).

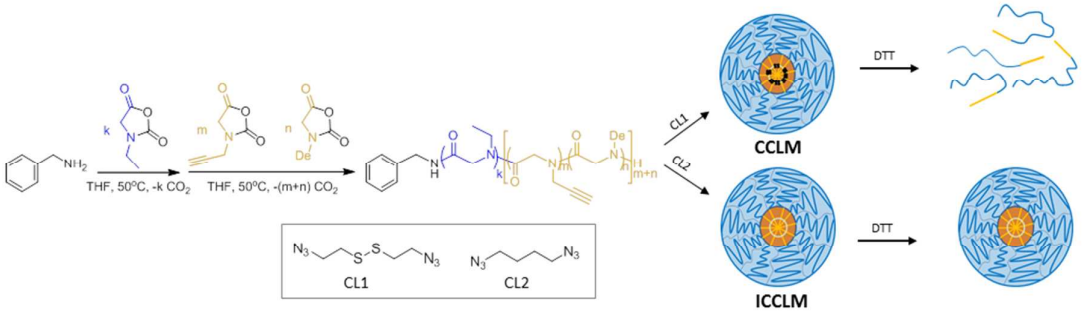

disulfide linkage which can be clea ved by appropriate reducing agents (*e.g.*, dithiothreitol, DTT) and the other does not (Scheme 12). DLS analysis of the core-crosslinked micelles (CCLMs) bearing disulfide linkages revealed that the micelles maintain a mono-modal size distribution in water. The hydrodynamic diameter of the CCLMs is notably decreased to 42.4 ± 0.8 nm as compared to the non-crosslinked micelle precursors (NCLMs) (d = 60.1 ± 0.9 nm) (Figure 21A). In DMF which is a non-selective solvent, the CCLMs became swelled but maintained the micellar structure (d = 59.2 ± 1.6 nm, PDI = 0.19) due to the covalent crosslinking in the micellar core. By contrast, the NCLMs become destabilized in dilute DMF solution, resulting in an increase of the hydrodynamic size, broadening of the size distribution (PDI = 0.41) and the appearance of unimers in the DLS analysis (Figure 21A). TEM analysis of both dried and uranyl acetate-stained CCLMs and NCLMs revealed the presence of mostly spherical micelles with some short cylinders, indicating that covalent crosslinking in the micellar core did not significantly alter the micellar morphology (Figure 21B). The average diameter of the CCLMs (21.1 ± 2.3 nm) is comparable to that of the NCLMs (22.8 ± 2.9 nm) in the dry state.

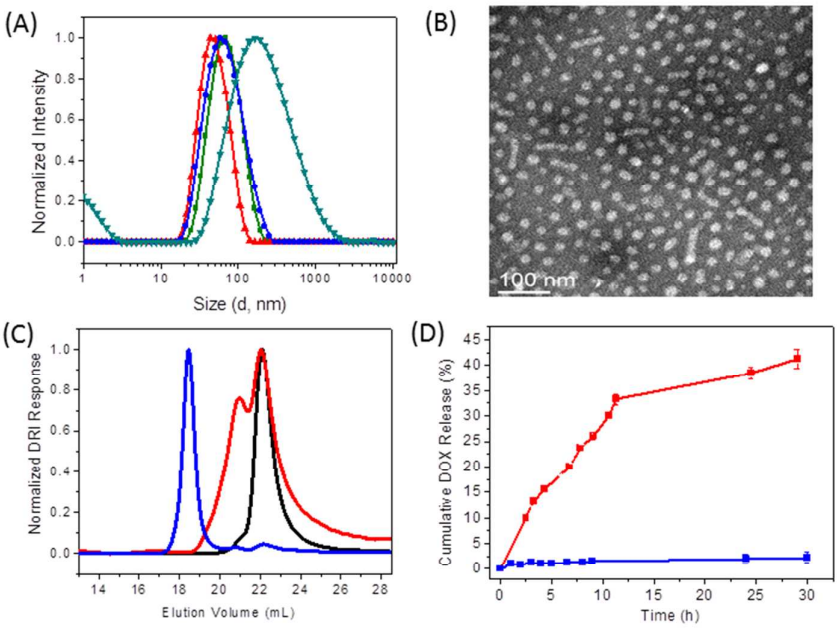

Figure 21. (A) DLS size distribution of the $E_{204}Pg_{13}D_{15}$-based NCLMs in water (-■-) or DMF (-▼-) and the corresponding CCLMs in water (-▲-) or DMF (-●-). The micellar solutions in water or DMF are kept at 0.5 mg·mL^{-1} or 0.05 mg·mL^{-1} respectively in the DLS studies. (B) TEM micrograph of the CCLMs based on the $E_{204}Pg_{13}D_{15}$ block copolypeptoids (stained with uranyl acetate). (C) SEC chromatograms of the $E_{204}Pg_{13}D_{15}$ unimer (—) and the corresponding CCLMs before (—) and after DTT treatment (—) in DMF/ 0.1 M LiBr. (D) Plots of cumulative percentage DOX release over time from the CCLMs with DTT (10 mM) (-■-) or without DTT presence (-■-).

The CCLMs bearing disulfide linkages were used to encapsulate hydrophobic molecules including fluorescent dye (1-anilinonaphthalene-8-sulfonic acid (1,8-ANS) or doxorubicin (DOX), a hydrophobic anticancer drug. A maximal 23% drug loading capacity and a 37% drug loading efficiency was obtained for DOX encapsulation. Upon in contact with DTT, the CCLMs were shown to disintegrate (Figure 21C) and release the DOX in a time-dependent manner (Figure 21D). Without DTT present, DOX release from CCLMs is minimal even after 30 h, strongly attesting to the effect of CCLM's destabilization via the cleavage of the disulfide crosslinkers by DTT on the drug release.

Temperature-responsive polypeptoid aggregates. A series of cyclic and linear amphiphilic block copolypeptoids poly(*N*-methyl glycine)-*b*-poly(*N*-decyl glycine) (*c*/*l*-PNMG-*b*-PNDG) bearing an amorphous solvophilic PNMG segment and a crystalline solvophobic PNDG segment have been synthesized by organo-mediated ROP of the corresponding R-NCA monomers using either NHC or benzyl amine initiators.[68] In dilute methanol solution at room temperature, the cyclic $PNMG_{105}$-*b*-$PNDG_{10}$ and linear $PNMG_{112}$-*b*-$PNDG_{16}$ were shown to form well-defined spherical micelles upon dissolution. The spherical micelles transformed into cylindrical micelles with uniform diameter and the length gradually increasing to microns over a period of 15 d (Figure 22). The cyclic micelles were shown to undergo the morphological transition at a faster rate than their linear analogs. The

morphological transition was attributed to the sidechain crystallization of the PNDG segment in the cylindrical micellar core, whereas no crystallization was observed in the spherical micelles. Upon heating above the melting temperature of the PNDG segment (58 °C), the cylindrical micelles reverse back to the spherical micelles. At semi-dilute concentration,[119] the polymer form gels comprised of entangled crystalline fibrils, which upon heating above the PNDG sidechain melting temperature, reverse to a solution due to the transformation of the cylindrical micelles back to the spherical micelles. The cyclic gels were shown to contain higher crystalline domains in the gel than the linear analogs, giving rise to enhanced gel stiffness. The thermo-reversible sol-gel transition was found to occur in a number of alcohol solvents (*e.g.*, methanol, ethanol, isopropanol).

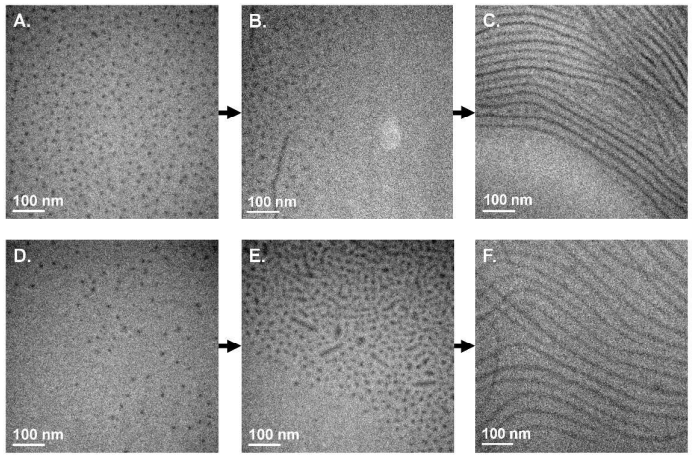

Figure 22. Cryo-TEM images obtained from dilute methanol solutions of the *c*-PNMG$_{105}$-*b*-PNDG$_{10}$ block copolypeptoid after 1 h (A), 2 h (B), and 15 d (C) in methanol and the linear counterpart (*l*-PNMG$_{112}$-*b*-PNDG$_{16}$) (D: 1h; E: 2h; F: 15 d).

Zhang *et al* reported the synthesis of a series of amphiphilic linear ABC triblock copolypeptoids bearing a hydrophobic, a hydrophilic, and a thermo-responsive segment (PNAlG) by sequential ROPs of the corresponding R-NCA monomers using benzyl amine initiators

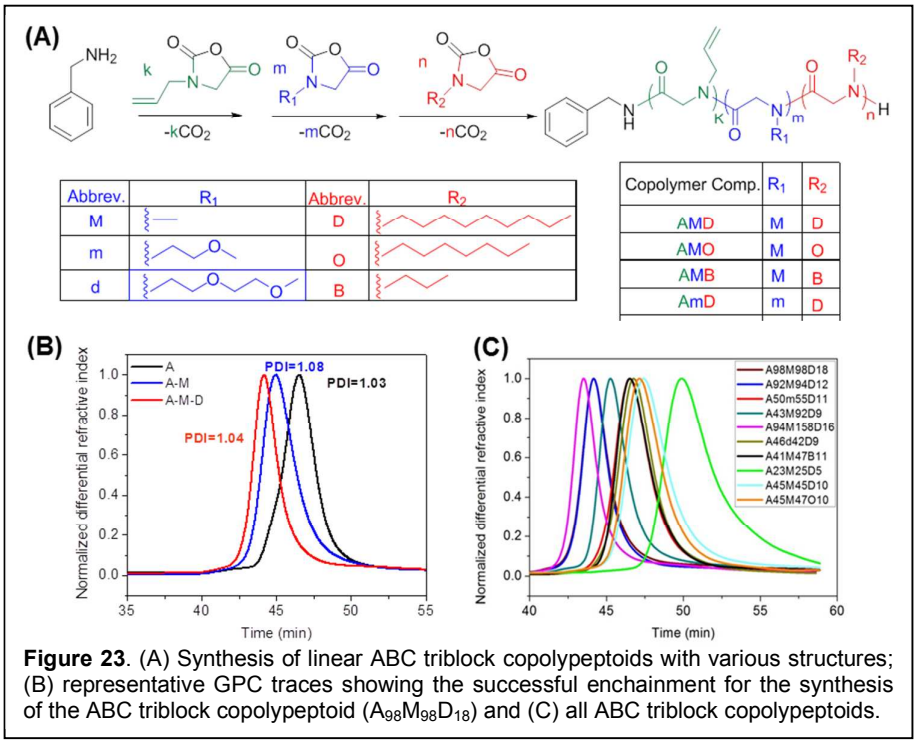

Figure 23. (A) Synthesis of linear ABC triblock copolypeptoids with various structures; (B) representative GPC traces showing the successful enchainment for the synthesis of the ABC triblock copolypeptoid ($A_{98}M_{98}D_{18}$) and (C) all ABC triblock copolypeptoids.

(Figure 23A).[89] The resulting polymers have well-defined structures and appear as mono-modal peaks in GPC chromatograms with narrow molecular weight distribution (PDI=1.04-1.15) (Figure 23B and 23C). The block copolypeptoids were shown to form spherical or short cylindrical micelles upon dissolution in dilute aqueous solution, depending on the polymer composition (Figure 24C). The semi-dilute polymer solutions (2.5-10%) were shown to undergo a reversible sol-to-gel transition with increasing temperature due to the hydrophobic collapses of the PNAlG segment above its cloud point (Figure 24A). The sol-to-gel transition is fully reversible and occurs in a narrow temperature window (Figure 24B). The gelation is rapid and occurs within seconds upon injection of the solution into an aqueous bath or onto a surface held above the gelation temperature. The gels can also be readily injected through a 20G syringe needle without breaking apart. The gelation temperature and the gel stiffness (Young's modulus E) can be tuned between 26.2-60 °C and 0.5-2346 Pa by controlling the polymer composition and polymer concentration. The gel was shown to consist of binodal micellar networks (Figure 24A) having a hierarchical structure with tunable pore sizes in the micron to tens of micron range (Figure 24D).

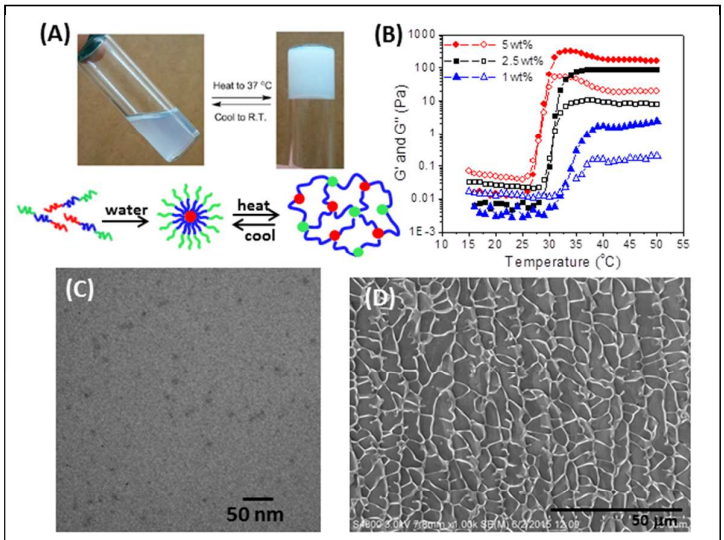

Figure 24. (A) Optical images and schematics showing the reversible sol-gel transition, (B) the plot of storage (G') and loss modulus (G") versus temperature for the aqueous solutions of $A_{98}M_{98}DG_{18}$ (Entry 1, Table 1) at different concentrations (1, 2.5 and 5 wt%); (C) cryo-TEM image showing the micelles of the $A_{92}M_{94}D_{12}$ polymer in dilute aqueous solution; (D) cryo-SEM image of the fractured $A_{92}M_{94}D_{12}$ (5 wt%) hydrogel interface.

Future challenges and outlook

Synthesis. Recent advances in controlled polymerization methods have enabled access to well-defined polypeptoids with controlled chain length, narrow chain length distribution, and diverse *N*-substituent structure. Synthesis of both linear and cyclic polypeptoids has enabled benchmarking of the fundamental physicochemical and biological properties of polypeptoids with varying *N*-substituents (*e.g.*, solubility, thermal properties, conformation and cytotoxicity, *etc.*). Synthetic strategies to enable access to polypeptoids with non-linear molecular architectures, well-defined monomer sequences, and tunable chain conformations

remain largely unexplored. Regarding the monomer sequence control in polypeptoids, one can envision the development of polymerization of appropriate substrates where the monomer sequence is defined during the substrate design and synthesis. These methods may complement the stepwise synthetic strategy (*i.e.*, sub-monomer method)[120] commonly used to access sequence-specific oligomeric peptoids. Design and synthesis of hybrid polymeric materials comprised of polypeptoid segments will also be a fruitful ground for future research. The synergistic combination of the unique properties of polypeptoids with those of other non-peptidomimetic polymers is likely to produce functional materials having unconventional properties.

Supramolecular self-assembly. Polypeptoids featuring a polar polyamide backbone with different substitution on the nitrogen are facially amphiphilic polymers. The polar amide functionalities confer strong dipole-dipole interactions that are absent in the majority of the conventional non-peptidomimetic polymers (*e.g.*, vinyl polymer, polyester, polyether). As a result of these structural attributes, polypeptoids tend to self-associate or aggregate in solution or at interfaces.[90,121,122] Understanding their supramolecular assemblies in solution or at the interface will be of fundamental importance and will have implications for practical uses of these polymers in solution-based applications. With advances in synthesis, understanding of how molecular interactions encoded in the *N*-substituent structures and monomer sequences impact the nano-scale and mesoscale assemblies of polypeptoids will be of significant interest in the rational design of polypeptoid polymers for targeted applications.

Materials applications. As polypeptoids exhibit enhanced protease stability, minimal cytotoxicity, and oxidative degradability, applications of polypeptoids are likely to be found in the fields of biomedicine and biotechnology. For example, investigation of polypeptoid-based drug delivery carriers,[92,98,99] gene delivery carriers, [79] and 3D culture/tissue-engineering scaffolds has started to emerge.[89] Demonstration of their unique properties and capabilities that are unrivaled by other non-polypeptoid-based systems will be critical in moving polypeptoids to the forefront of biomaterials applications.

Concluding remarks

The revived interests and recent research activities in polypeptoids have produced exciting results that indicate polypeptoids are an attractive and promising biomimetic platform for macromolecular and supramolecular engineering. Recent development of controlled polymerization methods have enabled access to structurally well-defined polypeptoids with controlled molecular characteristics (*e.g.*, HLB, charge characteristics, chain conformation, *etc.*) and architectures. We expect a bright future ahead for the further

development and application of polypeptoids as a design platform to access functional materials having a wide variety of potential uses in biomaterials or biomedical areas.

Acknowledgement

This work is supported by the National Science Foundation (CHE1609447) and Louisiana State University. AL and GLS were in part supported by the U.S. Department of Energy under EPSCoR Grant No. DE-SC0012432 with additional support from the Louisiana Board of Regents.

References.

[1] Kirshenbaum, K.; Barron, A. E.; Goldsmith, R. A.; Armand, P.; Bradley, E. K.; Truong, K. T. V.; Dill, K. A.; Cohen, F. E.; Zuckermann, R. N. "Sequence-Specific Polypeptoids: A Diverse Family of Heteropolymers with Stable Secondary Structure." *Proceedings of the National Academy of Sciences* **1998**, *95*, 4303-4308.

[2] Armand, P.; Kirshenbaum, K.; Goldsmith, R. A.; Farr-Jones, S.; Barron, A. E.; Truong, K. T. V.; Dill, K. A.; Mierke, D. F.; Cohen, F. E.; Zuckermann, R. N.; Bradley, E. K. "NMR Determination of the Major Solution Conformation of a Peptoid Pentamer with Chiral Side Chains." *Proceedings of the National Academy of Sciences* **1998**, *95*, 4309-4314.

[3] Wu, C. W.; Sanborn, T. J.; Zuckermann, R. N.; Barron, A. E. "Peptoid Oligomers with α-Chiral, Aromatic Side Chains: Effects of Chain Length on Secondary Structure." *Journal of the American Chemical Society* **2001**, *123*, 2958-2963.

[4] Wu, C. W.; Sanborn, T. J.; Huang, K.; Zuckermann, R. N.; Barron, A. E. "Peptoid Oligomers with α-Chiral, Aromatic Side Chains: Sequence Requirements for the Formation of Stable Peptoid Helices." *Journal of the American Chemical Society* **2001**, *123*, 6778-6784.

[5] Guo, L.; Li, J.; Brown, Z.; Ghale, K.; Zhang, D. "Synthesis and Characterization of Cyclic and Linear Helical Poly(α-peptoid)s by N-Heterocyclic Carbene-Mediated Ring-Opening Polymerizations of N-Substituted N-Carboxyanhydrides." *Peptide Science* **2011**, *96*, 596-603.

[6] Li, G.; Donghui, Z. *Synthesis and Characterization of Helix-Coil Block Copoly(α-peptoid)s* In *Non-Conventional Functional Block Copolymers*; American Chemical Society: 2011; Vol. 1066, p 71-79.

[7] Mannige, R. V.; Haxton, T. K.; Proulx, C.; Robertson, E. J.; Battigelli, A.; Butterfoss, G. L.; Zuckermann, R. N.; Whitelam, S. "Peptoid Nanosheets Exhibit a New Secondary-Structure Motif." *Nature* **2015**, *526*, 415-420.

[8] Robertson, E. J.; Battigelli, A.; Proulx, C.; Mannige, R. V.; Haxton, T. K.; Yun, L.; Whitelam, S.; Zuckermann, R. N. "Design, Synthesis, Assembly, and Engineering of Peptoid Nanosheets." *Accounts of Chemical Research* **2016**, DOI: 10.1021/acs.accounts.1025b00439

[9] Sanii, B.; Haxton, T. K.; Olivier, G. K.; Cho, A.; Barton, B.; Proulx, C.; Whitelam, S.; Zuckermann, R. N. "Structure-Determining Step in the Hierarchical Assembly of Peptoid Nanosheets." *ACS Nano* **2014**, *8*, 11674-11684.

[10] Sanii, B.; Kudirka, R.; Cho, A.; Venkateswaran, N.; Olivier, G. K.; Olson, A. M.; Tran, H.; Harada, R. M.; Tan, L.; Zuckermann, R. N. "Shaken, Not Stirred: Collapsing a Peptoid Monolayer To Produce Free-Floating, Stable Nanosheets." *Journal of the American Chemical Society* **2011**, *133*, 20808-20815.

[11] Kudirka, R.; Tran, H.; Sanii, B.; Nam, K. T.; Choi, P. H.; Venkateswaran, N.; Chen, R.; Whitelam, S.; Zuckermann, R. N. "Folding of a Single-Chain, Information-Rich Polypeptoid Sequence into a Highly Ordered Nanosheet." *Peptide Science* **2011**, *96*, 586-595.

[12] Cai, S.-L.; Zhang, W.-G.; Zuckermann, R. N.; Li, Z.-T.; Zhao, X.; Liu, Y. "The Organic Flatland—Recent Advances in Synthetic 2D Organic Layers." *Advanced Materials* **2015**, *27*, 5762-5770.

[13] Murnen, H. K.; Rosales, A. M.; Dobrynin, A. V.; Zuckermann, R. N.; Segalman, R. A. "Persistence Length of Polyelectrolytes with Precisely Located Charges." *Soft Matter* **2013**, *9*, 90-98.

[14] Secker, C.; Robinson, J. W.; Schlaad, H. "Alkyne-X Modification of Polypeptoids." *European Polymer Journal* **2015**, *62*, 394-399.

[15] Lahasky, S. H.; Hu, X.; Zhang, D. "Thermoresponsive Poly(α-peptoid)s: Tuning the Cloud Point Temperatures by Composition and Architecture." *ACS Macro Letters* **2012**, *1*, 580-584.

[16] Robinson, J. W.; Secker, C.; Weidner, S.; Schlaad, H. "Thermoresponsive Poly(N-C3 glycine)s." *Macromolecules* **2013**, *46*, 580-587.

[17] Robinson, J. W.; Schlaad, H. "A Versatile Polypeptoid Platform Based on N-Allyl Glycine." *Chemical Communications* **2012**, *48*, 7835-7837.

[18] Fetsch, C.; Grossmann, A.; Holz, L.; Nawroth, J. F.; Luxenhofer, R. "Polypeptoids from N-Substituted Glycine N-Carboxyanhydrides: Hydrophilic, Hydrophobic, and Amphiphilic Polymers with Poisson Distribution." *Macromolecules* **2011**, *44*, 6746-6758.

[19] Tao, X.; Du, J.; Wang, Y.; Ling, J. "Polypeptoids with Tunable Cloud Point Temperatures Synthesized from N-Substituted Glycine N-Thiocarboxyanhydrides." *Polymer Chemistry* **2015**, *6*, 3164-3174.

[20] Xuan, S.; Gupta, S.; Li, X.; Bleuel, M.; Schneider, G. J.; Zhang, D. "Synthesis and Characterization of Well-Defined PEGylated Polypeptoids as Protein-Resistant Polymers." *Biomacromolecules* **2017**, *18*, 951-964

[21] Lee, C.-U.; Li, A.; Ghale, K.; Zhang, D. "Crystallization and Melting Behaviors of Cyclic and Linear Polypeptoids with Alkyl Side Chains." *Macromolecules* **2013**, *46*, 8213-8223.

[22] Fetsch, C.; Luxenhofer, R. "Thermal Properties of Aliphatic Polypeptoids." *Polymers* **2013**, *5*, 112.

[23] Rosales, A. M.; Murnen, H. K.; Zuckermann, R. N.; Segalman, R. A. "Control of Crystallization and Melting Behavior in Sequence Specific Polypeptoids." *Macromolecules* **2010**, *43*, 5627-5636.

[24] Sun, J.; Teran, A. A.; Liao, X.; Balsara, N. P.; Zuckermann, R. N. "Crystallization in Sequence-Defined Peptoid Diblock Copolymers Induced by Microphase Separation." *Journal of the American Chemical Society* **2014**, *136*, 2070-2077.

[25] Miller, S. M.; Simon, R. J.; Ng, S.; Zuckermann, R. N.; Kerr, J. M.; Moos, W. H. "Proteolytic Studies of Homologous Peptide and N-Substituted Glycine Peptoid Oligomers." *Bioorganic & Medicinal Chemistry Letters* **1994**, *4*, 2657-2662.

[26] Miller, S. M.; Simon, R. J.; Ng, S.; Zuckermann, R. N.; Kerr, J. M.; Moos, W. H. "Comparison of the Proteolytic Susceptibilities of Homologous L-Amino Acid, D-Amino Acid, and N-Substituted Glycine Peptide and Peptoid Oligomers." *Drug Development Research* **1995**, *35*, 20-32.

[27] Ulbricht, J.; Jordan, R.; Luxenhofer, R. "On the Biodegradability of Polyethylene Glycol, Polypeptoids and Poly(2-oxazoline)s." *Biomaterials* **2014**, *35*, 4848-4861.

[28] Luxenhofer, R.; Fetsch, C.; Grossmann, A. "Polypeptoids: A Perfect Match for Molecular Definition and Macromolecular Engineering?" *Journal of Polymer Science Part A: Polymer Chemistry* **2013**, *51*, 2731-2752.

[29] Secker, C.; Brosnan, S. M.; Luxenhofer, R.; Schlaad, H. "Poly(α-Peptoid)s Revisited: Synthesis, Properties, and Use as Biomaterial." *Macromolecular Bioscience* **2015**, *15*, 881-891.

[30] Gangloff, N.; Ulbricht, J.; Lorson, T.; Schlaad, H.; Luxenhofer, R. "Peptoids and Polypeptoids at the Frontier of Supra- and Macromolecular Engineering." *Chemical Reviews* **2016**, *116*, 1753-1802.

[31] Klinker, K.; Barz, M. "Polypept(o)ides: Hybrid Systems Based on Polypeptides and Polypeptoids." *Macromolecular Rapid Communication* **2015**, *36*, 1943-1957.

[32] Zhang, D.; Lahasky, S. H.; Guo, L.; Lee, C.-U.; Lavan, M. "Polypeptoid Materials: Current Status and Future Perspectives." *Macromolecules* **2012**, *45*, 5833-5841.

[33] Leuchs, H.; Manasse., W. "Uber die Isomerie der Carbdthoxyl-glycyl-glycincstcr " *Ber. Dtsch. Chem. Ges.* **1907**, *40*, 3235-3249.

[34] Leuchs, H.; Geiger., W. "Uber die Anhydride von a-Amino-N -carbonsduren und die von a-Aminosduren." *Ber. Dtsch. Chem. Ges.* **1908**, *41*, 1721-1726.

[35] Wessely, F.; Riedl, K.; Tuppy, H. "Untersuchungen über α-Amino-N-carbonsäureanhydride VI." *Monatshefte für Chemie und verwandte Teile anderer Wissenschaften*, *81*, 861-872.

[36] Katchalski, E.; Sela, M. In *Advances in Protein Chemistry*; C.B. Anfinsen, M. L. A. K. B., John, T. E., Eds.; Academic Press: 1958; Vol. Volume 13, p 243-492.

[37] Guo, L.; Lahasky, S. H.; Ghale, K.; Zhang, D. "N-Heterocyclic Carbene-Mediated Zwitterionic Polymerization of N-Substituted N-Carboxyanhydrides toward Poly(α-peptoid)s: Kinetic, Mechanism, and Architectural Control." *Journal of American Chemical Society* **2012**, *134*, 9163-9171.

[38] Fuchs, F. "Über N-Carbonsäure-anhydride." *Berichte der deutschen chemischen Gesellschaft (A and B Series)* **1922**, *55*, 2943-2943.

[39] Levy, A. L. "Anhydro-N-Carboxy-DL-[beta]-Phenylalanine." *Nature* **1950**, *165*, 152-152.

[40] Kricheldorf, H. R.; Bösinger, K. "Mechanismus der NCA-Polymerisation, 3. Über die Amin katalysierte Polymerisation von Sarkosin-NCA und -NTA." *Die Makromolekulare Chemie* **1976**, *177*, 1243-1258.

[41] Tao, X.; Deng, Y.; Shen, Z.; Ling, J. "Controlled Polymerization of N-Substituted Glycine N-Thiocarboxyanhydrides Initiated by Rare Earth Borohydrides toward Hydrophilic and Hydrophobic Polypeptoids." *Macromolecules* **2014**, *47*, 6173-6180.

[42] Tao, X.; Deng, C.; Ling, J. "PEG-Amine-Initiated Polymerization of Sarcosine N-Thiocarboxyanhydrides Toward Novel Double-Hydrophilic PEG-b-Polysarcosine Diblock Copolymers." *Macromol. Rapid Commun.* **2014**, *35*, 875-881.

[43] Kricheldorf, H. R. "Polypeptides and 100 Years of Chemistry of α-Amino Acid N-Carboxyanhydrides." *Angewandte Chemie International Edition* **2006**, *45*, 5752-5784.

[44] Waley, S. G.; Watson, J. *J. Am. Chem. Soc.* **1948**, *70*, 2299–2300.

[45] Ballard, D. G. H.; Bamford, C. H. *J. Chem. Soc.* **1958**, 355–360.

[46] Waley, S. G.; Watson, J. *Proc. R. Soc. London, Ser. A* **1949**, *199*, 499–517.

[47] Szwarc, M. *The kinetics and mechanism of N-carboxy-α-amino-acid anhydride (NCA) polymerisation to poly-amino acids* In *Fortschritte der Hochpolymeren-Forschung*; Springer Berlin Heidelberg: **1965**; Vol. 4/1, p 1-65.

[48] Bamford, C. H.; Block, H.; Mason, D.; Openshaw, A. W. *SCI Monogr.* **1966**, *20*, 304–313.

[49] Sisido, M.; Imanishi, Y.; Higashimura, T. *Makromol. Chem.* **1977**, *178*, 3107–3114.

[50] Kricheldorf, H. R.; BÖsinger, K.*Makromol. Chem.* **1976**, *177*, 1243–1258.

[51] Kricheldorf, H. R.; von Lossow, C.; Schwarz, G. *Macromol. Chem. Phys.* **2004**, *205*, 918–924.

[52] Kricheldorf, H. R.; von Lossow, C.; Schwarz, G.; Fritsch, D. *Macromol. Chem. Phys.* **2005**, *206*, 1165–1170.

[53] Kricheldorf, H. R.; von Lossow, C.; Schwarz, G. *J. Polym. Sci., Part A: Polym. Chem.* **2006**, *44*, 4680–4695.

[54] Kricheldorf, H. R.; von Lossow, C.; Schwarz, G. *Macromolecules* **2005**, *38*, 5513–5518.

[55] Kricheldorf, H. R.; von Lossow, C.; Lomadze, N.; Schwarz, G. *J. Polym. Sci., Part A: Polym. Chem.* **2008**, *46*, 4012–4020.

[56] Fetsch, C.; Luxenhofer, R. "Highly Defined Multiblock Copolypeptoids: Pushing the Limits of Living Nucleophilic Ring-Opening Polymerization." *Macromolecular Rapid Communication* **2012**, *33*, 1708-1713.

[57] Pan, X.; Liu, Y.; Li, Z.; Cui, S.; Gebru, H.; Xu, J.; Xu, S.; Liu, J.; Guo, K. "Amphiphilic Polyoxazoline-block-Polypeptoid Copolymers by Sequential One-Pot Ring-Opening Polymerizations." *Macromolecular Chemistry and Physics* **2017**, *218*, 1600483.

[58] Gangloff, N.; Fetsch, C.; Luxenhofer, R. "Polypeptoids by Living Ring-Opening Polymerization of N-Substituted N-Carboxyanhydrides from Solid Supports." *Macromolecular Rapid Communications* **2013**, *34*, 997-1001.

[59] Schneider, M.; Fetsch, C.; Amin, I.; Jordan, R.; Luxenhofer, R. "Polypeptoid Brushes by Surface-Initiated Polymerization of N-Substituted Glycine N-Carboxyanhydrides." *Langmuir* **2013**, *29*, 6983-6988.

[60] Schneider, M.; Tang, Z.; Richter, M.; Marschelke, C.; Förster, P.; Wegener, E.; Amin, I.; Zimmermann, H.; Scharnweber, D.; Braun, H.-G.; Luxenhofer, R.; Jordan, R. "Patterned Polypeptoid Brushes." *Macromolecular Bioscience* **2016**, *16*, 75-81.

[61] Lu, L.; Lahasky, S.; Zhang, D.; Garno, J. C. "Directed Growth of Polymer Nanorods using Surface-Initiated Ring-Opening Polymerization of N-Allyl N-Carboxyanhydride." *ACS Applied Materials & Interfaces* **2016**, *8*, 4014-4022.

[62] Chan, B. A.; Xuan, S.; Horton, M.; Zhang, D. "1,1,3,3-Tetramethylguanidine-Promoted Ring-Opening Polymerization of N-Butyl N-Carboxyanhydride Using Alcohol Initiators." *Macromolecules* **2016**, *49*, 2002-2012.

[63] Tao, X.; Zheng, B.; Kricheldorf, H. R.; Ling, J. "Are N-substituted glycine N-thiocarboxyanhydride monomers really hard to polymerize?" *Journal of Polymer Science Part A: Polymer Chemistry* **2017**, *55*, 404-410.

[64] Unpublished results.

[65] Tao, X.; Zheng, B.; Bai, T.; Zhu, B.; Ling, J. "Hydroxyl Group Tolerated Polymerization of N-Substituted Glycine N-Thiocarboxyanhydride Mediated by Aminoalcohols: A Simple Way to α-Hydroxyl-ω-aminotelechelic Polypeptoids." *Macromolecules* **2017**, *50*, 3066-3077.

[66] Brown, H. A.; Waymouth, R. M. "Zwitterionic Ring-Opening Polymerization for the Synthesis of High Molecular Weight Cyclic Polymers." *Accounts of Chemical Research* **2013**, *46*, 2585-2596.

[67] Guo, L.; Zhang, D. "Cyclic Poly(α-peptoid)s and Their Block Copolymers from N-Heterocyclic Carbene-Mediated Ring-Opening Polymerizations of N-Substituted N-Carboxylanhydrides." *Journal of American Chemical Society* **2009**, *131*, 18072-18074.

[68] Lee, C.-U.; Smart, T. P.; Guo, L.; Epps, T. H.; Zhang, D. "Synthesis and Characterization of Amphiphilic Cyclic Diblock Copolypeptoids from N-Heterocyclic Carbene-Mediated Zwitterionic Polymerization of N-Substituted N-Carboxyanhydride." *Macromolecules* **2011**, *44*, 9574-9585

[69] Lahasky, S. H.; Serem, W. K.; Guo, L.; Garno, J. C.; Zhang, D. "Synthesis and Characterization of Cyclic Brush-Like Polymers by N-Heterocyclic Carbene-Mediated

Zwitterionic Polymerization of N-Propargyl N-Carboxyanhydride and the Grafting-to Approach." *Macromolecules* **2011**, *44*, 9063-9074.

[70] Li, A.; Lu, L.; Li, X.; He, L.; Do, C.; Garno, J. C.; Zhang, D. "Amidine-Mediated Zwitterionic Ring-Opening Polymerization of N-alkyl N-Carboxyanhydride: Mechanism, Kinetics and Architecture Elucidation." *Macromolecules* **2016**, 49, 1163-1171.

[71] Du, P.; Li, A.; Li, X.; Zhang, Y.; Do, C.; He, L.; Rick, S., John, V. J.; Kumar, R. and Zhang, D. "Aggregation of Cyclic Polypeptoids bearing Zwitterionic End-groups with Attractive Dipole-Dipole and Solvophobic Interactions: A Study by Small-Angle Neutron Scattering and Molecular Dynamics Simulation." *Physical Chemistry Chemical Physics* **2017**, *19*, 14388-14400.

[72] Lahasky, S. H.; Lu, L.; Huberty, W. A.; Cao, J.; Guo, L.; Garno, J. C.; Zhang, D. "Synthesis and Characterization of Thermo-responsive Polypeptoid Bottlebrushes." *Polymer Chemistry* **2014**, *5*, 1418-1426.

[73] Hörtz, C.; Birke, A.; Kaps, L.; Decker, S.; Wächtersbach, E.; Fischer, K.; Schuppan, D.; Barz, M.; Schmidt, M. "Cylindrical Brush Polymers with Polysarcosine Side Chains: A Novel Biocompatible Carrier for Biomedical Applications." *Macromolecules* **2015**, *48*, 2074-2086.

[74] Nakamura, R.; Aoi, K.; Okada, M. "Interactions of Enzymes and a Lectin with a Chitin-Based Graft Copolymer Having Polysarcosine Side Chains." *Macromolecular Bioscience* **2004**, *4*, 610-615.

[75] Nakamura, R.; Aoi, K.; Okada, M. "Controlled Synthesis of a Chitosan-Based Graft Copolymer Having Polysarcosine Side Chains Using the NCA Method with a Carboxylic Acid Additive." *Macromolecular Rapid Communications* **2006**, *27*, 1725-1732.

[76] Aoi, K.; Hatanaka, T.; Tsutsumiuchi, K.; Okada, M.; Imae, T. "Synthesis of a novel star-shaped dendrimer by radial-growth polymerization of sarcosine N-carboxyanhydride initiated with poly(trimethyleneimine) dendrimer." *Macromolecular Rapid Communications* **1999**, *20*, 378-382.

[77] Cui, S.; Pan, X.; Gebru, H.; Wang, X.; Liu, J.; Liu, J.; Li, Z.; Guo, K. "Amphiphilic star-shaped poly(sarcosine)-block-poly(ε-caprolactone) diblock copolymers: one-pot synthesis, characterization, and solution properties." *Journal of Materials Chemistry B* **2017**, *5*, 679-690.

[78] Holm, R.; Weber, B.; Heller, P.; Klinker, K.; Westmeier, D.; Docter, D.; Stauber, R. H.; Barz, M. "Synthesis and Characterization of Stimuli-Responsive Star-Like Polypept(o)ides: Introducing Biodegradable PeptoStars." *Macromolecular Bioscience* **2017**, *17*, 1600514.

[79] Zhu, L.; Simpson, J. M.; Xu, X.; He, H. Zhang, D.; Yin, L. "Cationic Polypeptoids with Optimized Molecular Characteristics towards Efficient Non-Viral Gene Delivery." *ACS Appl. Mater. Interfaces* **2017**, *9*, 23476-23486.

[80] Secker, C.; Brosnan, S. M.; Limberg, F. R. P.; Braun, U.; Trunk, M.; Strauch, P.; Schlaad, H. "Thermally Induced Crosslinking of Poly(N-Propargyl Glycine)." *Macromolecular Chemistry and Physics* **2015**, *216*, 2080-2085.

[81] Secker, C.; Völkel, A.; Tiersch, B.; Koetz, J.; Schlaad, H. "Thermo-Induced Aggregation and Crystallization of Block Copolypeptoids in Water." *Macromolecules* **2016**, *49*, 979-985.

[82] Ma, J.; Xuan, S.; Guerin, A.; Zhang, D. and Kuroda, D. G. "Unusual Molecular Mechanism behind the Thermal Response of Polypeptoids in Aqueous Solution." *Physical Chemistry Chemical Physics* **2017**, *19*, 10878-10888.

[83] Fasman, G. D.; Blout, E. R. "Copolymers of L-Proline and Sarcosine: Synthesis and Physical-Chemical Studies." *Biopolymers* **1963**, *1*, 99-109.

[84] Unpublished results.

[85] Sarid, S.; Berger, A.; Katchalski, E. "Proline Iminopeptidase." *Journal of Biological Chemistry* **1959**, *284*, 1740-1746.

[86] Halliwell, B.; Gutteridge, J. M. C. *Free Radicals in Biology and Medicine*; 3rd ed.; Clarendon Press: Oxford, UK, **1999**.

[87] Fetsch, C.; Flecks, S.; Gieseler, D.; Marschelke, C.; Ulbricht, J.; van Pée, K.-H.; Luxenhofer, R. "Self-Assembly of Amphiphilic Block Copolypeptoids with C2-C5 Side Chains in Aqueous Solution." *Macromolecular Chemistry and Physics* **2015**, *216*, 547-560.

[88] Li, A.; Zhang, D. "Synthesis and Characterization of Cleavable Core-Crosslinked Micelles based on Amphiphilic Block Copolypeptoids as Smart Drug Carriers." *Biomacromolecules* **2016**, *17*, 852-861.

[89] Xuan, S.; Lee, C.-U.; Chen, C.; Doyle, A. B.; Zhang, Y.; Guo, L.; John, V. T.; Hayes, D.; Zhang, D. "Thermoreversible and Injectable ABC Polypeptoid Hydrogels: Controlling the Hydrogel Properties through Molecular Design." *Chemistry of Materials* **2016**, *28*, 727-737.

[90] Zhang, Y.; Xuan, S.; Owoseni, O.; Omarova, M.; Li, X.; Saito, M. E.; He, J.; McPherson, G. L.; Raghavan, S. R.; Zhang, D.; John, V. T. "Amphiphilic Polypeptoids Serve as the Connective Glue to Transform Liposomes into Multilamellar Structures with Closely Spaced Bilayers." *Langmuir* **2017**, *33*, 2780-2789.

[91] Maurer, P. H.; Subrahmanyam, D.; Katchalski, E.; Blout, E. R. "Antigenicity of Polypeptides[poly(a-amino acids)]." *Journal of Immunology* **1959**, *83*, 193-197.

[92] Hara, E.; Ueda, M.; Makino, A.; Hara, I.; Ozeki, E.; Kimura, S. "Factors Influencing in Vivo Disposition of Polymeric Micelles on Multiple Administrations." *ACS Medicinal Chemistry Letters* **2014**, *5*, 873-877.

[93] Whittall, N.; Moran, D. M.; Wheeler, A. W.; Cottam, G. P. "Suppression of Murine IgE Responses with Amino Acid Polymer/Allergen Conjugates." *International Archives of Allergy and Immunology* **1985**, *76*, 354-360.

[94] Wheeler, A. W.; Henderson, D. C.; Garman, A. J.; Moran, D. M. "Suppression of Murine IgE Responses with Amino Acid Polymer/Allergen Conjugates." *International Archives of Allergy and Immunology* **1985**, *76*, 361-368.

[95] Moran, D. M.; Wheeler, A. W.; Henderson, D. C.; Whittall, N. "Suppression of Murine IgE Responses with Amino Acid Polymer/Allergen Conjugates." *International Archives of Allergy and Immunology* **1986**, *81*, 357-362.

[96] Cook, R. M.; Henderson, D. C.; Wheeler, A. W.; Moran, D. M. "Suppression of Murine IgE Responses with Amino Acid Polymer/Allergen Conjugates." *International Archives of Allergy and Immunology* **1986**, *80*, 355-360.

[97] Henderson, D. C.; Wheeler, A. W.; Moran, D. M. "Suppression of Murine IgE Responses with Amino Acid Polymer/Allergen Conjugates." *International Archives of Allergy and Immunology* **1987**, *82*, 208-211.

[98] Hara, E.; Ueda, M.; Kim, C. J.; Makino, A.; Hara, I.; Ozeki, E.; Kimura, S. "Suppressive Immune Response of Poly(sarcosine) Chains in Peptide-Nanosheets in Contrast to Polymeric Micelles." *Journal of Peptide Science* **2014**, *20*, 570-577.

[99] Hara, E.; Makino, A.; Kurihara, K.; Yamamoto, F.; Ozeki, E.; Kimura, S. "Pharmacokinetic Change of Nanoparticulate Formulation “Lactosome” on Multiple Administrations." *International Immunopharmacology* **2012**, *14*, 261-266.

[100] Joo Kim, C.; Hara, E.; Shimizu, A.; Sugai, M.; Kimura, S. "Activation of B1a Cells in Peritoneal Cavity by T Cell-Independent Antigen Expressed on Polymeric Micelle." *Journal of Pharmaceutical Sciences* **2015**, *104*, 1839-1847.

[101] Birke, A.; Huesmann, D.; Kelsch, A.; Weilbaecher, M.; Xie, J.; Bros, M.; Bopp, T.; Becker, C.; Landfester, K.; Barz, M. "Polypeptoid-block-polypeptide Copolymers: Synthesis, Characterization, and Application of Amphiphilic Block Copolypept(o)ides in Drug Formulations and Miniemulsion Techniques." *Biomacromolecules* **2014**, *15*, 548-557.

[102] Holm, R.; Klinker, K.; Weber, B.; Barz, M. "Synthesis of Amphiphilic Block Copolypept(o)ides by Bifunctional Initiators: Making PeptoMicelles Redox Sensitive." *Macromolecular Rapid Communications* **2015**, *36*, 2083-2091.

[103] Klinker, K.; Schäfer, O.; Huesmann, D.; Bauer, T.; Capelôa, L.; Braun, L.; Stergiou, N.; Schinnerer, M.; Dirisala, A.; Miyata, K.; Osada, K.; Cabral, H.; Kataoka, K.; Barz, M. "Secondary-Structure-Driven Self-Assembly of Reactive Polypept(o)ides: Controlling Size, Shape, and Function of Core Cross-Linked Nanostructures." *Angewandte Chemie International Edition* **2017**, *56*, 1-7.

[104] Cui, S.; Wang, X.; Li, Z.; Zhang, Q.; Wu, W.; Liu, J.; Wu, H.; Chen, C.; Guo, K. "One-Pot Glovebox-Free Synthesis, Characterization, and Self-Assembly of Novel Amphiphilic Poly(Sarcosine-b-Caprolactone) Diblock Copolymers." *Macromol. Rapid Commun.* **2014**, *35*, 1954-1959.

[105] Kanzaki, T.; Horikawa, Y.; Makino, A.; Sugiyama, J.; Kimura, S. "Nanotube and Three-Way Nanotube Formation with Nonionic Amphiphilic Block Peptides." *Macromolecular Bioscience* **2008**, *8*, 1026-1033.

[106] Ueda, M.; Makino, A.; Imai, T.; Sugiyama, J.; Kimura, S. "Rational Design of Peptide Nanotubes for Varying Diameters and Lengths." *Journal of Peptide Science* **2011**, *17*, 94-99.

[107] Ueda, M.; Makino, A.; Imai, T.; Sugiyama, J.; Kimura, S. "Transformation of Peptide Nanotubes into a Vesicle via Fusion Driven by Stereo-Complex Formation." *Chemical Communications* **2011**, *47*, 3204-3206.

[108] Ueda, M.; Makino, A.; Imai, T.; Sugiyama, J.; Kimura, S. "Tubulation on Peptide Vesicles by Phase-Separation of a Binary Mixture of Amphiphilic Right-Handed and Left-Handed Helical Peptides." *Soft Matter* **2011**, *7*, 4143-4146.

[109] Ueda, M.; Makino, A.; Imai, T.; Sugiyama, J.; Kimura, S. "Temperature-Triggered Fusion of Vesicles Composed of Right-Handed and Left-Handed Amphiphilic Helical Peptides." *Langmuir* **2011**, *27*, 4300-4304.

[110] Ueda, M.; Makino, A.; Imai, T.; Sugiyama, J.; Kimura, S. "Versatile Peptide Rafts for Conjugate Morphologies by Self-Assembling Amphiphilic Helical Peptides." *Polymer Journal* **2013**, *45*, 509-515.

[111] Matsui, H.; Ueda, M.; Makino, A.; Kimura, S. "Molecular Assembly Composed of a Dendrimer Template and Block Polypeptides Through Stereocomplex Formation." *Chemical Communications* **2012**, *48*, 6181-6183.

[112] Uesaka, A.; Ueda, M.; Makino, A.; Imai, T.; Sugiyama, J.; Kimura, S. "Self-Assemblies of Triskelion A2B-Type Amphiphilic Polypeptide Showing pH-Responsive Morphology Transformation." *Langmuir* **2012**, *28*, 6006-6012.

[113] Makino, A.; Hara, E.; Hara, I.; Ozeki, E.; Kimura, S. "Size Control of Core–Shell-type Polymeric Micelle with a Nanometer Precision." *Langmuir* **2014**, *30*, 669-674.

[114] Brosnan, S. M.; Schlaad, H.; Antonietti, M. "Aqueous Self-Assembly of Purely Hydrophilic Block Copolymers into Giant Vesicles." *Angewandte Chemie International Edition* **2015**, *54*, 9715-9718.

[115] Douy, A.; Gallot, B. "New Amphipathic Lipopeptides, 1. Synthesis and Mesomorphic Structures of Lipopeptides with Polysarcosine Peptidic Chains." *Die Makromolekulare Chemie* **1986**, *187*, 465-483.

[116] Gervais, M.; Douy, A.; Gallot, B.; Erre, R. "Surface Analysis of Lipopeptides using X-ray Photoelectron Spectroscopy: I. Lipopeptides with Polysarcosine Peptidic Chains." *Journal of Colloid and Interface Science* **1988**, *125*, 146-154.

[117] Gallot, B.; Hassan, H. H. "Lyotropic Lipo-Amino-Acids: Synthesis and Structural Study." *Molecular Crystals and Liquid Crystals Incorporating Nonlinear Optics* **1989**, *170*, 195-214.

[118] Fetsch, C.; Gaitzsch, J.; Messager, L.; Battaglia, G.; Luxenhofer, R. "Self-Assembly of Amphiphilic Block Copolypeptoids – Micelles, Worms and Polymersomes." *Scientific Reports* **2016**, *6*, 33491.

[119] Lee, C.-U.; Lu, L.; Chen, J.; Garno, J. C.; Zhang, D. "Crystallization-Driven Thermoreversible Gelation of Coil-Crystalline Cyclic and Linear Diblock Copolypeptoids." *ACS Macro Letter* **2013**, *2*, 436-440.

[120] Knight, A. S.; Zhou, E. Y.; Francis, M. B.; Zuckermann, R. N. "Sequence Programmable Peptoid Polymers for Diverse Materials Applications." *Advanced Materials* **2015**, *27*, 5665-5691.

[121] Robertson, E. J.; Battigelli, A.; Proulx, C.; Mannige, R. V.; Haxton, T. K.; Yun, L.; Whitelam, S.; Zuckermann, R. N. "Design, Synthesis, Assembly, and Engineering of Peptoid Nanosheets." *Accounts of Chemical Research* **2016**, *49*, 379-389.

[122] Robertson, E. J.; Nehls, E. M.; Zuckermann, R. N. "Structure–Rheology Relationship in Nanosheet-Forming Peptoid Monolayers." *Langmuir* **2016**, *32*, 12146-12158.

The chapter from which this Review was adapted appeared in the book "Polymers for Biomedicine: Synthesis, Characterization, and Applications" edited Carmen Scholz, published by John Wiley & Sons, Inc. (ISBN: 978-1-118-96657-0). Print and online versions are available at http://www.wiley.com/WileyCDA/WileyTitle/productCd-1118966570.html .

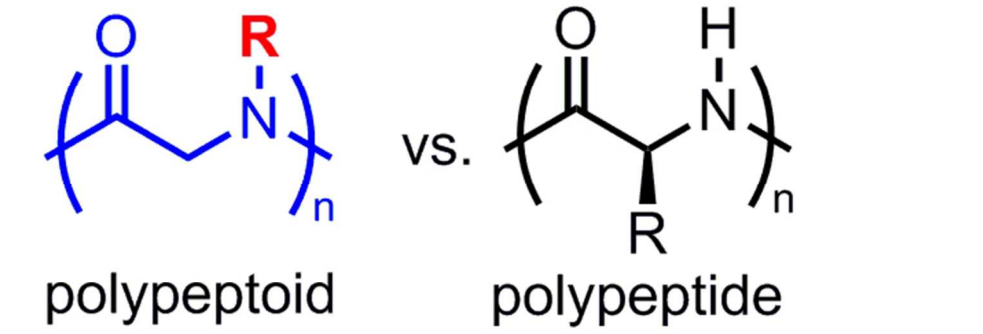

backbone: hydrophilic with strong dipole-dipole interactions
sidechain: tuning the HLB, charge characteristics and chain conformation

Figure 1

61x42mm (300 x 300 DPI)

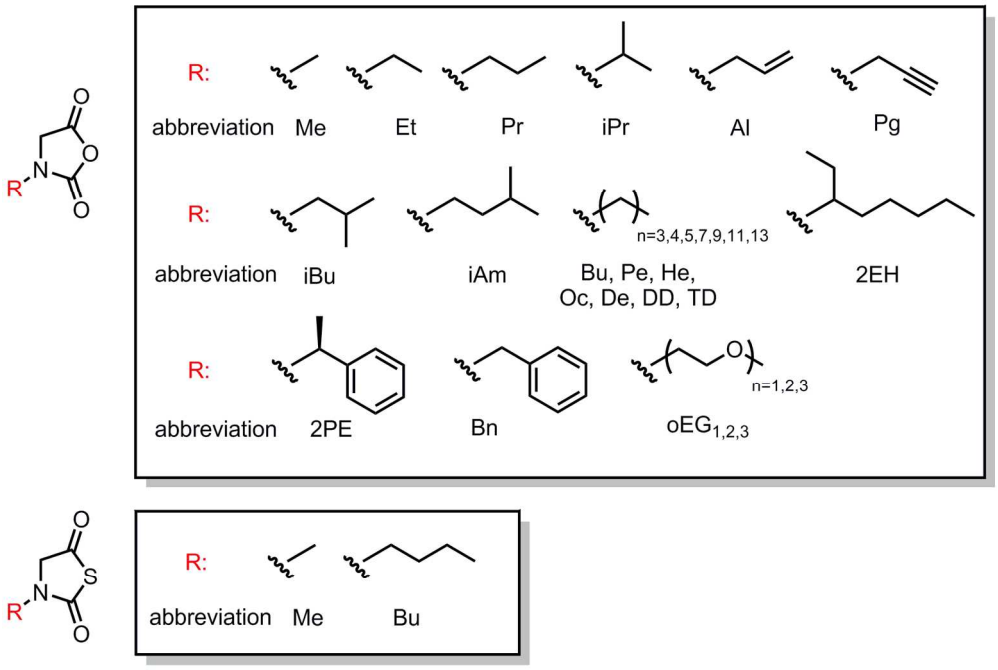

Figure 2

156x104mm (300 x 300 DPI)

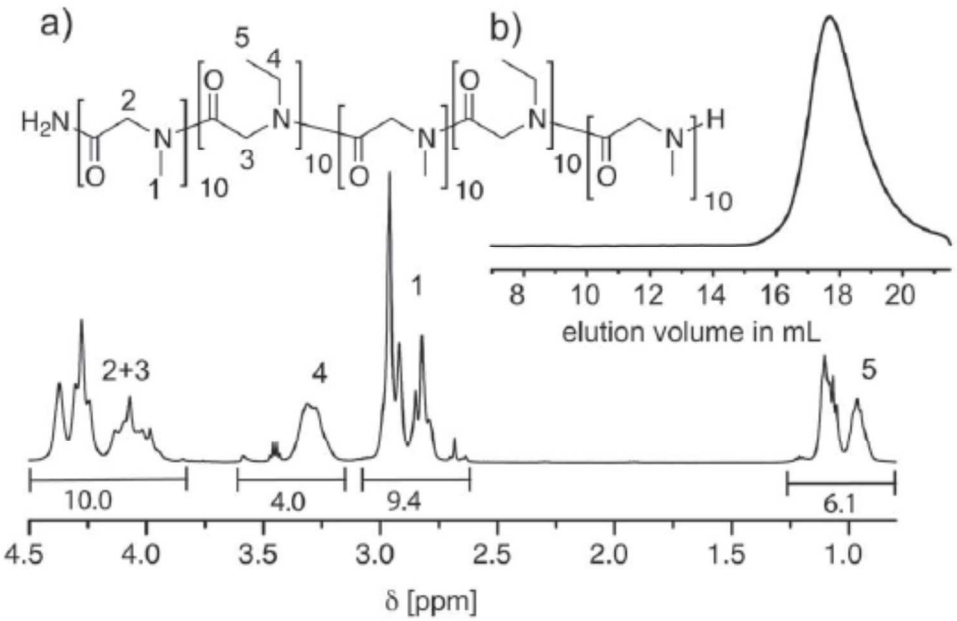

Figure 3

130x88mm (300 x 300 DPI)

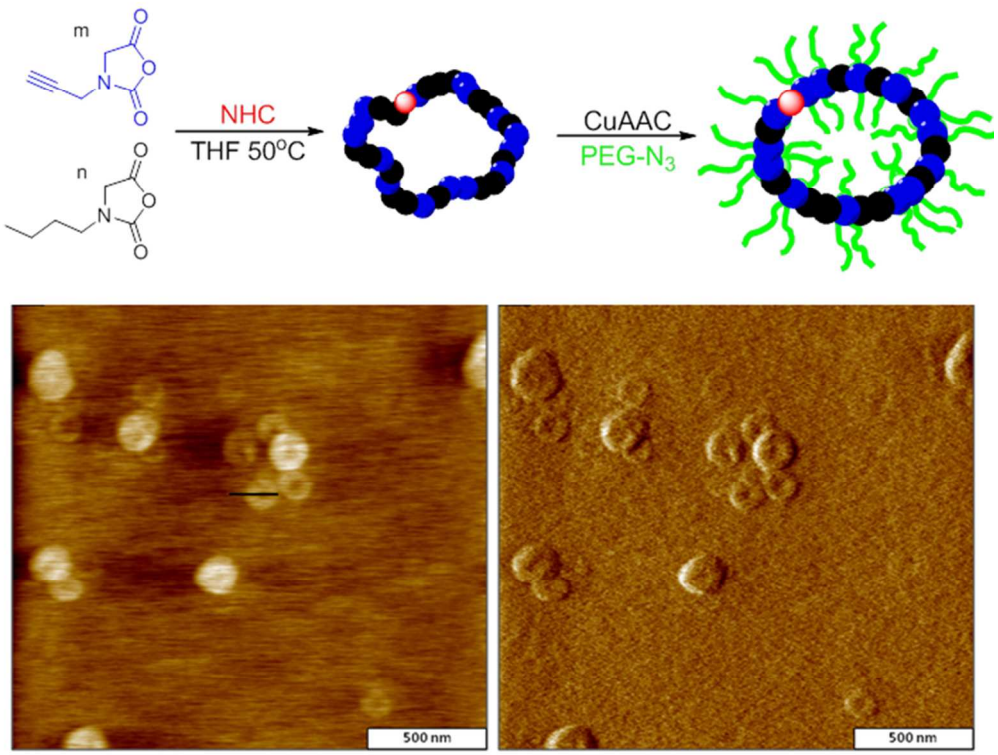

Figure 4

73x57mm (600 x 600 DPI)

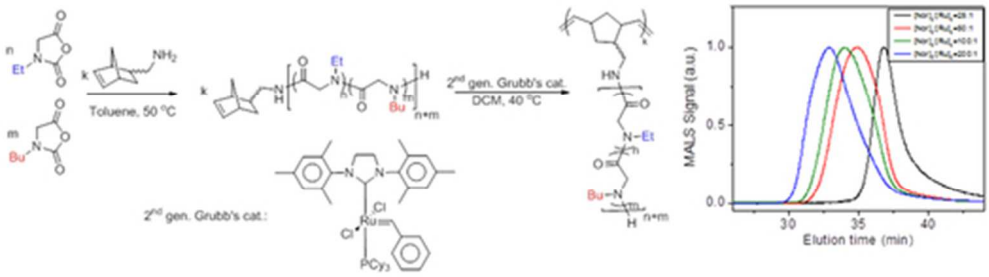

Figure 5

44x12mm (300 x 300 DPI)

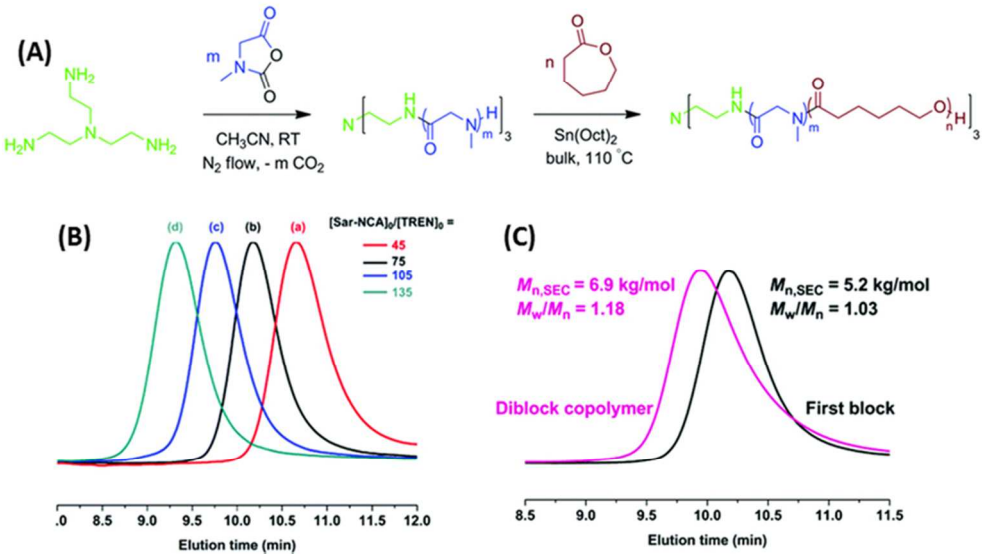

Figure 6

75x42mm (300 x 300 DPI)

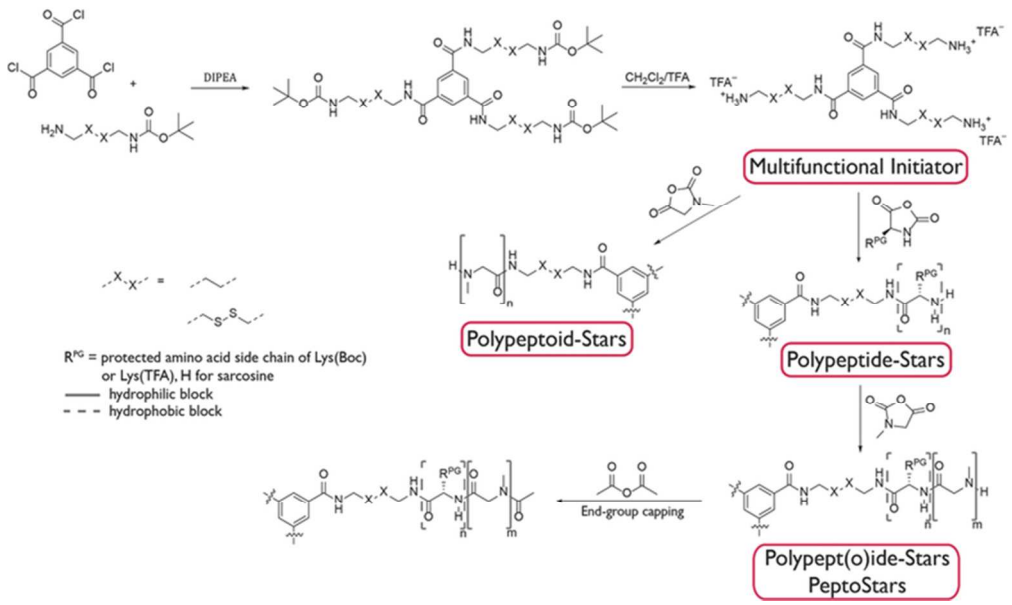

Figure 7

94x55mm (300 x 300 DPI)

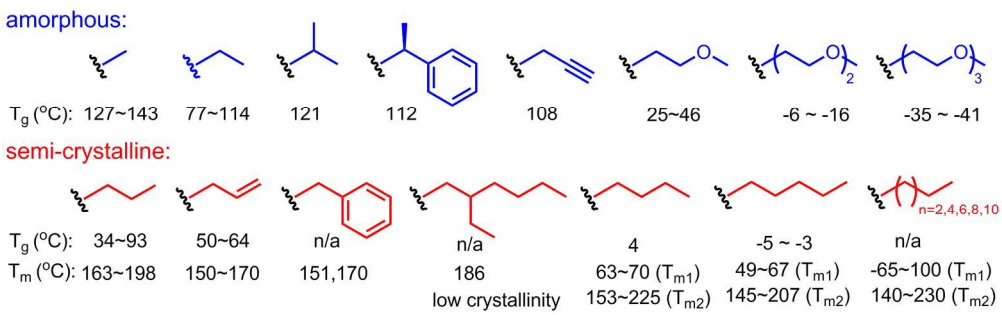

Figure 8

183x57mm (300 x 300 DPI)

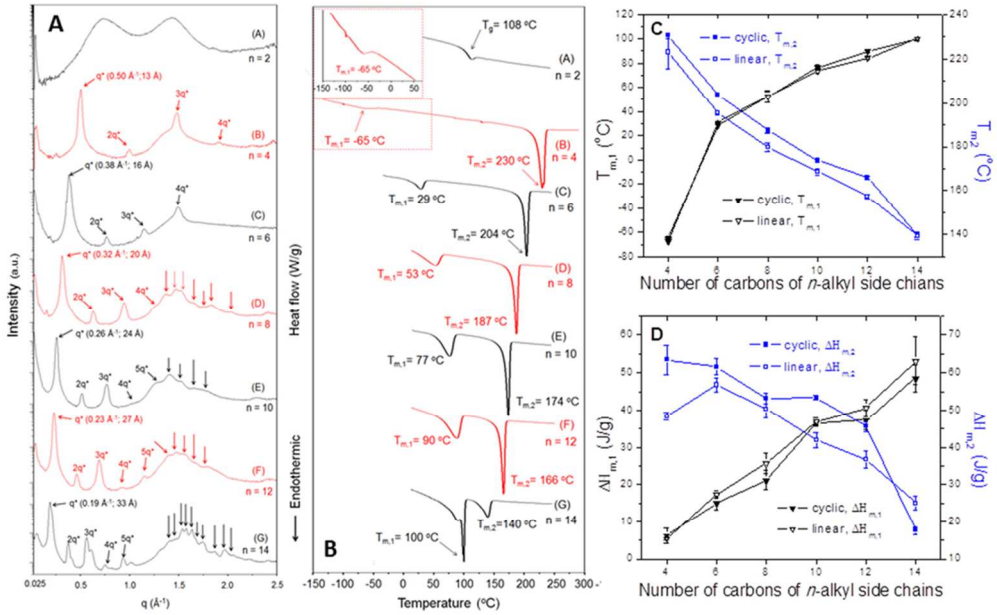

Figure 9

95x60mm (300 x 300 DPI)

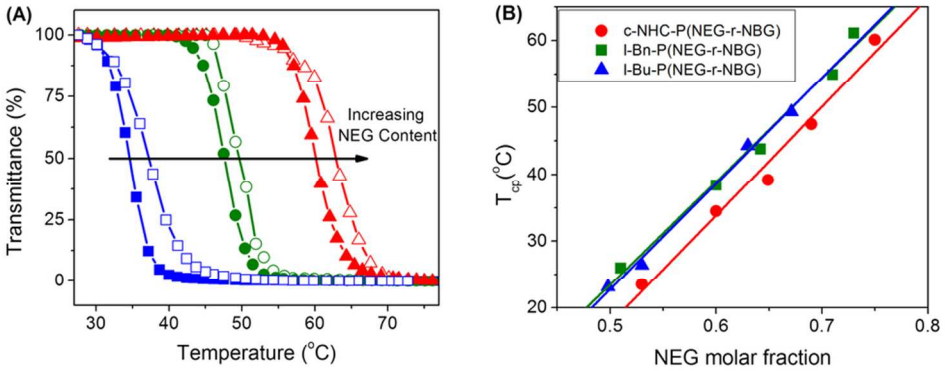

Figure 10

43x17mm (600 x 600 DPI)

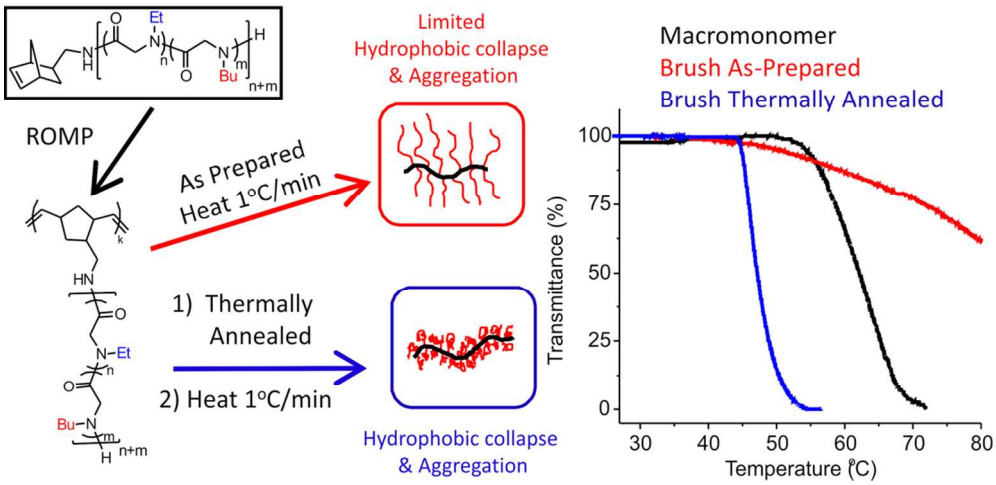

Figure 11

51x24mm (600 x 600 DPI)

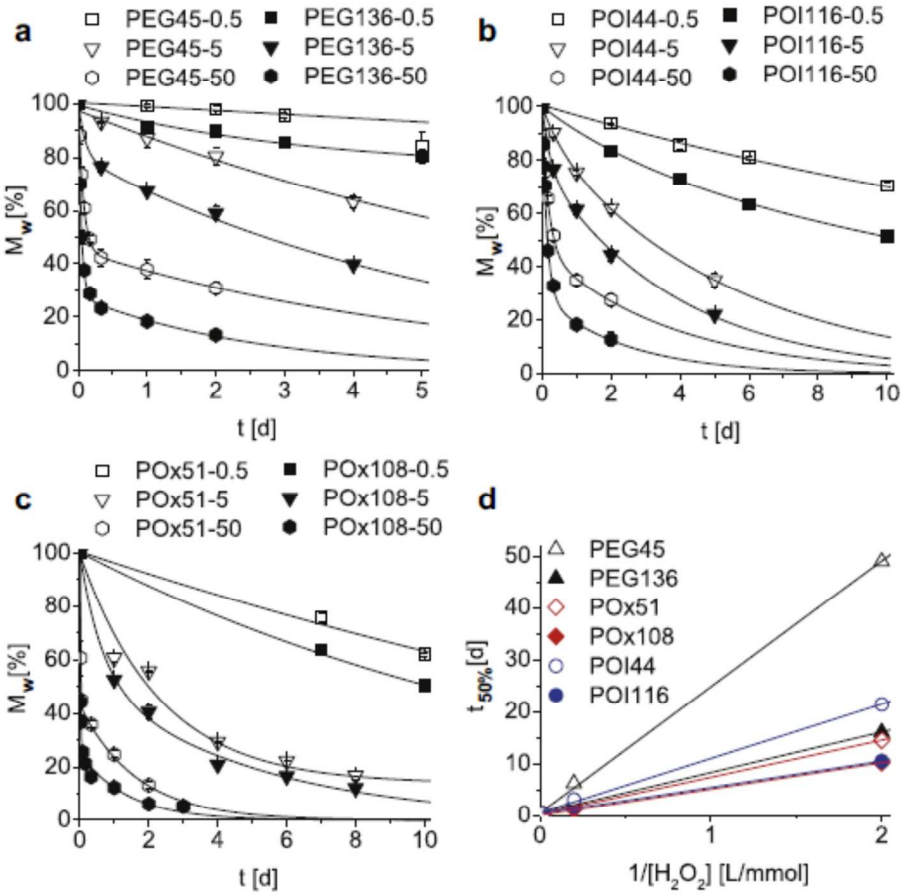

Figure 12

86x80mm (600 x 600 DPI)

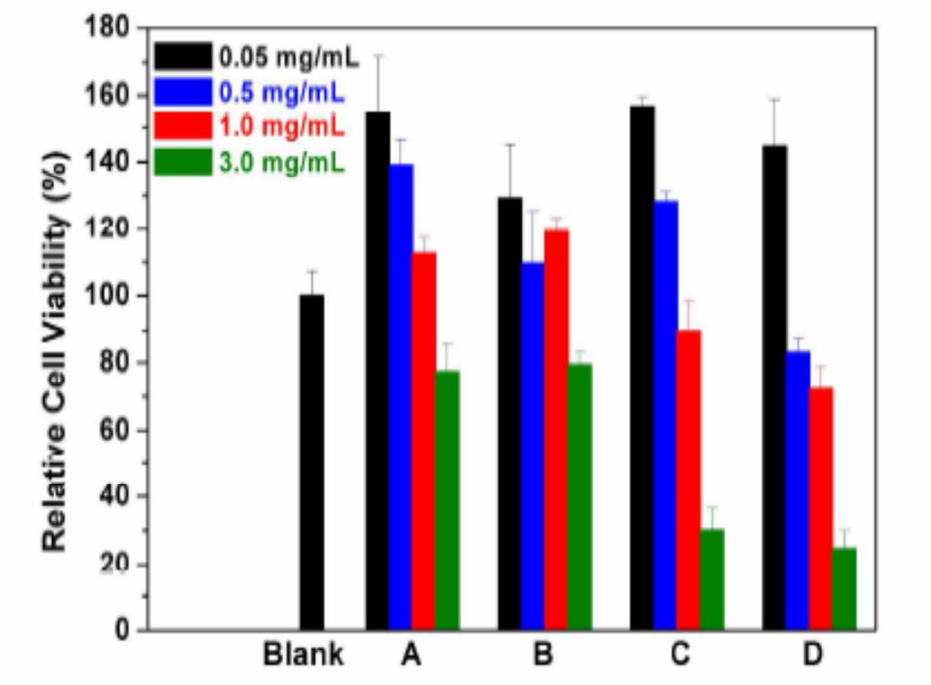

58x41mm (600 x 600 DPI)

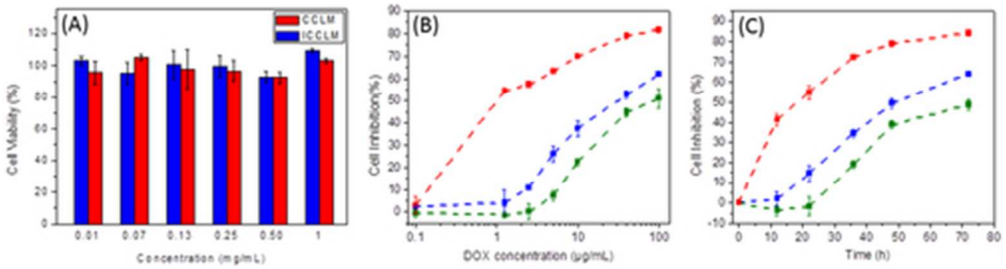

Figure 14

42x11mm (300 x 300 DPI)

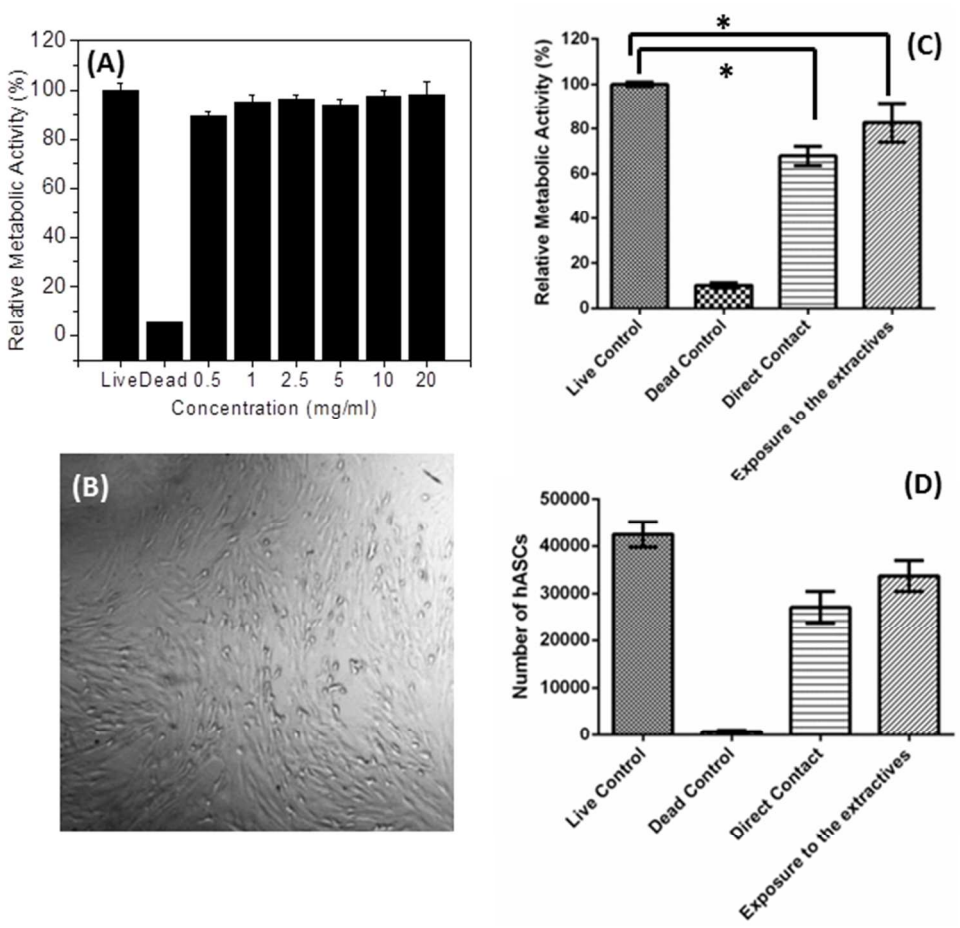

Figure 15

93x86mm (600 x 600 DPI)

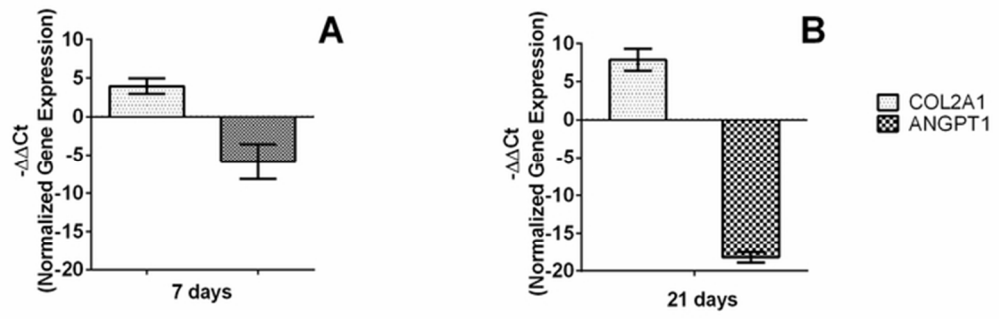

Figure 16

29x9mm (600 x 600 DPI)

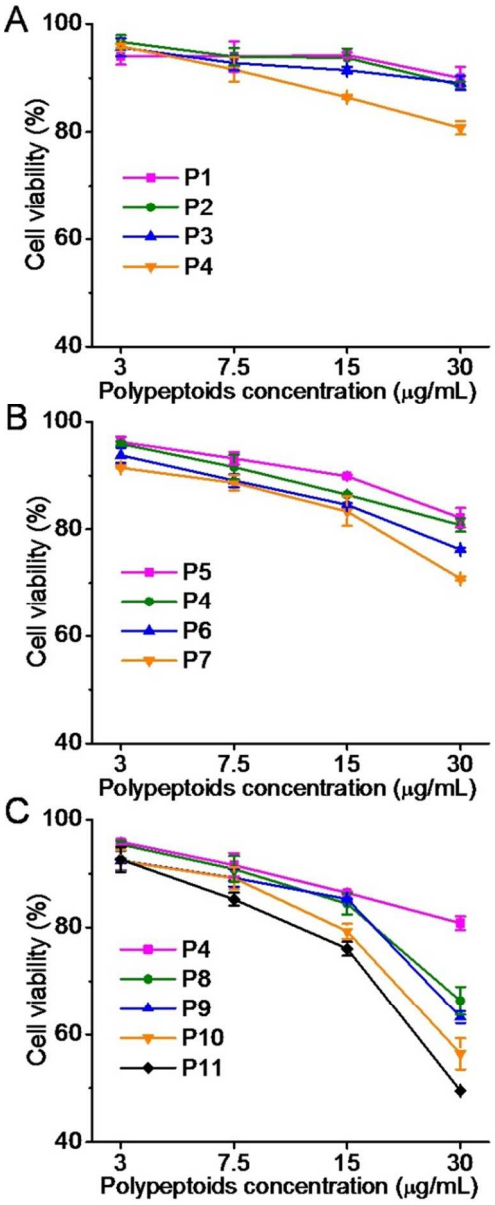

Figure 17

131x320mm (300 x 300 DPI)

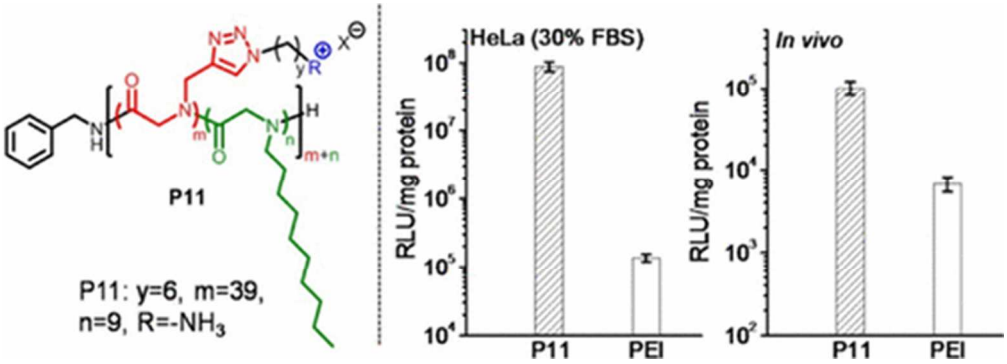

Figure 18

44x15mm (600 x 600 DPI)

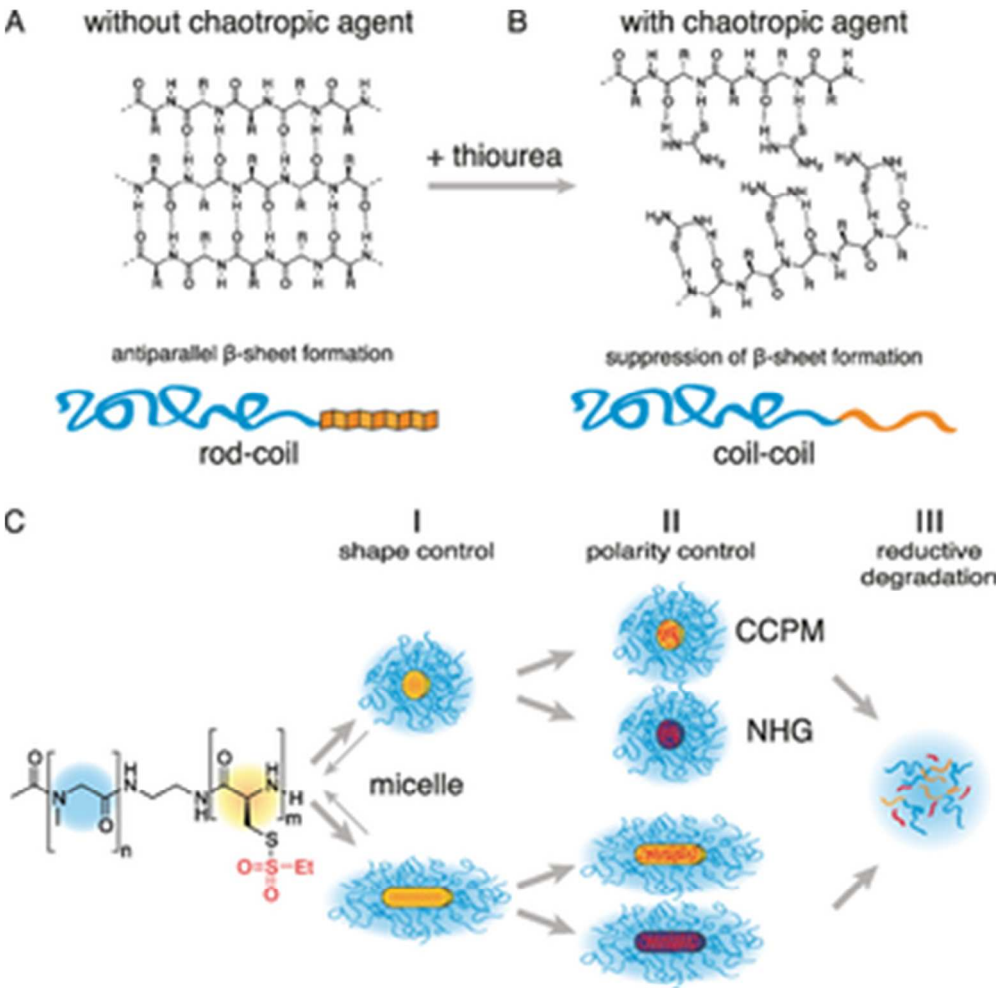

Figure 19

110x109mm (600 x 600 DPI)

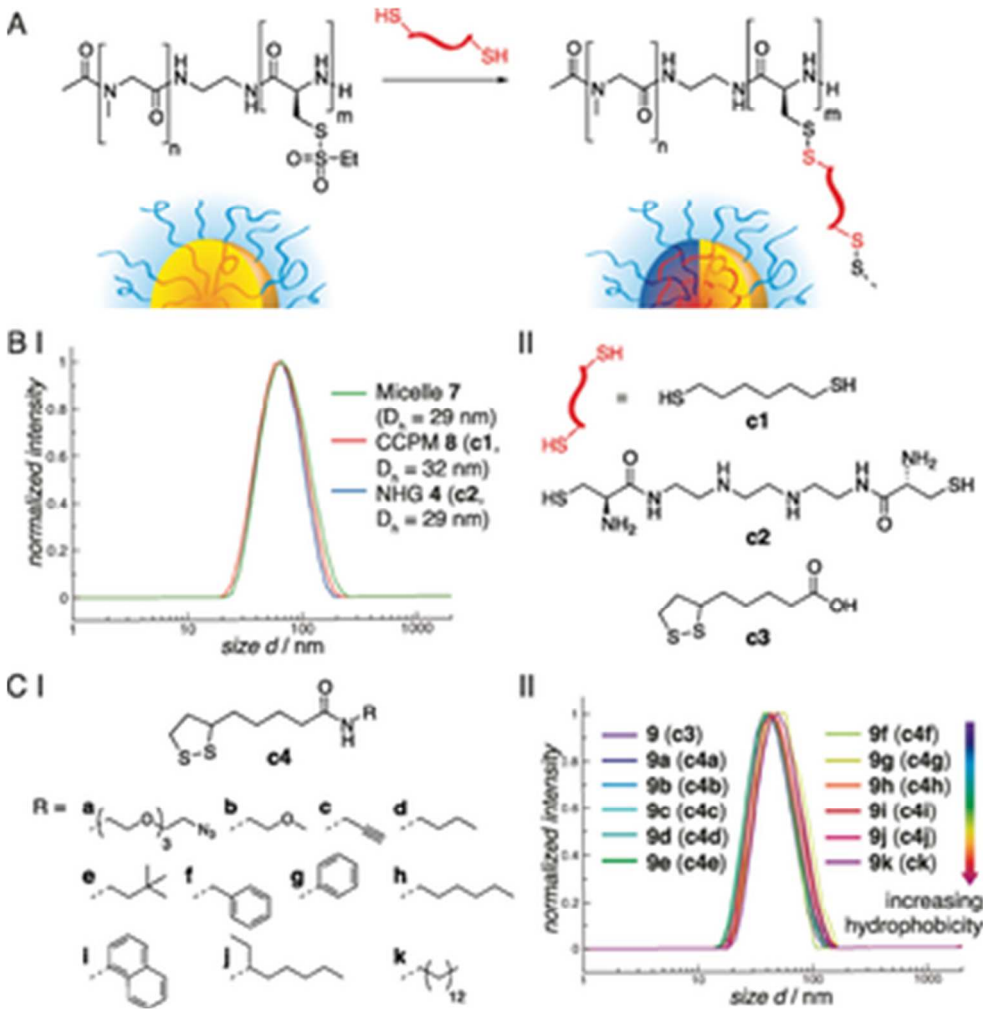

Figure 20

105x105mm (600 x 600 DPI)

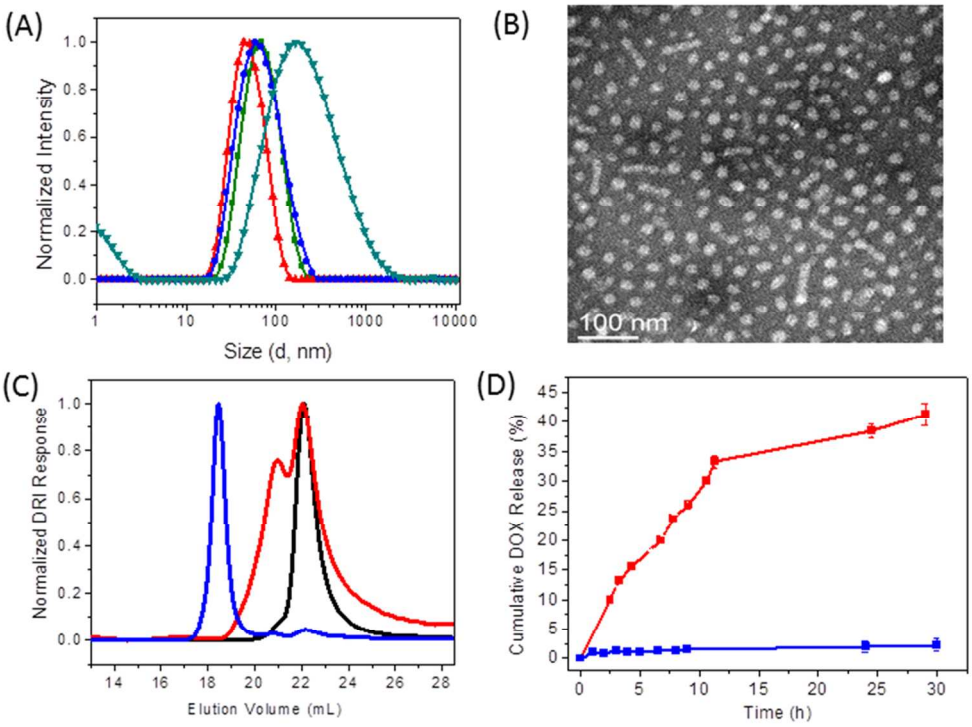

Figure 21

89x66mm (600 x 600 DPI)

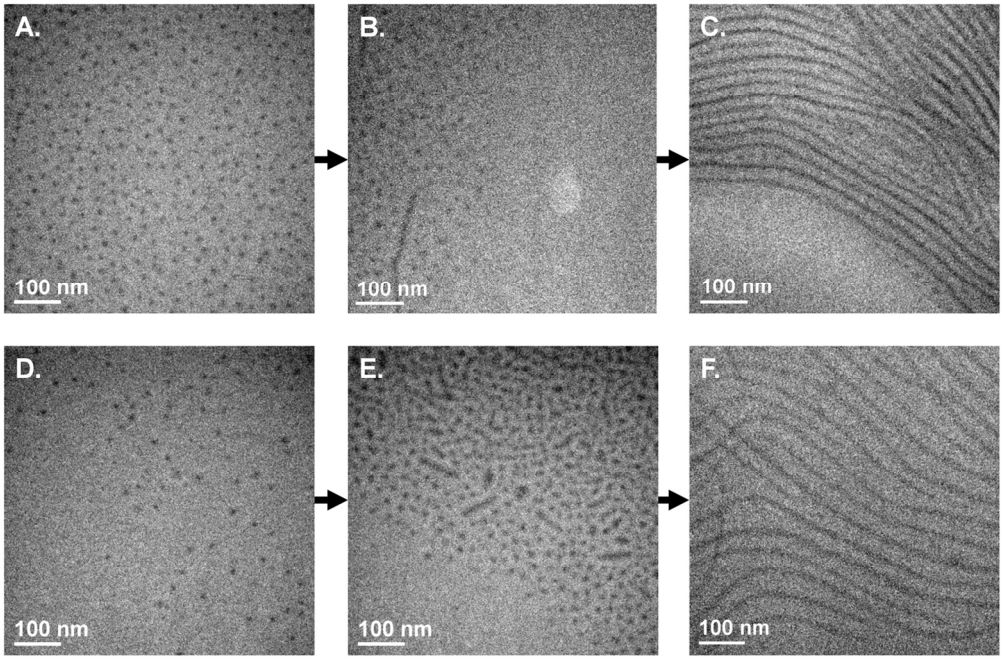

Figure 22

63x42mm (600 x 600 DPI)

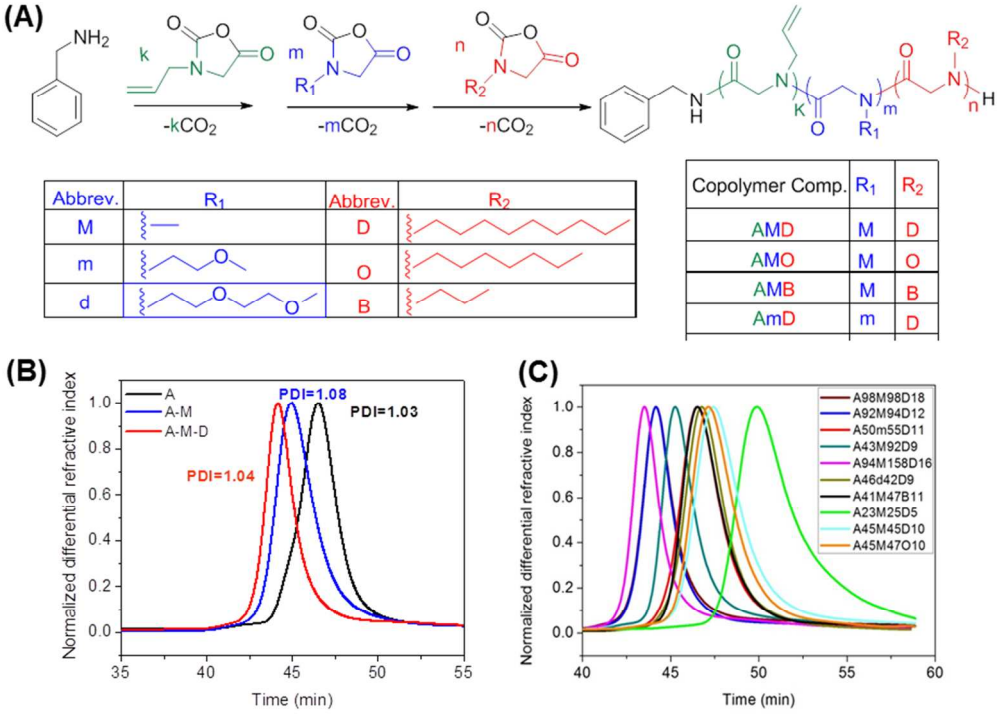

Figure 23

88x63mm (600 x 600 DPI)

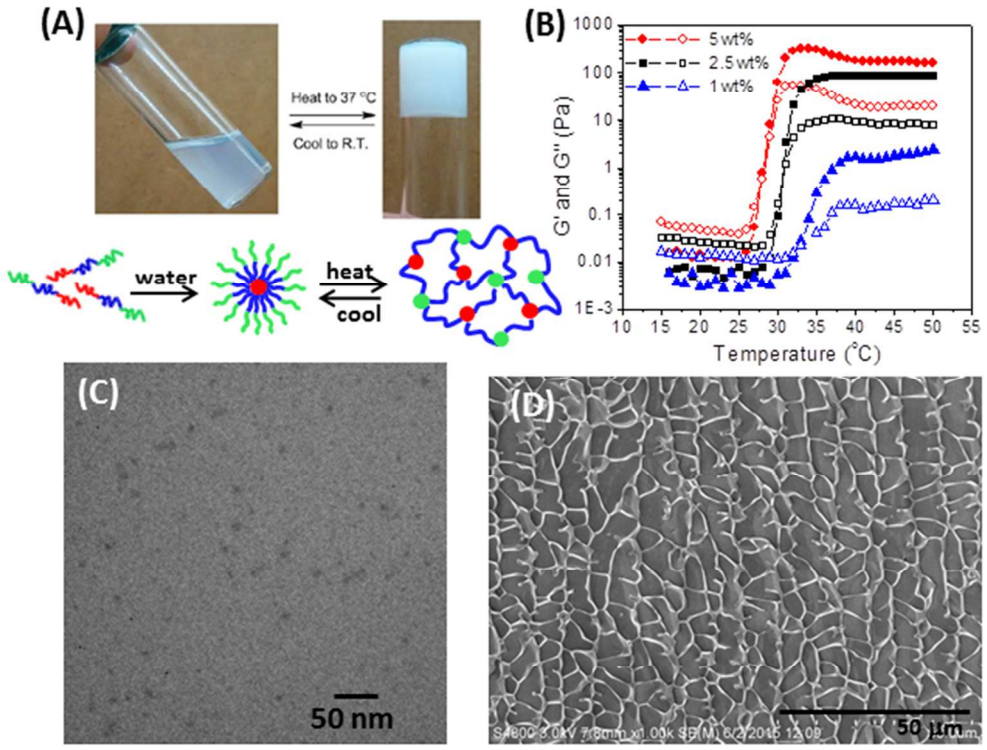

Figure 24

74x56mm (600 x 600 DPI)

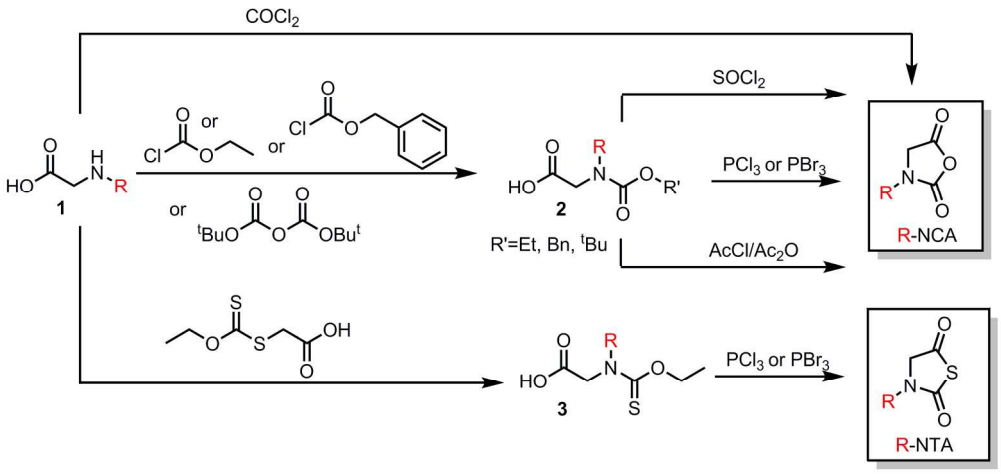

Scheme 1

187x87mm (300 x 300 DPI)

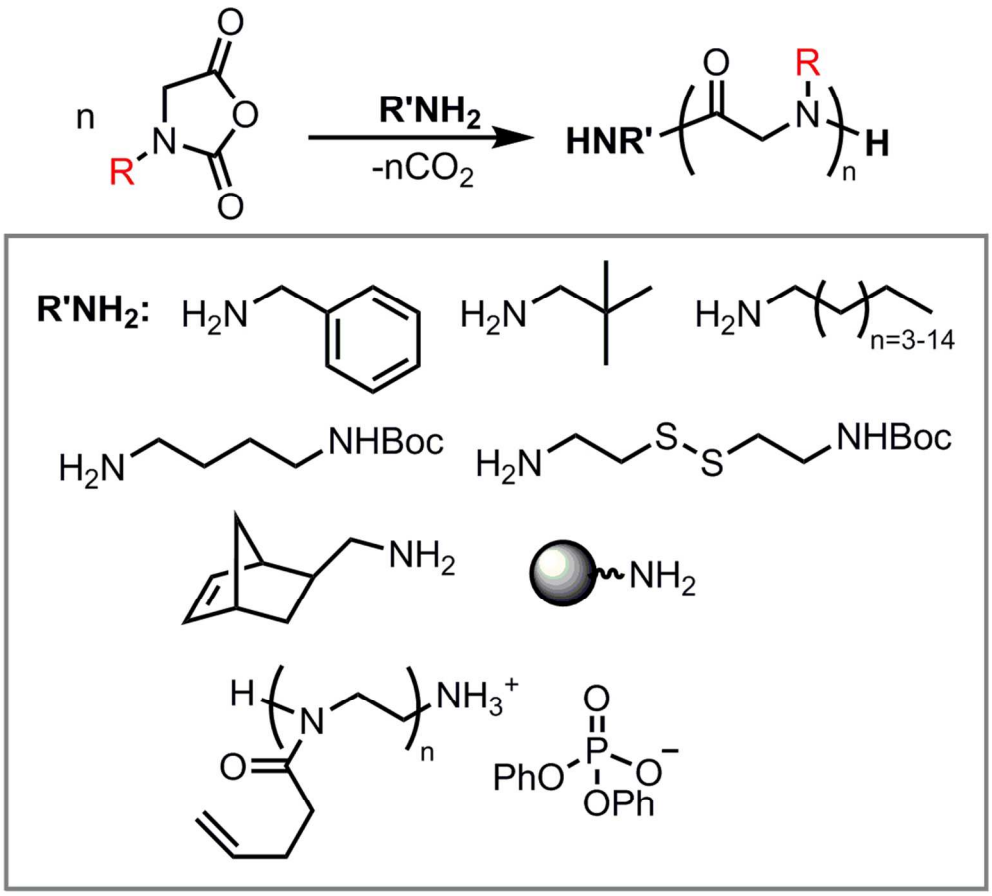

Scheme 2

96x87mm (300 x 300 DPI)

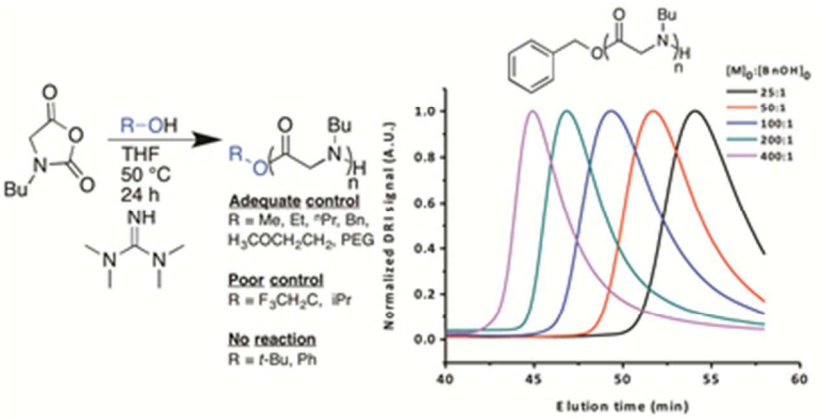

Scheme 3

108x54mm (96 x 96 DPI)

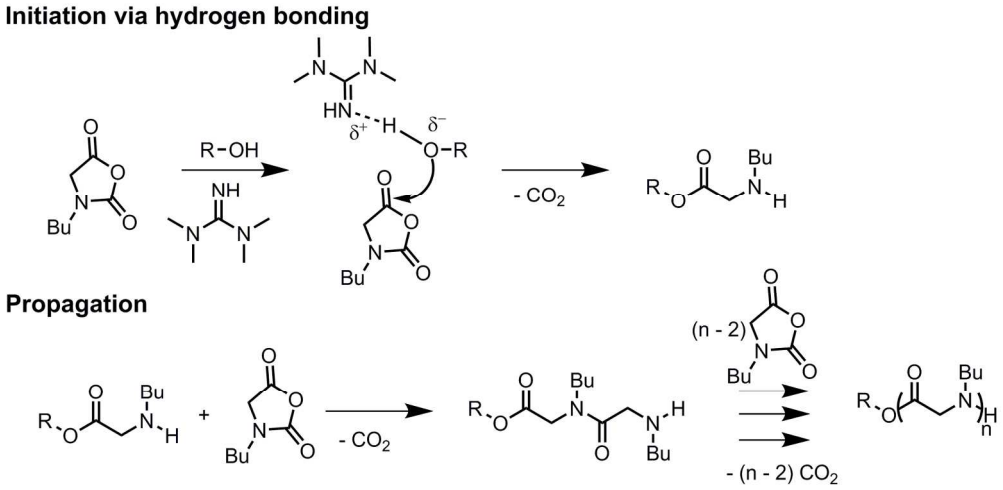

Scheme 4

173x85mm (300 x 300 DPI)

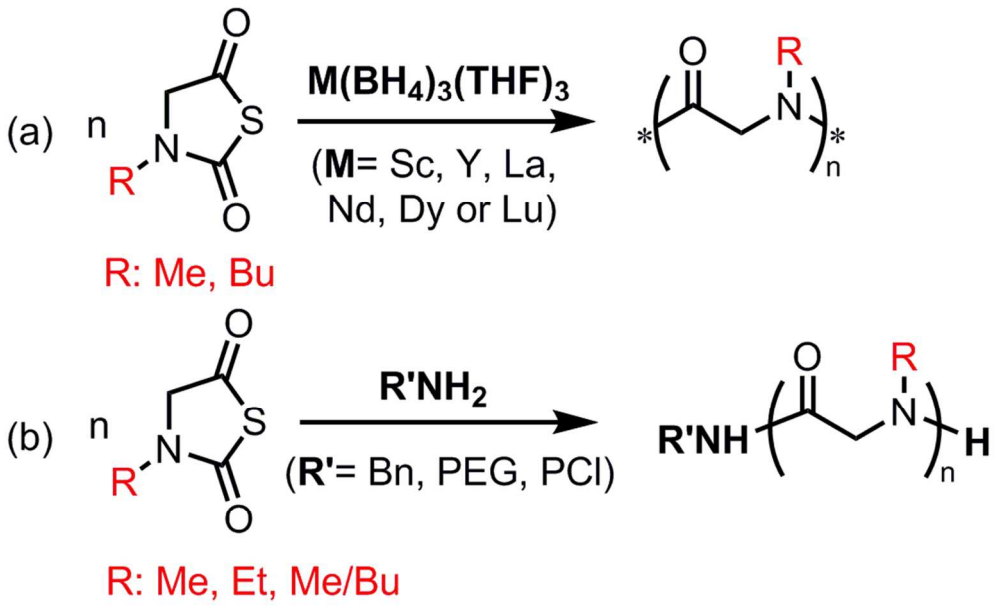

Scheme 5

91x56mm (300 x 300 DPI)

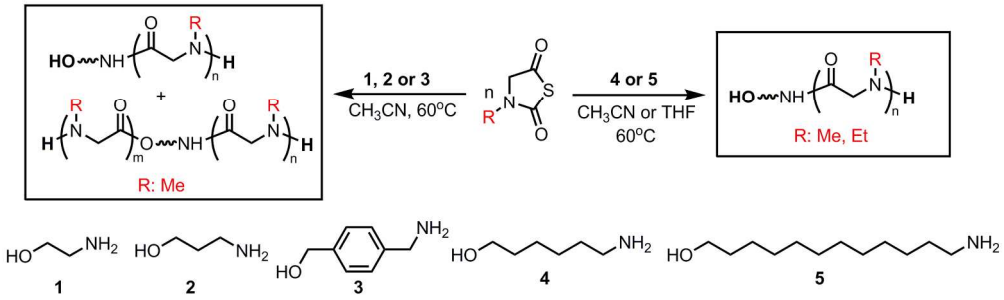

Scheme 6

199x60mm (300 x 300 DPI)

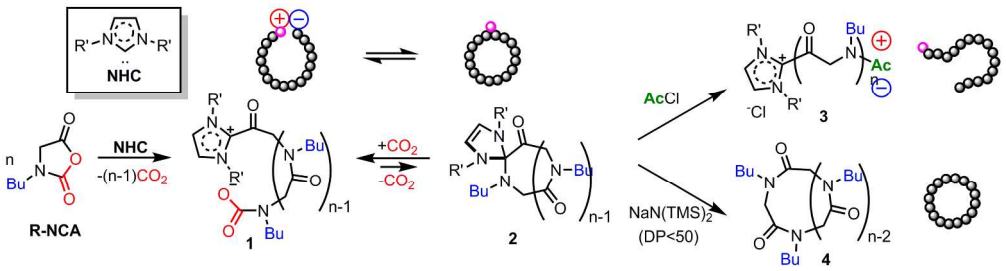

Scheme 7

219x59mm (300 x 300 DPI)

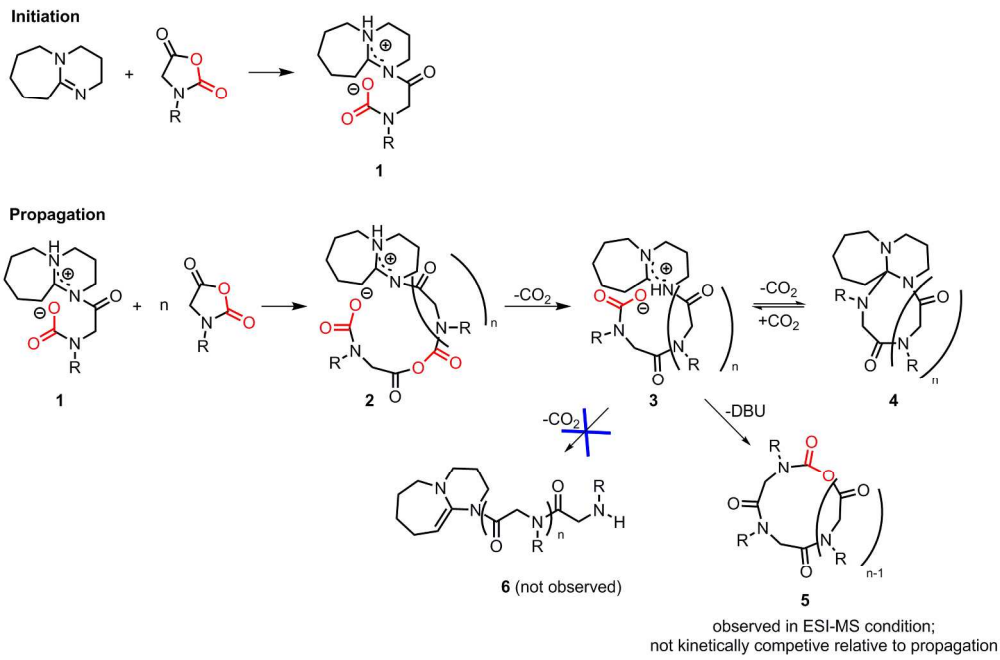

Scheme 8

213x140mm (300 x 300 DPI)

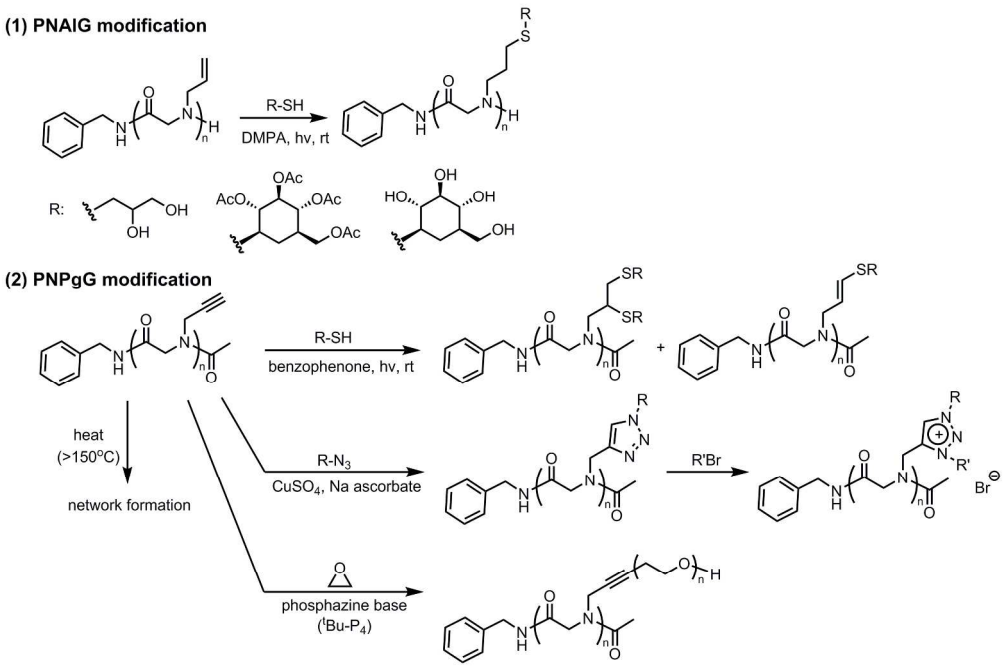

Scheme 9

228x151mm (300 x 300 DPI)

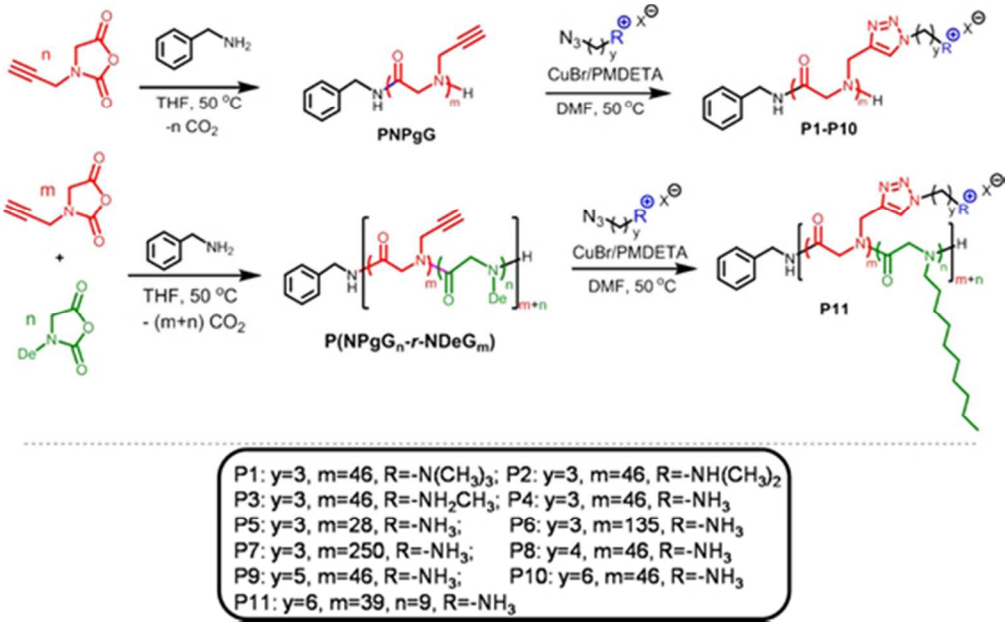

P1: y=3, m=46, R=-N(CH$_3$)$_3$; P2: y=3, m=46, R=-NH(CH$_3$)$_2$
P3: y=3, m=46, R=-NH$_2$CH$_3$; P4: y=3, m=46, R=-NH$_3$
P5: y=3, m=28, R=-NH$_3$; P6: y=3, m=135, R=-NH$_3$
P7: y=3, m=250, R=-NH$_3$; P8: y=4, m=46, R=-NH$_3$
P9: y=5, m=46, R=-NH$_3$; P10: y=6, m=46, R=-NH$_3$
P11: y=6, m=39, n=9, R=-NH$_3$

Scheme 10

150x92mm (96 x 96 DPI)

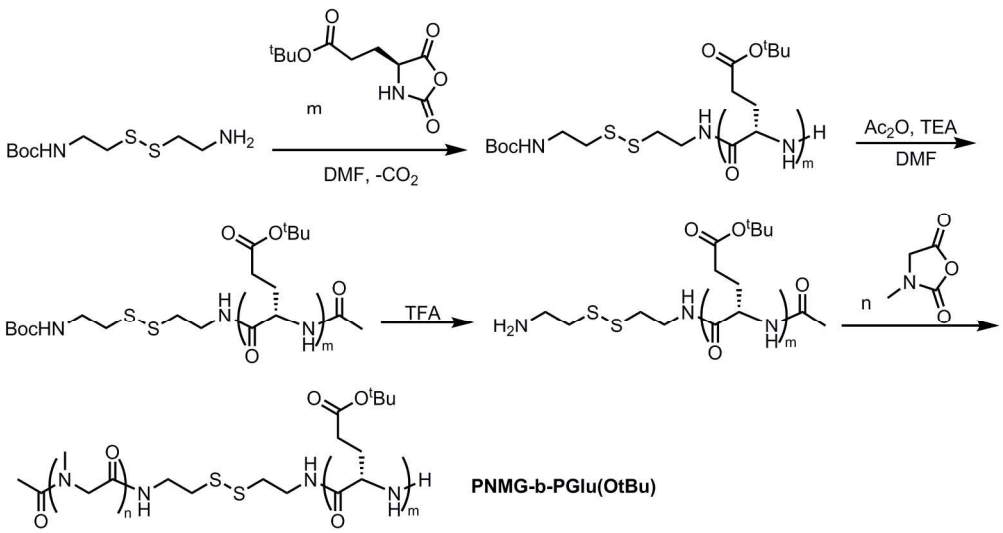

Scheme 11

185x97mm (300 x 300 DPI)

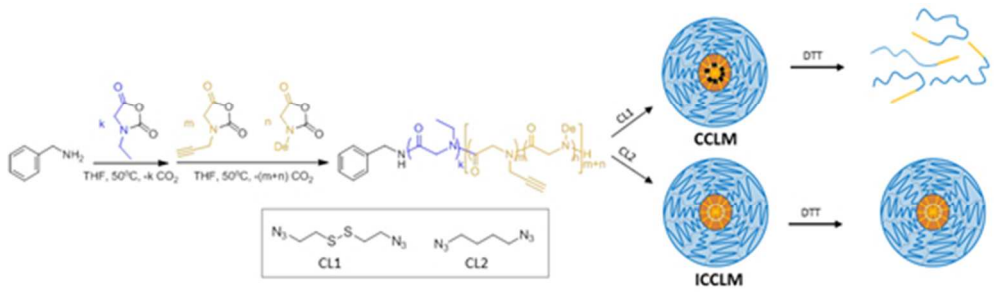

Scheme 12

153x46mm (96 x 96 DPI)